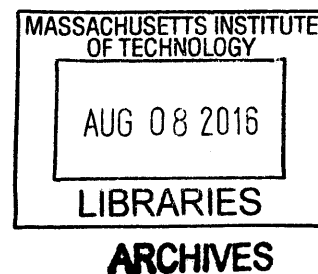


SMALL-MOLECULE INHIBITION OF GENERAL TRANSCRIPTIONAL  
REGULATORS IN CANCER

BY

JESSICA REDDY

B.S. Biological Sciences  
University of California, Irvine, 2005



Submitted to the Department of Biology in Partial Fulfillment  
of the Requirements for the Degree of

Doctor of Philosophy in Biology

at the

Massachusetts Institute of Technology

July 2016 [September 2016]

© 2016 Massachusetts Institute of Technology. All rights reserved.

Signature redacted

Signature of Author: \_\_\_\_\_

Department of Biology  
July 29, 2016

Signature redacted

Certified by: \_\_\_\_\_

Richard A. Young  
Professor of Biology  
Thesis Supervisor

Signature redacted

Accepted by: \_\_\_\_\_

Amy E. Keating  
Professor of Biology  
Co-chair, Biology Graduate Committee

# **SMALL-MOLECULE INHIBITION OF GENERAL TRANSCRIPTIONAL REGULATORS IN CANCER**

By

Jessica Reddy

Submitted to the Department of Biology on July 29, 2016 in Partial Fulfillment of the Requirements for the Degree of Doctor of Philosophy in Biology

## **Abstract**

Transcription is frequently deregulated in cancer, but targeting of transcriptional processes for cancer therapy has thus far been limited to nuclear receptors. Recent studies, however, have suggested that inhibitors of various general transcriptional regulators can be used in cancer therapy because expression of some oncogenes is disproportionately sensitive to these inhibitors. Here, I describe the cellular and molecular effects of inhibiting a general transcriptional regulator, CDK7, in T-cell acute lymphoblastic leukemia (T-ALL) cells. Because tumor cells commonly evolve resistance to individual therapies, I have also investigated the potentially synergistic effects of combining two compounds that target transcriptional regulators – the CDK7-inhibitor THZ1 and the BRD4-inhibitor JQ1 – and suggest a model describing the molecular basis of the synergistic effects I observed. My research provides insight into the effects of these inhibitors of general transcriptional regulators on tumor cell behavior and gene expression programs.

Thesis supervisor: Dr. Richard Young  
Title: Professor

*Dedicated to my father, Bobby Reddy, Sr.  
You have my everlasting love, respect, and gratitude.*

## Acknowledgements

Few words can describe how grateful I am for my advisor Prof. Rick Young, for his patience and belief in me. Rick has showed me the necessity of optimism in scientific research, coupled with the importance of preparing for worst-case scenarios (usually with aviation-related analogies). His mentorship has helped cultivate my scientific voice and trained me in the art of crystalizing one's ideas through writing. He has taught me how to bring deep thinking to problems and how to make the most compelling arguments. Always emphasizing the importance of prioritization and flexibility, he instilled the habit of frequent re-evaluation in order to pursue the most important scientific questions.

I thank my graduate committee advisors Prof. Phillip Sharp, Prof. David Page, and Prof. Piyush Gupta for providing support and helpful suggestions, especially in finishing my PhD studies. Prof. Angela Koehler from the Department of Biological Engineering at MIT is one of my role models, and I thank her for serving on my thesis committee.

I thank Prof. Trevor Siggers and Prof. Martha Bulyk for giving me an opportunity to study the intricacies of DNA binding specificities; this was an excellent place to start thinking about the regulation of transcription in development and disease. In addition, remembering Trevor's positive approach to science helped me through several moments during my graduate training.

Tony Lee has been invaluable throughout the years. He has consistently helped me take a step back, remove any intellectual blinders and see the forest from the trees. Tony believed in my scientific abilities from Day One. He has brought structure to my thinking as well as scholarship and sophistication to my communication style.

Alla Sigova has been a trusted friend, mentor, colleague, and role model. She has helped me in unquantifiable ways a countless number of times and has always possessed an unfaltering belief in my abilities as a scientist and leader. Most importantly, Alla has always reminded me, through words and by example that the most fulfilling way to approach one's life's work is to fully dedicate the mind, heart, and soul to it.

It has been an honor working with and learning from Nick Kwiatkowski, Brian Abraham, Alla Sigova, Peter Rahl, and Michael Seyffert during my studies in drugging transcriptional regulators. Nick has been extremely patient with me and taught me everything I know about chemical biology. He always was one to drop everything to help me. I have been incredibly fortunate to be surrounded by such talented teachers.

I thank members of the Young lab who have become some of my dearest friends: Lee Lawton, Garrett Frampton, Ana D'Alessio, Zi Peng Fan, Lars Anders,



and honorary member Johanna Goldmann. I also thank past and present members of the Young lab who have provided scientific support.

I thank my bay-mate Daniel Dadon for being a close friend and colleague over the years. Dan continuously inspires me to suspend doubts and think big when attacking scientific problems. There is a certain bond you share with someone who is going through his or her own transformative process alongside you.

I thank Amy Mitchell for helping me distill my dreams into concrete goals and grow from the inevitable obstacles of this chapter of life.

My mother Chia-Chuan Reddy has experienced this journey with me in a way that only a mother could. Her love has fueled every piece of success I have had.

My father Prof. Bobby Reddy, Sr. was my very first academic and life mentor, and his words of wisdom are with me every moment of every day. His visionary thinking and brilliance has been an inspiration for me to do something that could change the world.

Lastly, I'd like to thank my older brother ("guh-guh") Bobby Reddy, Jr. Bobby has supported me for the last twenty-eight years in every facet of life. I have eternal respect for his entrepreneurial passion, persistence, and obsessiveness to do what he can to improve healthcare. He has taught me the following: perseverance, fearlessness, and most importantly, what it means to *hustle*.

"There is a vitality, a life force, an energy, a quickening that is translated through you into action, and because there is only one of you in all of time, this expression is unique. And if you block it, it will never exist through any other medium and it will be lost. The world will not have it. It is not your business to determine how good it is nor how valuable nor how it compares with other expressions. (...) Keep the channel open... No artist is pleased. [There is] no satisfaction whatever at any time. There is only a queer divine dissatisfaction, a blessed unrest that keeps us marching and makes us more alive than the others."

Martha Graham

## Table of Contents

Title page.....	1
Abstract.....	2
Acknowledgements.....	4
Chapter 1: Introduction.....	8
Chapter 2: Targeting transcription regulation in cancer with a covalent CDK7 inhibitor.....	53
Chapter 3: Small-molecule inhibition of functionally related transcriptional co-factors produces synergistic effects in T-cell acute lymphoblastic leukemia.....	78
Chapter 4: Conclusions and future directions.....	116
Appendix: Supplemental material for Chapter 2.....	132

## Chapter 1: Introduction

---

### Preface

Transcriptional processes are typically dysregulated in cancer cells (Bhagwat and Vakoc, 2015; Lee and Young, 2013; Brien et al., 2016; Cancer Genome Atlas Research Network, 2013; Villicana et al., 2014; Hnisz et al., 2013). Transcription factors (TFs) play direct and specific roles in tumorigenesis, which makes them attractive candidate drug targets, but with the exception of nuclear receptors, small molecule inhibition of transcription factors has proven difficult. Recent studies have revealed that inhibition of general transcriptional regulators (GTRs), which are transcriptional control proteins that generally function at many active genes, may provide an alternative method to inhibit dysregulated transcription in tumor cells (Loven et al., 2013; Kwiatkowski et al., 2014). This surprising result is thought to be due to several features of dysregulated tumor cells, including the development of exceptional “dependencies” on the GTRs at certain dysregulated genes such as *MYC*.

The two GTRs that are the focus of this discussion are BRD4 and CDK7, for which various chemical probes have been synthesized and studied by a group of collaborating laboratories directed by Jay Bradner, Nathanael Gray and Richard Young (Delmore et al., 2010; Kwiatkowski et al., 2014.) These groups reported that inhibition of the general transcriptional regulator BRD4 with the small-molecule competitive inhibitor JQ1 could result in gene-selective effects in

tumor cells (Delmore et al., 2010). This observation countered an expectation that inhibiting a general factor would cause global, non-selective effects on transcription. Instead, JQ1 treatment resulted in selective down-regulation of the *MYC* oncogene in Multiple Myeloma cells. These results suggested that tumor cells might be especially dependent on certain general transcriptional regulators and that inhibitors of other GTRs might produce similar gene-selective effects in tumor cells.

Indeed, an irreversible inhibitor (THZ1) of CDK7 and CDK12, which are kinases that function in general transcription initiation and elongation, was found to produce gene-selective effects on oncogenes in T-cell acute lymphoblastic leukemia (T-ALL) cells (Kwiatkowski et al., 2014). These results, which are described in Chapter 2, indicate that inhibition of CDK7/CDK12 produces gene-selective effects on oncogenes as well as proliferative effects in T-ALL cells.

Although BRD4 and CDK7/12 are both involved in general transcriptional control (Fig. 1), they have different mechanistic functions, which led to the hypothesis that they might show synergistic effects when their inhibitors are used in combination. I tested this hypothesis and found, as described in Chapter 3, that T-ALL cells are sensitive to both THZ1 or JQ1, but the treatment of T-ALL cells with a combination of THZ1 and JQ1 produces synergistic anti-proliferative effects and more profound effects on the T-ALL gene expression program than treatment with either inhibitor alone. My results indicate that different genes are especially dependent on CDK7 and BRD4 for their transcription, and suggest that the loss of expression of the combined set with both inhibitors mediates the

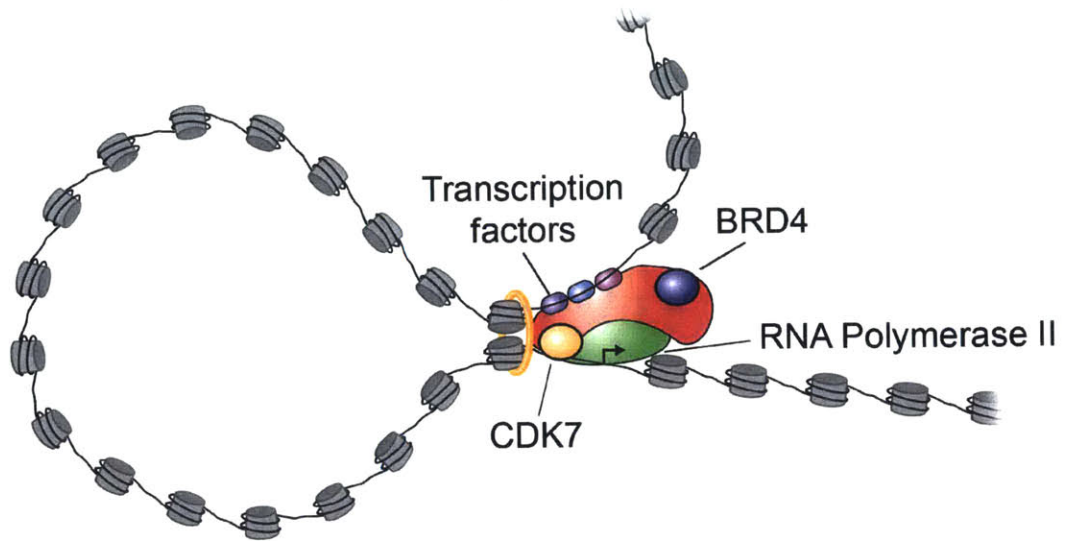


**Figure 1**

**Figure 1 | CDK7 and BRD4 function in transcriptional regulation through distinct yet inter-connected roles.** CDK7, in association with TFIIH, is involved in transcription initiation through phosphorylation of the CTD of Pol II. BRD4, in association with Mediator, functions in transcription elongation through recruitment of P-TEFb.

cellular synergism. I describe below some of the underlying transcriptional mechanisms that may contribute to these observations, reviewing 1) transcriptional regulatory processes in normal cells and 2) transcriptional dysregulation and selected approaches that have been used for development of new therapeutics. I then discuss recent efforts to develop and understand the effects of inhibitors of general transcriptional regulators, and then finish with a discussion of transcriptional therapies employing combinations of drugs.

## **Transcriptional regulatory processes**

### *Overview*

During transcription initiation, transcription factors bind DNA regulatory regions called enhancers and interact with cofactors and the transcription initiation apparatus (Fuda et al., 2009; Jonkers and Lis, 2015; Adelman and Lis, 2012; Taatjes, 2010; Roeder, 2005; Conaway and Conaway, 2011). Cofactors, which include Mediator, BRD4 and P300, are typically defined as proteins involved in transcriptional regulation that do not bind DNA. The transcription initiation apparatus includes General Transcription Factors (also known as Basal Transcription Factors) and RNA Polymerase II (Pol II). The transcription initiation apparatus includes general transcription factors, such as the CDK7-containing TFIIF complex.

During transcription initiation, the carboxy terminal domain (CTD) of Pol II, which contains fifty-two heptad repeats (Tyr<sub>1</sub>-Ser<sub>2</sub>-Pro<sub>3</sub>-Thr<sub>4</sub>-Ser<sub>5</sub>-Pro<sub>6</sub>-Ser<sub>7</sub>), is



phosphorylated by CDK7 (a component of the General Transcription Factor TFIIF) on Serine 5, which stimulates the release of Pol II from promoters. Following promoter release, Pol II molecules typically transcribe 20-50 nucleotides and then pause (Sikorski and Buratowski, 2009; Fuda et al., 2009; Jonkers and Lis, 2015; Adelman and Lis, 2012). The release from pausing occurs through the action of the CDK9-containing complex, Positive Transcription Elongation Factor (P-TEFb), which is recruited to chromatin by BRD4. P-TEFb phosphorylates the Pol II CTD on Serine 2 as well as the pause control factors DSIF and NELF, resulting in productive elongation.

### *Transcription Factors and Enhancers*

Transcription factors (TFs) typically contain DNA-binding domains (DBDs) and activation domains. In mammalian cells, there are at least 23 different types of DBDs, with the most common domains containing zinc fingers, homeodomains, and helix-loop-helix motifs (Luscombe et al., 2000; Vaquerizas et al., 2009). The sequences bound by these DBDs usually span 6-10 basepairs. The activation domain is typically a separate domain that interacts with transcriptional cofactors such as Mediator or P300.

Enhancers contain clusters of TF binding sites (Bulger and Groudine, 2011; Calo and Wysocka, 2013; Carey, 1998; Lelli et al., 2012; Levine and Tijan, 2003; Maston et al., 2006; Ong and Corces, 2011; Panne, 2008; Spitz and Furlong, 2012). Enhancers generally span a few hundred base pairs to multiple kilobases (Bernstein et al., 2012; Heintzman et al., 2009; Thurman et al., 2012),

and in mammalian cells can operate over large distances (megabases) (Herz et al., 2014). The term enhancer was originally used to describe specific regulatory regions that contribute to developmental control, but is now more widely used to describe regulatory regions that influence the activity of specific genes.

Each cell type is thought to have a specific set of perhaps 10,000 or so active enhancers, and it has been estimated that mammalian cells have, in aggregate, a million enhancers (Bernstein et al., 2012). Recent studies have revealed that clustered enhancers bound by unusually high levels of the transcription apparatus, called super-enhancers, regulate genes with prominent roles in cell identity (Whyte et al., 2013; Parker et al., 2013; Hnisz et al., 2013).

Transcription factors make homotypic and heterotypic interactions with other transcription factors and co-regulators. Interactions involving TFs with other proteins and DNA are typically cooperative, such that binding affinities are enhanced in the presence of other protein-protein and protein-DNA interactions (Giese et al., 1995; Kim and Maniatis, 1997; Thanos and Maniatis, 1995). Cooperative binding allows for synergistic transcriptional outputs in response to signals without proportional changes in TF concentration (Ptashne, 2014). Crystallography revealed these cooperative interactions at the *IFNB1* locus, in which molecules of ATF2/c-JUN, IRF3/IRF7, and NFκB were bound in concert to the enhancer, forming what is called an “enhancesome” structure (Panne et al., 2007).

### *Cofactors*

Transcriptional cofactors, which include Mediator, BRD4 and P300, are proteins that play important roles in transcriptional regulation but do not bind DNA directly. These proteins and their functions have been reviewed extensively elsewhere (Taatjes, 2010; Roeder, 2005; Conaway and Conaway, 2011; Lee and Workman, 2007; Ferri et al., 2016), so I will focus comments briefly only on BRD4, which is targeted in experiments described here.

First co-purified with the Mediator co-activator complex, BRD4 is a member of the Bromodomain and Extra Terminal domain (BET) family involved in transcriptional activation (Jiang et al., 1998; Ferri et al., 2016). BRD4 contains N-terminal bromodomains that recognize acetylated lysine residues on histone tails and other proteins. Post-translational modification of lysine residues on histones play regulatory roles in transcription. Acetylated histones are typically associated with active transcription, due to increased chromatin accessibility. Consistently, ChIP-seq studies showed that BRD4 co-occupies the genome at promoters and enhancers of active genes (Loven et al., 2013). BRD4 directly interacts with the PTEFb kinase CDK9 and is required for PTEFb recruitment and pause release (Jang et al., 2005; Yang et al., 2005).

### *Transcription initiation apparatus*

The transcription initiation apparatus consists of the promoter-associated General Transcription Factors (TFIIA, B, D, E, F and H) and RNA Polymerase II. This apparatus has been reviewed extensively (Sikorski and Buratowski, 2009;

Sainsbury et al., 2015; Lee and Young, 2000), so I will focus discussion on TFIIH, which contains CDK7.

TFIIH is a multi-subunit complex that functions in transcription and DNA repair (Compe and Egly, 2012). ATP-dependent helicase activity of TFIIH subunit XPB facilitates promoter opening during transcription initiation. CDK7, Cyclin H, and co-factor MAT1 form the CDK-activating complex (CAK) that associates with core TFIIH. CAK has functions in cell cycle control, through T-loop phosphorylation of cyclin-dependent kinases, and transcription (Lolli and Johnson, 2005). The TFIIH subunits XPD and XPB both have helicase activity and are critical for nucleotide excision repair in response to DNA damage (Compe and Egly, 2016).

CDK7 appears to play roles in Pol II pausing and pause release (Laroche et al., 2012; Nilsson et al., 2015). CDK7 can phosphorylate, in addition to Pol II, the pausing factors DRB Sensitivity Inducing Factor (DSIF) and Negative Elongation Factor (NELF), thus facilitating Pol II retention at promoter-proximal pause sites. Productive elongation only occurs after phosphorylation of Pol II CTD on Serine 2 and DSIF by P-TEFb, as well as dissociation of NELF. CDK7, through its CAK activity, has also been shown to phosphorylate CDK9 for its full activation, suggesting a role for CDK7 in pause release. It is thought that the role of CDK7 in initiation, pausing, and pause release by phosphorylating substrates critical to each of these processes creates an incoherent feedforward loop (IFFL), where the input signal both activates and inhibits the output (Alon, 2007). It is thought that the IFFL network motif causes a time delay and, in this

case, may create a window for recruitment of factors involved in co-transcriptional RNA maturation processes. These factors, including capping enzyme and splicing factors, are recruited to phosphorylated CTD of Pol II, which acts as a binding platform. Loss of CDK7 activity is therefore expected to result in defects in promoter clearance, pausing, pause release, capping, and post-transcriptional processes (Glover-Cutter et al., 2009; Larochelle et al., 2012).

## **Transcriptional dysregulation and therapeutic approaches**

### *Overview*

Tumor cells often exhibit transcriptional dysregulation as a consequence of inappropriate expression of an early lineage master transcription factor and/or a loss of proper interactions with gene regulatory DNA. Drugs that target the nuclear hormone receptor (NHR) family of TFs have been among the most successful approaches for therapeutic treatment of transcriptional dysregulation (Bhagwat and Vakoc, 2015). Targeting other TFs have been challenging because they lack substrate or ligand-binding domains that can be bound by small molecules, and because some of the more frequent TF mutations in cancer involve loss of DNA binding by factors such as P53. New attempts to target TFs have often involved perturbing DNA-protein or protein-protein interactions, although these potential inhibitors tend to lack potency as only a few of them have achieved sub-micromolar potencies (Koehler, 2010).

### *Dysregulated master transcription factors drive oncogenic programs in cancer cells*

Cancer cells are often driven by oncogenic master TFs, which are usually lineage transcription factors that are normally expressed during early developmental stages. For example, T-ALLs originate from a developmental arrest in thymocyte development and, in 15-30% of cases, are caused by small intrachromosomal deletions that place the early lineage regulator TAL1 under transcriptional control of a highly expressed neighboring gene in T cells (Van Vlierberghe and Ferrando, 2012). TAL1 co-occupies regulatory regions of most active genes in T-ALL with other hematopoietic MTFs RUNX1, MYB, GATA3 (Sanda et al., 2008; Mansour et al., 2014).

### *TFs and aberrant interactions with other regulatory proteins*

Changes in protein-protein interactions involving TFs are prevalent during cancer pathogenesis. In promyelocytic leukemias (PMLs), over-expression of a fusion protein, PML-retinoic acid receptor alpha (RARA), results in inappropriate interactions with co-repressor complexes. These repressive complexes inhibit the expression of myeloid differentiation genes and arrest cells in an immature myeloid state (Rice and de The, 2014). Similarly, TAL1, an oncogenic TF in T-ALL, can induce leukemia through aberrant recruitment of the SIN3A co-repressor complex to genes normally activated by E47/HEB/P300 (O'Neil et al., 2004). In addition, a study assessing the leukemogenic activity of NOTCH1 found that regions within its transactivation domain were sufficient to induce T-ALLs in

100% of mice, suggesting that interactions with other co-regulators are critical for the transformative capability of NOTCH1 (Aster et al., 2000).

### *Mutations affecting DBDs*

Mutations altering the structure of transcription factor DBDs can change their binding affinity to DNA and thus contribute to a tumorigenic state (Joerger and Fersht, 2007). For example, mutations of the tumor suppressor *P53* are most commonly found in its DBD. The arginine 273 amino acid within the *P53* DBD makes direct contacts with DNA, and this interaction is weakened 700-1,000 times through the A273H somatic mutation (Ang et al., 2006). Mutations in residues that do not directly contact DNA can also affect DNA-binding affinity of transcription factors. The TGF- $\beta$  signaling effector TF SMAD4, which is mutated in pancreatic and colorectal cancers, binds DNA through a specific  $\beta$ -hairpin motif within its DBD. Two mutations, Y95N and N129K, that are located outside the  $\beta$ -hairpin motif, have been shown to abrogate SMAD4-DNA binding, likely from destabilization of the domain as a whole (Koyama et al., 1999; Jones and Kern, 2000). Mutations within the DBD of CCCTC-binding factor (CTCF), a widely expressed transcription factor with a vast array of targets, have been found in cancer (Filippova et al., 2002). These mutations alter the binding of CTCF to certain regulatory sequences, but not others, which results in aberrant expression of genes related to cell proliferation (*MYC*, *ARF*, *PIM1*, *PLK*, and *IGF2*) without affecting other targets. These examples demonstrate that mutations in DBDs affecting specific TF-DNA contacts can play critical roles in cancer pathogenesis.

### *Nuclear hormone receptors as targets in cancer therapy*

Nuclear hormone receptor (NHR) agonists and antagonists are among the most successful cancer drugs (Bhagwat and Vakoc, 2015). NHRs contain domains that are regulated by ligands, such as vitamins or hormones, and can be targeted through competitive binding of agonists or antagonists (Yan and Higgins, 2013). All-trans retinoic acid (ATRA) is a retinoic acid receptor agonist and has been used to treat acute PMLs, leading to clinical remission in 90% of patients (Lo-Coco et al., 2013). ATRA binds the PML-RARA ligand-binding domain and changes its conformation to interact with co-activators, rather than co-repressors, which results in terminal differentiation of the cells. Other NHRs have been successfully targeted in cancer through glucocorticoid receptor agonists (Inaba et al., 2010; Pui and Evan, 2006; Lonial et al., 2011), as well as estrogen receptor and androgen receptor antagonists (Huang et al., 2014; Carver, 2014; Howell 2006; Aragon-Ching 2014).

### *New approaches to target TFs*

Small molecules and peptide inhibitors have been used to disrupt TF protein-protein interactions. These PPIs usually involve large, flat interaction surfaces that lack well-defined hydrophobic binding pockets. Interaction surfaces often contain intrinsically-disordered regions that change conformation upon interaction with the dimerizing protein (Koehler, 2010). Small molecules can stabilize these intrinsically-disordered regions which prevents binding of the



interacting protein.

MYC dimerization with the TF MAX is required for its DNA binding, and chemical library screening has led to the identification of inhibitors that perturb this interaction (Berg et al., 2002; Koehler, 2010). These compounds have been shown to inhibit transcription driven by MYC in reporter assays as well as expression of its gene targets in cells. In addition, the MDM2 E3 ubiquitin ligase, that interacts with and degrades P53, has been targeted with compounds that disrupt this interaction, such as the small molecule RG7112, and are currently in clinical trials for liposarcoma and acute leukemia (Yan and Higgins, 2013). However, high effective concentrations ( $> 10 \mu\text{M}$ ) are required for most small molecules that inhibit TF PPIs. Peptide inhibitors have also been developed, but stability and permeability issues have limited this approach (Johnston and Carroll, 2015).

#### *Approaches to target specific transcription factor-DNA interactions*

Two main approaches have been used to target specific TF-DNA interactions and include small molecules and TF decoy oligonucleotides (Yan and Higgins, 2013). Some compounds, like mithramycin and anthracyclines, bind preferentially to G/C-rich DNA sequences and have been shown to compete for binding at promoters with transcription factors that have G/C-containing DNA-binding motifs, such as SP1 (Mansinlla and Portugal, 2008). In addition, polyamides containing N-methylpyrrole and N-methylimidazole can be designed to bind specific DNA sequences to sterically inhibit TF binding. For example, a

polyamide designed to bind sites recognized by the immune system TF NF- $\kappa$ B was able to block its binding to promoters of the genes *IL6* and *IL8* (Raskatov et al., 2012). This approach has been limited, however, since polyamides bind minor grooves of DNA, rather than major grooves where most TFs make specific contacts. Alternatively, oligonucleotides containing TF binding sites can be used as decoys to sequester them away from DNA. One such decoy oligonucleotide has been created for the TF STAT3 and is currently under clinical evaluation. This approach, however, has been limited due to low *in vivo* stability and inefficient delivery of oligonucleotides into nuclei (Yan and Higgins, 2013).

## **Developing inhibitors of general transcriptional regulators**

### *Overview*

Recent studies have revealed that tumor cells acquire exceptional “dependencies” on general transcriptional regulators such as MYC and dysregulated early lineage transcription factors. I review below the chemical probes and target proteins that have been used in these studies and briefly describe evidence that the dependencies are associated with super-enhancer-driven genes.

### *JQ1 is a competitive inhibitor of BRD4 with anti-tumor activity*

JQ1 is a thieno-triazolo-1,4-diazepine that inhibits BRD4 through competitive binding to the acetyl-lysine binding site of BET bromodomains (Filippakopoulos et al., 2010). Co-crystal structure and docking simulations

revealed hydrogen bonding and hydrophobic interactions with JQ1 and conserved and non-conserved residues within the acetyl-lysine binding pocket of BRD4. Selectivity profiling demonstrated selectivity toward BET bromodomains over other bromodomain families, with the highest affinity for BRD4 over other BET bromodomains. Fluorescence recovery after photobleaching (FRAP) experiments revealed displacement of BRD4 molecules from chromatin with JQ1 treatment, indicating inhibition of BRD4 in cells.

JQ1 and its effects have been studied in numerous tumor types, including aggressive cancers that are refractory to current chemotherapeutics (Ferri et al., 2016; Shi and Vakoc, 2014; Chapuy et al., 2013; Zuber et al., 2011; Dawson et al., 2011; Roderick et al., 2014; Knoechel et al., 2014; Ott et al., 2012; Mertz et al., 2011; Asangani et al., 2014; Shu et al., 2016). The foundational studies in Multiple Myeloma cells with JQ1 presented an unexpected finding – BRD4 inhibition resulted in selective and profound down-regulation of *MYC* (Delmore et al., 2011). The idea that inhibition of a general transcriptional regulator could result in gene-selective effects seemed counterintuitive. Subsequent investigation revealed that transcription of *MYC* was driven by an especially large super-enhancer in these cells (Loven et al., 2013), and BRD4 occupancy at this super-enhancer was found to be disproportionately sensitive to JQ1 treatment. Consistently, transcription elongation, as measured by the distribution of Pol II ChIP-seq signal across promoters and gene bodies, was reduced to a greater extent at the *MYC* gene than other genes. Furthermore, genome-wide loss in BRD4 signal following JQ1 treatments tended to be greater at enhancers with

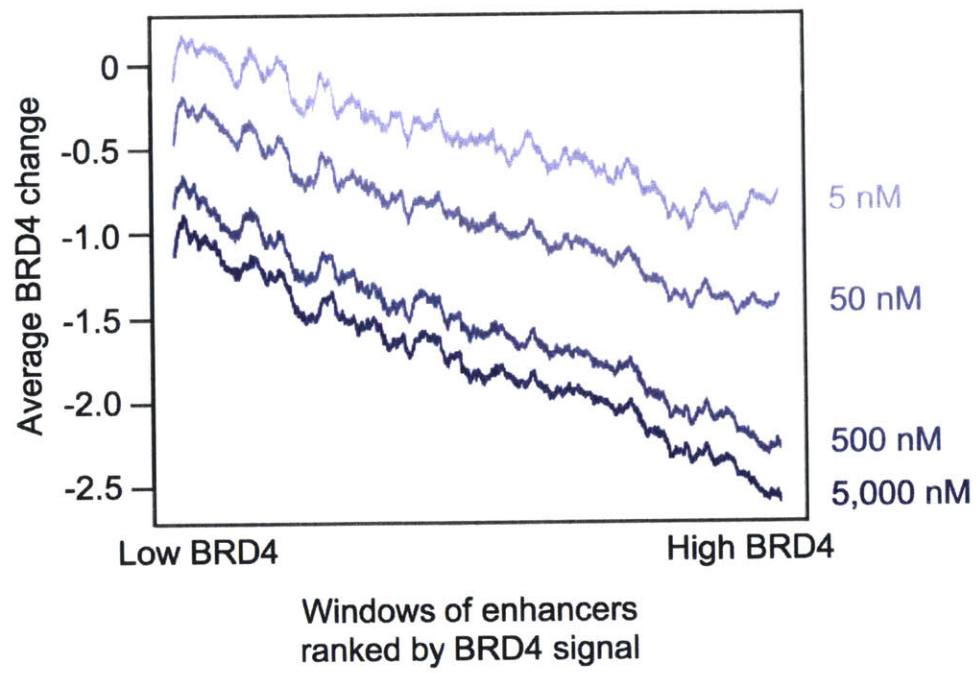


**Figure 2**

**Figure 2 | Enhancers with higher levels of BRD4 occupancy tend to be more sensitive to JQ1 treatment in Multiple Myeloma cells.** Enhancers in MM1.S cells were ranked based on levels of BRD4 ChIP-seq signal (x-axis) and average  $\log_2$  fold-changes in BRD4 occupancy following JQ1 treatment (5 nM, 50 nM, 500 nM, 5,000 nM) were plotted. Each data-point represents average change in signal for 200 enhancers.

higher BRD4 signal (Fig. 2). These results provided a mechanistic model to explain why BRD4 inhibition could produce gene-selective effects.

Since the development of JQ1 as a lead compound, Tensha Therapeutics has generated an optimized analogue, called TEN-010, which is currently in phase I/II clinical trials for multiple solid and hematological malignancies (NCT02308761; NCT01987362). Several BET bromodomain inhibitors, including I-BET762 (GSK; Nicodeme et al., 2010), OTX015 (Oncoethix - Merk; Coude et al., 2015), RVX-208 (Resverlogix; Bailey et al., 2010), I-BET151 (GSK; Dawson et al., 2011), and PFLI-1 (Pfizer; Picaud et al., 2013), have been developed in the academic and commercial sectors, which have triazolodiazepines structures or more dissimilar scaffolds. Currently, there are ~20 clinical trials with BET bromodomain inhibitors.

*THZ1 is a covalent inhibitor of CDK7 that has anti-proliferative effects in tumor cells*

THZ1 is a phenylaminopyrimidine that covalently interacts with a cysteine residue (C312) present outside the CDK7 kinase domain (Kwiatkowski et al., 2014). Selectivity among the CDKs is conferred through the unique presence of C312 on CDK7, but CDK12 and CDK13 also contain accessible cysteine residues and were shown to be reactive to THZ1 at high doses. Screening with a panel of ~1,500 cancer lines revealed that T-ALL cells were among the most sensitive to THZ1, with IC<sub>50</sub>s <250 nM. THZ1 treatment resulted in apoptotic responses in T-ALL cells. THZ1 treatment led to selective effects on critical T-ALL oncogenes, including the MTF *RUNX1*, which is hematopoietic TF normally

required for emergence of the first hematopoietic stem cells. *RUNX1* is an MTF in T-ALL cells and regulates most active genes with the core transcriptional regulatory circuit. Enhancer profiling revealed that *RUNX1* is associated with one of the largest SEs in T-ALL cells, and this SE was bound by CDK7. The profound down-regulation of *RUNX1* with THZ1 likely played key roles in the cellular response to THZ1 as its effects on gene expression phenocopied that with *RUNX1* shRNA knockdown. These results provided another example of exquisite sensitivity of tumor cells to inhibition of a GTR, presumably resulting from selective effects on critical SE-driven oncogenic MTFs (Kwiatkowski et al., 2014).

THZ1 has been shown to potently suppress the growth of tumor cells that currently lack targeted therapeutics, including *MYCN*-driven neuroblastoma (NB), small cell lung cancer (SCLC), and triple-negative breast cancer cells (TNBC) (Chipumuro et al., 2014; Christensen et al., 2014; Wang et al., 2015). SCLC is the most malignant subtype of lung cancer, and oncogenic drivers have not been well defined. THZ1 caused dramatic down-regulation of proto-oncogenes, such as *SOX2* and *NFB*, and lineage-specific TFs, such as *ASCL1*, that were shown to be associated with SEs and contribute to cellular responses to the inhibitor. TNBC cells were likewise found to be highly vulnerable to THZ1, likely due to down-regulation of a group of lineage-specific TFs and signaling factors. These studies further confirmed the susceptibility of tumor cells to CDK7 inhibition. Since the development of THZ1 as a lead compound, Syros Pharmaceuticals generated an optimized analogue SY-1365, and in April 2016 announced Phase

I/II clinical trials to commence during the first half of 2017 for acute myeloid leukemias (AMLs).

*Tumor cell super-enhancers drive aberrant transcriptional programs*

Super-enhancers that drive oncogenes are acquired by somatic alterations in cancer cells (Loven et al., 2013; Hnisz et al., 2013; Chapuy et al., 2013; Christensen et al., 2014; Chipumuro et al., 2014). Effector transcription factors of signaling pathways co-occupy enhancers with master TFs (Mullen et al., 2011), and inputs from these pathways have been shown converge at super-enhancers (Hnisz et al., 2015). For example, NOTCH1, the most commonly mutated gene in T-ALLs, co-occupies regulatory regions with T-ALL master TFs (unpublished data) and regulates the expression of genes critical to T-ALL biology, including *MYC* (Weng et al., 2006).

Cancer cells can acquire super-enhancers through a variety of genetic and non-genetic mechanisms. Disease-associated single nucleotide polymorphisms (SNPs) that are located in enhancer sequences can influence transcription factor binding, either increasing or decreasing affinity to DNA. For example, the rs6983267 risk variant on chromosome 8q24 lies within a binding site for the Wnt-pathway effector TF TCF4 and is associated with increased *MYC* expression. This variant creates a higher-affinity TCF4 binding site (GATGAAAGT to GATGAAAGG) that has 1.5-times greater transcriptional activity than wild-type sequences in reporter assays (Tuupanen et al., 2009). Furthermore, removing a region containing rs6983267 from a murine model of



colorectal cancer reduced the formation of cancerous polyps, demonstrating the importance of this SNP in tumorigenesis (Sur et al., 2012). In addition, genome sequencing projects have discovered focal amplification of enhancer regions, including those associated with *MYC* in multiple myeloma and *MYCN* in neuroblastomas. Super-enhancers can also drive oncogene expression through chromosomal translocations, as exemplified by *IGH* enhancer regions juxtaposed to *MYC* in Burkitt's lymphoma and in *IRF4* in multiple myeloma as well as enhancers juxtaposing *GFI* in medulloblastoma cells (Northcott et al., 2014). These SEs are critical for maintenance of oncogene expression as CRISPR/Cas9-mediated removal of regions results in decreased expression of oncogenes and tumor cell viability (Northcott et al., 2014). Cancer cells can also acquire super-enhancers that are absent in the cell-of-origin through non-genetic changes, including inappropriate re-activation of tissue-specific enhancers (Hnisz et al., 2013; Mansour et al., 2014).

#### *Cancer cells are dependent on high-level transcription of oncogenic TFs*

Since tumor cells possess addiction to oncogenes, they in turn appear to be addicted to GTRs that contribute to their high-level expression. In this way, cancer cells appear to possess “transcriptional addictions” or dependencies. A common theme is that oncogenic TFs that are highly vulnerable to GTR inhibition tend to be relatively short-lived, consistent with the requirement for super-enhancers to drive continuous, uninterrupted transcription (Fig. 3). This feature likely contributes to their sensitivity, as their steady-state expression levels will be

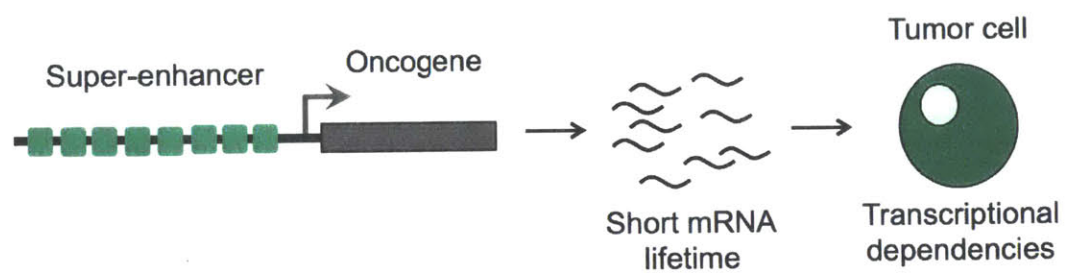


Figure 3

**Figure 3 | A model that explains tumor cell sensitivity to inhibitors of general transcriptional regulators involves super-enhancer association, the unstable nature of certain oncogenes, and tumor cell dependency on oncogenes.**

among the first to decline following GTR inhibitor administration. For example, *MYC* has one of the shortest mRNA half-lives in cells, predicted to be ~20 minutes. Furthermore, our studies estimated the mRNA half-life of *RUNX1* to be ~2 hours, as opposed to the ~7 hours reflecting the half-life of average mRNA molecules (unpublished). Taken together, SE association and the short-lived nature of oncogenic TFs contribute to their disproportionate sensitivity to GTR inhibitors.

### **Combination therapy**

In addition to JQ1 and THZ1, many other GTR inhibitors are either FDA-approved or in clinical or pre-clinical development. Collectively, these compounds inhibit various layers of transcriptional control, several of which have been shown to cause synergistic effects when treated together. Combination therapy is a critical aspect of current-day cancer therapeutics, and targeting multiple transcriptional regulators could be a method to inhibit multiple oncogenic programs as well as reduce outgrowth of resistant cells. In the next section, I explain the rationale for combination inhibition in cancer therapy and discuss the benefits of combining multiple GTR inhibitors. I also present examples of clinically relevant GTR inhibitors that have been previously shown to synergize with JQ1 and other BET inhibitors.

*Combination therapy is a way to reduce toxic side effects and the likelihood of resistance*

Combination therapy is becoming a gold standard in cancer treatment as it

can help lower doses necessary for treatment, limit the emergence of resistant clones, and inhibit multiple oncogenic processes at once (Fouquier and Guedj, 2015). Synergism between inhibitors results in disproportionate increases in efficacy and allows for decreased dosages and unwanted systemic toxicities. As an example, clinical usage of the DNA methyltransferase inhibitor 5-azacytidine was at first limited due to severe hematologic toxicity, but these effects were lessened when treated in combination with histone deacetylase inhibitors (Thurn et al., 2011). The Pol II inhibitor actinomycin D, which intercalates DNA and stabilizes the open complex intermediate, has been associated with detrimental side effects as monotherapy, but is currently used routinely in treating Wilm's tumor with other chemotherapeutic agents, vincristine and doxorubicin (Stellrecht and Chen, 2011; Malogolowkin et al., 2008). Furthermore, since cancer progression occurs through a step-wise multigenic process (Vogelstein, 2013), combination therapy allows for targeting of more than one of these events.

The major limitation of targeted therapeutics is the inevitable development of resistance (Lowe et al., 2004). The two main forms are: acquired resistance, which reflects adaptations to drug-imposed selective pressure, and primary resistance, which refers to cells that are inherently resistant to the drug. Combination therapy can reduce acquired resistance as there is a lower probability of developing adaptations to more agents than just one. Mutations that increase the activity of drug efflux pumps or render target proteins inaccessible to the drug are possible genetic mechanisms to acquire resistance. In addition, recent studies indicate that resistant clones can form

through changes in the transcriptional regulatory landscape. For example, although murine MLL-AF9 AML cells are normally sensitive to JQ1, prolonged sublethal doses resulted in JQ1-resistant cells that had normal expression levels of oncogenes, but these oncogenes were driven by alternative enhancers that had become active (Rathert et al., 2015; Fong et al., 2015). A new active enhancer, indicated by a focal gain in H3K27ac ChIP-seq signal, was observed near MYC, as well as loss of activity from a 3' enhancer known to drive *MYC* expression in JQ1-sensitive cells. Genes in the Wnt signaling pathway were up-regulated in JQ1-resistant cells, and transcriptional activity of the acquired enhancers were found to be dependent on the Wnt effector TF TCF4. These results demonstrate that plasticity in enhancer activity allowed for maintenance of expression of critical oncogenes, in the absence of BRD4, but through the action of a different transcriptional regulator. Furthermore, JQ1-resistant cells were found to be sensitive to small-molecule inhibition of the Wnt pathway.

Cells with primary resistance are inherently resistant to the drug, and these cells can outgrow as sensitive cells are diminished with the treatment. Within heterogenous population of tumor cells, those with primary resistance are likely driven by oncogenic programs that facilitate this insensitivity, and often represent cancer stem cells (Fong et al., 2015; Knoechel et al., 2014). Alternative enhancers can also facilitate resistance in these cells. The same Wnt-dependent enhancer was shown to drive expression of MYC in the primary resistant MLL-AF9 AML cells as with those that acquired resistance, and were found to represent leukemic stem cells (Rathert et al., 2015; Fong et al.,

2015). Cells with primary resistance to Notch pathway inhibitors were found to be leukemic stem cells in T-ALL (Knoechel et al., 2014,) and were instead sensitive to JQ1. These results show that fractions of heterogeneous tumor cell populations can be reliant on different transcriptional programs to maintain expression of key oncogenes. The combined use of multiple GTR inhibitors could thus be a way to suppress a larger fraction of cells if each one targets a specific “transcriptional dependency”.

In summary, combining multiple GTR inhibitors could reduce effective inhibitor doses, thus limiting off-target effects, and also decrease the chances of acquired and primary resistance. As I discuss in this thesis, it appears that different oncogenic TFs can be especially dependent on certain GTRs, so multiple GTR inhibitors could inhibit different oncogenic TFs. This strategy may therefore be a way to inhibit different oncogenic TFs within a given cell, as well as different cells within a heterogeneous population of tumor cells.

#### *Combination therapy with Pan-kinase inhibitors*

Kinase inhibitors that are potent against transcriptional CDKs CDK7 and CDK9 have been studied in the clinical setting for numerous cancers, but generally lack selectivity as they also can inhibit cell cycle CDKs to various degrees. JQ1 has been shown to synergize with Pan-kinase inhibitors that have activity for transcriptional CDKs, CDK7 and CDK9 (Baker et al., 2015). These inhibitors, including flavopiridol and dinaciclib, are competitive inhibitors for the ATP binding site. Flavopiridol, or alvocidib, has selectivity toward CDK9 over

CDK7 in in vitro kinase assays (IC<sub>50</sub>: CDK9, 6 nM; CDK7, 300 nM) and inhibits phosphorylation of Pol II CTD on Serine 5 and Serine 2, thus inhibiting transcription initiation and elongation. Flavopiridol was first used to treat refractory high-risk chronic lymphocytic leukemia (CLL), and its anti-tumor activity was attributed to inhibition of the transcriptional CDKs rather than cell cycle kinases as these cells have low levels of proliferation (Mariaule and Belmont, 2014; Stellrecht and Chen, 2011). Two issues arose in clinical trials that limited its clinical potential: 1) the drug bound plasma proteins, reducing its free concentration and requiring exorbitantly high doses, and 2) acute tumor lysis syndrome. However, flavopiridol was granted orphan drug status in 2014 for AML, and has been studied as a mono-therapy, and importantly, in combination with multiple chemotherapeutics. Dinaciclib is a pan-CDK inhibitor that also inhibits CDK9 to a greater extent than CDK7 (IC<sub>50</sub>: CDK9, 4 nM; CDK7, 70 nM) that has been shown to inhibit Pol II Serine 2 phosphorylation. It is currently in clinical trials as part of combination treatments for multiple tumor types, including Stage III-IV pancreatic cancer, multiple myeloma, and CLL (Mariaule and Belmont, 2014).

Both flavopiridol and dinaciclib have been evaluated in combination with JQ1 in osteosarcoma cells, and both combinations were shown to produce synergistic effects on cell proliferation and survival (Baker et al., 2015). Although the mechanistic basis of these synergistic effects are unknown, it is possible that functional interplay among CDK7, CDK9, and BRD4 plays a role. CDK7, CDK9, and BRD4 have all been shown to regulate gene-selective transcription programs



(Kanin et al., 2007; Garriga et al., 2010; Loven et al., 2010), but the extent to which they are overlapping require further study. However, CDK7, CDK9, and BRD4 have been shown to co-occupy super-enhancers, enhancers, and promoters (Loven et al., 2013; this thesis), and both BRD4 and CDK7 regulate CDK9 activity, through recruitment to chromatin and phosphorylation, respectively, so it is likely that the three proteins share a set of targets. Studies have also suggested that BRD4 possesses kinase activity for Pol II CTD on Serine 2 and that both CDK7 and CDK9 can regulate BRD4 through phosphorylation (Devaiah et al., 2012; Devaiah and Singer, 2012). Functionally, CDK7 generally plays a more distinct role in initiation as compared to BRD4 and CDK9 in elongation. Therefore, a combined and interdependent effect on one or more regulatory processes in transcription initiation and elongation likely contributes to the cellular synergism.

Most other GTR inhibitors target chromatin or epigenetic regulators that have catalytic domains, and more recently, bromodomains, in light of the success of BET inhibition. Chromatin regulators with catalytic activities can deposit or remove post-translational modifications on histone N-terminal tails, which affect local accessibility of chromatin to TFs and co-regulators, thus dictating activating or repressive transcriptional states of target genes.

#### *Combination therapy with BRD4 inhibitors*

Histone acetyltransferases (HATs) are transcriptional co-activators that acetylate lysine amino acids on histone tails and other nuclear proteins (Lee and

Workman, 2007). Acetylated lysine are associated with increased levels of transcription and are substrates for bromodomain-containing proteins, including BRD4. CBP and p300 are closely related HATs that acetylate histone tails and recruit TFs for transcriptional activation. Currently, multiple inhibitors have been developed that target the HAT catalytic domains, including CBP646, or bromodomains of CBP/p300, including I-CBP-112 and CBP30, and pre-clinical studies have demonstrated anti-proliferative effects in cancer cells, such as leukemias and prostate cancer (Picaud et al., 2015; Hay et al., 2014; Hammitzsch et al., 2015). Recently, inhibitors selective for bromodomains in CBP/p300 have been shown to have synergistic effects with JQ1 on human leukemia and primary T cell survival. This synergistic response could be due to down-regulation of targets shared by CBP/p300 and BRD4 as CBP/p300 activity generates substrates that can be bound by BRD4. Consistently, comparison of the transcriptional responses between CBP/p300 and BET inhibitors revealed an overlap in sensitive genes, including the anti-inflammatory cytokine *IL10* and the vascular cell adhesion protein 1 (*VCAM1*). However, despite both drugs primarily inhibiting inflammatory genes, CBP/p300 inhibition resulted in a smaller set of sensitive genes than JQ1 treatment. Although p300 and BRD4 co-occupy genomic sites (Roe et al., 2015), the bromodomains of BRD4 can interact with acetylated substrates that are deposited by HATs other than CBP/p300 (Filippakopoulos and Knapp, 2014) as there are at least 15 human proteins with HAT activity (Lee and Workman, 2007). However, inhibition of p300 catalytic activity with CBP646 resulted in decreased expression of MYC to similar extents

as BET bromodomain inhibition, and overall transcriptional changes phenocopies that with JQ1, suggesting that p300 and BRD4 are functionally interdependent (Roe et al., 2015). CBP646 decreased histone acetylation as well as BRD4 occupancy. This suggests that p300 and BRD4 operate together in regulating key oncogenes. Additionally, this differential sensitivity can be due to genes that are especially dependent on BRD4 as compared to p300. Synergy between HAT and BET inhibition could therefore result from combined inhibition of acetylase activity and acetyl-lysine interaction at genes in a combinatorial fashion.

The methyltransferase DOT1L catalyzes the addition of H3K79me2, which is typically associated with active transcription. DOT1L was first implicated in cancer pathogenesis when it was shown to interact with MLL fusion proteins in MLL-driven leukemias (Cai et al., 2015). Several members of the Super Elongation Complex, which also contains P-TEFb, are known fusion partners with MLL. EPZ-5676 is currently in Phase I clinical trials for pediatric patients with relapsed or refractory leukemias (AML and ALLs) and Myelodysplastic syndromes with MLL rearrangements (NCT02141828; NCT01684150). Recently, the SGC0946 and BET inhibitor I-BET were shown to cause synergistic effects in MLL-driven leukemias (Gilan et al., 2016). DOT1L and BRD4 were found part of distinct biochemical complexes, and SGC0946 and I-BET treatments resulted in largely different changes in the gene expression program, but for those sensitive to both inhibitors, DOT1L inhibition resulted in decreased BRD4 occupancy, which was demonstrated to be mediated by DOT1L recruitment of p300.

## **Conclusions**

Transcriptional mis-regulation is a ubiquitous feature in cancer. As direct effectors of aberrant transcriptional programs, transcription factors are ideal targets and drugging them usually involves inhibition of protein-DNA or protein-protein interactions. These approaches, however, have been challenging due to the large interaction surfaces necessary to inhibit and lack of obvious mimicable substrates. It is therefore not surprising that targeting nuclear hormone receptors with molecules against their ligand-binding domains have been the most successful transcription factor inhibition strategies.

General transcriptional co-regulators serve as promising targets because many of them contain enzymatic activities or ligand binding domains, allowing for the development of substrate analogues as inhibitors. These regulators are thought to function generally in transcriptional regulation in normal cells, which may limit the therapeutic window necessary for treatment. However, recent studies have demonstrated gene-selective effects with inhibitors of transcriptional co-regulators in cancer cells, due at least in part to the exquisite sensitivity of expression driven by super-enhancers to the drugs. Super-enhancers tend to drive critical oncogenes, including master transcription factors, and it is becoming increasingly apparent that several general transcriptional regulators preferentially occupy super-enhancers and that small-molecules against these regulators could be a way to selectively inhibit oncogene expression.

This thesis describes the development and characterization of one such

inhibitor – THZ1—that targets the TFIIH kinase CDK7. In addition, since combining inhibitors together can allow for reduced effective doses and limit the emergence of resistance, we combined THZ1 with an inhibitor targeting a different general transcriptional regulator, BRD4, with the small-molecule, JQ1. My work demonstrates the efficacy of transcriptional inhibitors in reducing tumor cell growth and supports the need for the development of additional transcriptional inhibitors.

## References

- Adelman, K., and Lis, J.T. (2012). Promoter-proximal pausing of RNA polymerase II: emerging roles in metazoans. *Nat Rev Genet* 13, 720-731.
- Alon, U. (2007). Network motifs: theory and experimental approaches. *Nat Rev Genet* 8, 450-461.
- Ang, H.C., Joerger, A.C., Mayer, S., and Fersht, A.R. (2006). Effects of common cancer mutations on stability and DNA binding of full-length p53 compared with isolated core domains. *J Biol Chem* 281, 21934-21941.
- Aragon-Ching, J.B. (2014). The evolution of prostate cancer therapy: targeting the androgen receptor. *Front Oncol* 4, 295.
- Asangani, I.A., Dommeti, V.L., Wang, X., Malik, R., Cieslik, M., Yang, R., Escara-Wilke, J., Wilder-Romans, K., Dhanireddy, S., Engelke, C., *et al.* (2014). Therapeutic targeting of BET bromodomain proteins in castration-resistant prostate cancer. *Nature* 510, 278-282.
- Aster, J.C., Xu, L., Karnell, F.G., Patriub, V., Pui, J.C., and Pear, W.S. (2000). Essential roles for ankyrin repeat and transactivation domains in induction of T-cell leukemia by notch1. *Mol Cell Biol* 20, 7505-7515.
- Bailey, D., Jahagirdar, R., Gordon, A., Hafiane, A., Campbell, S., Chatur, S., Wagner, G.S., Hansen, H.C., Chiacchia, F.S., Johansson, J., *et al.* (2010). RVX-208: a small molecule that increases apolipoprotein A-I and high-density lipoprotein cholesterol in vitro and in vivo. *J Am Coll Cardiol* 55, 2580-2589.
- Baker, E.K., Taylor, S., Gupte, A., Sharp, P.P., Walia, M., Walsh, N.C., Zannettino, A.C., Chalk, A.M., Burns, C.J., and Walkley, C.R. (2015). BET inhibitors induce apoptosis through a MYC independent mechanism and synergise with CDK inhibitors to kill osteosarcoma cells. *Sci Rep* 5, 10120.
- Berg, T., Cohen, S.B., Desharnais, J., Sonderegger, C., Maslyar, D.J., Goldberg, J., Boger, D.L., and Vogt, P.K. (2002). Small-molecule antagonists of Myc/Max dimerization inhibit Myc-induced transformation of chicken embryo fibroblasts. *Proceedings of the National Academy of Sciences of the United States of America* 99, 3830-3835.
- Bhagwat, A.S., and Vakoc, C.R. (2015). Targeting Transcription Factors in Cancer. *Trends Cancer* 1, 53-65.

Brien, G.L., Valerio, D.G., and Armstrong, S.A. (2016). Exploiting the Epigenome to Control Cancer-Promoting Gene-Expression Programs. *Cancer cell* 29, 464-476.

Bulger, M., and Groudine, M. (2011). Functional and mechanistic diversity of distal transcription enhancers. *Cell* 144, 327-339.

Cai, S.F., Chen, C.W., and Armstrong, S.A. (2015). Drugging Chromatin in Cancer: Recent Advances and Novel Approaches. *Molecular cell* 60, 561-570.

Calo, E., and Wysocka, J. (2013). Modification of enhancer chromatin: what, how, and why? *Molecular cell* 49, 825-837.

Cancer Genome Atlas Research, N. (2013). Genomic and epigenomic landscapes of adult de novo acute myeloid leukemia. *N Engl J Med* 368, 2059-2074.

Carey, M. (1998). The enhanceosome and transcriptional synergy. *Cell* 92, 5-8.

Carver, B.S. (2014). Strategies for targeting the androgen receptor axis in prostate cancer. *Drug Discov Today* 19, 1493-1497.

Chapuy, B., McKeown, M.R., Lin, C.Y., Monti, S., Roemer, M.G., Qi, J., Rahl, P.B., Sun, H.H., Yeda, K.T., Doench, J.G., *et al.* (2013). Discovery and characterization of super-enhancer-associated dependencies in diffuse large B cell lymphoma. *Cancer cell* 24, 777-790.

Christensen, C.L., Kwiatkowski, N., Abraham, B.J., Carretero, J., Al-Shahrour, F., Zhang, T., Chipumuro, E., Herter-Sprie, G.S., Akbay, E.A., Altabef, A., *et al.* (2014). Targeting transcriptional addictions in small cell lung cancer with a covalent CDK7 inhibitor. *Cancer cell* 26, 909-922.

Compe, E., and Egly, J.M. (2012). TFIIH: when transcription met DNA repair. *Nat Rev Mol Cell Biol* 13, 343-354.

Compe, E., and Egly, J.M. (2016). Nucleotide Excision Repair and Transcriptional Regulation: TFIIH and Beyond. *Annu Rev Biochem* 85, 265-290.

Conaway, R.C., and Conaway, J.W. (2011). Function and regulation of the Mediator complex. *Curr Opin Genet Dev* 21, 225-230.

Consortium, E.P. (2012). An integrated encyclopedia of DNA elements in the human genome. *Nature* 489, 57-74.

Coude, M.M., Braun, T., Berrou, J., Dupont, M., Bertrand, S., Masse, A., Raffoux, E., Itzykson, R., Delord, M., Riveiro, M.E., *et al.* (2015). BET inhibitor OTX015 targets BRD2 and BRD4 and decreases c-MYC in acute leukemia cells. *Oncotarget* 6, 17698-17712.

Dawson, M.A., Prinjha, R.K., Dittmann, A., Giotopoulos, G., Bantscheff, M., Chan, W.I., Robson, S.C., Chung, C.W., Hopf, C., Savitski, M.M., *et al.* (2011). Inhibition of BET recruitment to chromatin as an effective treatment for MLL-fusion leukaemia. *Nature* 478, 529-533.

Delmore, J.E., Issa, G.C., Lemieux, M.E., Rahl, P.B., Shi, J., Jacobs, H.M., Kastiris, E., Gilpatrick, T., Paranal, R.M., Qi, J., *et al.* (2011). BET bromodomain inhibition as a therapeutic strategy to target c-Myc. *Cell* 146, 904-917.

Devaiah, B.N., Lewis, B.A., Cherman, N., Hewitt, M.C., Albrecht, B.K., Robey, P.G., Ozato, K., Sims, R.J., 3rd, and Singer, D.S. (2012). BRD4 is an atypical kinase that phosphorylates serine2 of the RNA polymerase II carboxy-terminal domain. *Proceedings of the National Academy of Sciences of the United States of America* 109, 6927-6932.

Devaiah, B.N., and Singer, D.S. (2012). Cross-talk among RNA polymerase II kinases modulates C-terminal domain phosphorylation. *J Biol Chem* 287, 38755-38766.

Ferri, E., Petosa, C., and McKenna, C.E. (2016). Bromodomains: Structure, function and pharmacology of inhibition. *Biochem Pharmacol* 106, 1-18.

Filippakopoulos, P., and Knapp, S. (2014). Targeting bromodomains: epigenetic readers of lysine acetylation. *Nat Rev Drug Discov* 13, 337-356.

Filippakopoulos, P., Qi, J., Picaud, S., Shen, Y., Smith, W.B., Fedorov, O., Morse, E.M., Keates, T., Hickman, T.T., Felletar, I., *et al.* (2010). Selective inhibition of BET bromodomains. *Nature* 468, 1067-1073.

Filippova, G.N., Qi, C.F., Ulmer, J.E., Moore, J.M., Ward, M.D., Hu, Y.J., Loukinov, D.I., Pugacheva, E.M., Klenova, E.M., Grundy, P.E., *et al.* (2002). Tumor-associated zinc finger mutations in the CTCF transcription factor selectively alter its DNA-binding specificity. *Cancer Res* 62, 48-52.

Fong, C.Y., Gilan, O., Lam, E.Y., Rubin, A.F., Ftouni, S., Tyler, D., Stanley, K., Sinha, D., Yeh, P., Morison, J., *et al.* (2015). BET inhibitor resistance emerges from leukaemia stem cells. *Nature* 525, 538-542.

Foucquier, J., and Guedj, M. (2015). Analysis of drug combinations: current methodological landscape. *Pharmacol Res Perspect* 3, e00149.

Fuda, N.J., Ardehali, M.B., and Lis, J.T. (2009). Defining mechanisms that regulate RNA polymerase II transcription in vivo. *Nature* 461, 186-192.



Garriga, J., Xie, H., Obradovic, Z., and Grana, X. (2010). Selective control of gene expression by CDK9 in human cells. *J Cell Physiol* 222, 200-208.

Giese, K., Kingsley, C., Kirshner, J.R., and Grosschedl, R. (1995). Assembly and function of a TCR alpha enhancer complex is dependent on LEF-1-induced DNA bending and multiple protein-protein interactions. *Genes Dev* 9, 995-1008.

Gilan, O., Lam, E.Y., Becher, I., Lugo, D., Cannizzaro, E., Joberty, G., Ward, A., Wiese, M., Fong, C.Y., Ftouni, S., *et al.* (2016). Functional interdependence of BRD4 and DOT1L in MLL leukemia. *Nat Struct Mol Biol* 23, 673-681.

Glover-Cutter, K., Larochelle, S., Erickson, B., Zhang, C., Shokat, K., Fisher, R.P., and Bentley, D.L. (2009). TFIIH-associated Cdk7 kinase functions in phosphorylation of C-terminal domain Ser7 residues, promoter-proximal pausing, and termination by RNA polymerase II. *Mol Cell Biol* 29, 5455-5464.

Hammitzsch, A., Tallant, C., Fedorov, O., O'Mahony, A., Brennan, P.E., Hay, D.A., Martinez, F.O., Al-Mossawi, M.H., de Wit, J., Vecellio, M., *et al.* (2015). CBP30, a selective CBP/p300 bromodomain inhibitor, suppresses human Th17 responses. *Proceedings of the National Academy of Sciences of the United States of America* 112, 10768-10773.

Hay, D.A., Fedorov, O., Martin, S., Singleton, D.C., Tallant, C., Wells, C., Picaud, S., Philpott, M., Monteiro, O.P., Rogers, C.M., *et al.* (2014). Discovery and optimization of small-molecule ligands for the CBP/p300 bromodomains. *J Am Chem Soc* 136, 9308-9319.

Heintzman, N.D., Hon, G.C., Hawkins, R.D., Kheradpour, P., Stark, A., Harp, L.F., Ye, Z., Lee, L.K., Stuart, R.K., Ching, C.W., *et al.* (2009). Histone modifications at human enhancers reflect global cell-type-specific gene expression. *Nature* 459, 108-112.

Herz, H.M., Hu, D., and Shilatifard, A. (2014). Enhancer malfunction in cancer. *Molecular cell* 53, 859-866.

Hnisz, D., Abraham, B.J., Lee, T.I., Lau, A., Saint-Andre, V., Sigova, A.A., Hoke, H.A., and Young, R.A. (2013). Super-enhancers in the control of cell identity and disease. *Cell* 155, 934-947.

Hnisz, D., Schuijers, J., Lin, C.Y., Weintraub, A.S., Abraham, B.J., Lee, T.I., Bradner, J.E., and Young, R.A. (2015). Convergence of developmental and oncogenic signaling pathways at transcriptional super-enhancers. *Molecular cell* 58, 362-370.

Howell, A. (2006). Pure oestrogen antagonists for the treatment of advanced breast cancer. *Endocr Relat Cancer* 13, 689-706.

- Huang, B., Warner, M., and Gustafsson, J.A. (2015). Estrogen receptors in breast carcinogenesis and endocrine therapy. *Mol Cell Endocrinol* 418 Pt 3, 240-244.
- Inaba, H., and Pui, C.H. (2010). Glucocorticoid use in acute lymphoblastic leukaemia. *Lancet Oncol* 11, 1096-1106.
- Jang, M.K., Mochizuki, K., Zhou, M., Jeong, H.S., Brady, J.N., and Ozato, K. (2005). The bromodomain protein Brd4 is a positive regulatory component of P-TEFb and stimulates RNA polymerase II-dependent transcription. *Molecular cell* 19, 523-534.
- Jiang, Y.W., Veschambre, P., Erdjument-Bromage, H., Tempst, P., Conaway, J.W., Conaway, R.C., and Kornberg, R.D. (1998). Mammalian mediator of transcriptional regulation and its possible role as an end-point of signal transduction pathways. *Proceedings of the National Academy of Sciences of the United States of America* 95, 8538-8543.
- Joerger, A.C., and Fersht, A.R. (2007). Structure-function-rescue: the diverse nature of common p53 cancer mutants. *Oncogene* 26, 2226-2242.
- Johnston, S.J., and Carroll, J.S. (2015). Transcription factors and chromatin proteins as therapeutic targets in cancer. *Biochim Biophys Acta* 1855, 183-192.
- Jones, J.B., and Kern, S.E. (2000). Functional mapping of the MH1 DNA-binding domain of DPC4/SMAD4. *Nucleic Acids Res* 28, 2363-2368.
- Jonkers, I., and Lis, J.T. (2015). Getting up to speed with transcription elongation by RNA polymerase II. *Nat Rev Mol Cell Biol* 16, 167-177.
- Kanin, E.I., Kipp, R.T., Kung, C., Slattery, M., Viale, A., Hahn, S., Shokat, K.M., and Ansari, A.Z. (2007). Chemical inhibition of the TFIIH-associated kinase Cdk7/Kin28 does not impair global mRNA synthesis. *Proceedings of the National Academy of Sciences of the United States of America* 104, 5812-5817.
- Kim, T.K., and Maniatis, T. (1997). The mechanism of transcriptional synergy of an in vitro assembled interferon-beta enhanceosome. *Molecular cell* 1, 119-129.
- Knoechel, B., Roderick, J.E., Williamson, K.E., Zhu, J., Lohr, J.G., Cotton, M.J., Gillespie, S.M., Fernandez, D., Ku, M., Wang, H., *et al.* (2014). An epigenetic mechanism of resistance to targeted therapy in T cell acute lymphoblastic leukemia. *Nat Genet* 46, 364-370.
- Koehler, A.N. (2010). A complex task? Direct modulation of transcription factors with small molecules. *Curr Opin Chem Biol* 14, 331-340.

Koyama, M., Ito, M., Nagai, H., Emi, M., and Moriyama, Y. (1999). Inactivation of both alleles of the DPC4/SMAD4 gene in advanced colorectal cancers: identification of seven novel somatic mutations in tumors from Japanese patients. *Mutat Res* 406, 71-77.

Kwiatkowski, N., Zhang, T., Rahl, P.B., Abraham, B.J., Reddy, J., Ficarro, S.B., Dastur, A., Amzallag, A., Ramaswamy, S., Tesar, B., *et al.* (2014). Targeting transcription regulation in cancer with a covalent CDK7 inhibitor. *Nature* 511, 616-620.

Larochelle, S., Amat, R., Glover-Cutter, K., Sanso, M., Zhang, C., Allen, J.J., Shokat, K.M., Bentley, D.L., and Fisher, R.P. (2012). Cyclin-dependent kinase control of the initiation-to-elongation switch of RNA polymerase II. *Nat Struct Mol Biol* 19, 1108-1115.

Lee, K.K., and Workman, J.L. (2007). Histone acetyltransferase complexes: one size doesn't fit all. *Nat Rev Mol Cell Biol* 8, 284-295.

Lee, T.I., and Young, R.A. (2013). Transcriptional regulation and its misregulation in disease. *Cell* 152, 1237-1251.

Lelli, K.M., Slattery, M., and Mann, R.S. (2012). Disentangling the many layers of eukaryotic transcriptional regulation. *Annu Rev Genet* 46, 43-68.

Levine, M., and Tjian, R. (2003). Transcription regulation and animal diversity. *Nature* 424, 147-151.

Lo-Coco, F., Avvisati, G., Vignetti, M., Thiede, C., Orlando, S.M., Iacobelli, S., Ferrara, F., Fazi, P., Cicconi, L., Di Bona, E., *et al.* (2013). Retinoic acid and arsenic trioxide for acute promyelocytic leukemia. *N Engl J Med* 369, 111-121.

Lolli, G., and Johnson, L.N. (2005). CAK-Cyclin-dependent Activating Kinase: a key kinase in cell cycle control and a target for drugs? *Cell Cycle* 4, 572-577.

Lonial, S., Mitsiades, C.S., and Richardson, P.G. (2011). Treatment options for relapsed and refractory multiple myeloma. *Clin Cancer Res* 17, 1264-1277.

Loven, J., Hoke, H.A., Lin, C.Y., Lau, A., Orlando, D.A., Vakoc, C.R., Bradner, J.E., Lee, T.I., and Young, R.A. (2013). Selective inhibition of tumor oncogenes by disruption of super-enhancers. *Cell* 153, 320-334.

Lowe, S.W., Cepero, E., and Evan, G. (2004). Intrinsic tumour suppression. *Nature* 432, 307-315.

Luscombe, N.M., Austin, S.E., Berman, H.M., and Thornton, J.M. (2000). An overview of the structures of protein-DNA complexes. *Genome Biol* 1, REVIEWS001.

Malogolowkin, M., Cotton, C.A., Green, D.M., Breslow, N.E., Perlman, E., Miser, J., Ritchey, M.L., Thomas, P.R., Grundy, P.E., D'Angio, G.J., *et al.* (2008). Treatment of Wilms tumor relapsing after initial treatment with vincristine, actinomycin D, and doxorubicin. A report from the National Wilms Tumor Study Group. *Pediatr Blood Cancer* 50, 236-241.

Mansilla, S., and Portugal, J. (2008). Sp1 transcription factor as a target for anthracyclines: effects on gene transcription. *Biochimie* 90, 976-987.

Mansour, M.R., Abraham, B.J., Anders, L., Berezovskaya, A., Gutierrez, A., Durbin, A.D., Etschin, J., Lawton, L., Sallan, S.E., Silverman, L.B., *et al.* (2014). Oncogene regulation. An oncogenic super-enhancer formed through somatic mutation of a noncoding intergenic element. *Science* 346, 1373-1377.

Mariaule, G., and Belmont, P. (2014). Cyclin-dependent kinase inhibitors as marketed anticancer drugs: where are we now? A short survey. *Molecules* 19, 14366-14382.

Maston, G.A., Evans, S.K., and Green, M.R. (2006). Transcriptional regulatory elements in the human genome. *Annu Rev Genomics Hum Genet* 7, 29-59.

Mertz, J.A., Conery, A.R., Bryant, B.M., Sandy, P., Balasubramanian, S., Mele, D.A., Bergeron, L., and Sims, R.J., 3rd (2011). Targeting MYC dependence in cancer by inhibiting BET bromodomains. *Proceedings of the National Academy of Sciences of the United States of America* 108, 16669-16674.

Nicodeme, E., Jeffrey, K.L., Schaefer, U., Beinke, S., Dewell, S., Chung, C.W., Chandwani, R., Marazzi, I., Wilson, P., Coste, H., *et al.* (2010). Suppression of inflammation by a synthetic histone mimic. *Nature* 468, 1119-1123.

Nilson, K.A., Guo, J., Turek, M.E., Brogie, J.E., Delaney, E., Luse, D.S., and Price, D.H. (2015). THZ1 Reveals Roles for Cdk7 in Co-transcriptional Capping and Pausing. *Molecular cell* 59, 576-587.

Northcott, P.A., Lee, C., Zichner, T., Stutz, A.M., Erkek, S., Kawauchi, D., Shih, D.J., Hovestadt, V., Zapatka, M., Sturm, D., *et al.* (2014). Enhancer hijacking activates GFI1 family oncogenes in medulloblastoma. *Nature* 511, 428-434.

O'Neil, J., Shank, J., Cusson, N., Murre, C., and Kelliher, M. (2004). TAL1/SCL induces leukemia by inhibiting the transcriptional activity of E47/HEB. *Cancer cell* 5, 587-596.

Ong, C.T., and Corces, V.G. (2011). Enhancer function: new insights into the regulation of tissue-specific gene expression. *Nat Rev Genet* 12, 283-293.

Ott, C.J., Kopp, N., Bird, L., Paranal, R.M., Qi, J., Bowman, T., Rodig, S.J., Kung, A.L., Bradner, J.E., and Weinstock, D.M. (2012). BET bromodomain inhibition targets both c-Myc and IL7R in high-risk acute lymphoblastic leukemia. *Blood* 120, 2843-2852.

Panne, D. (2008). The enhanceosome. *Curr Opin Struct Biol* 18, 236-242.

Panne, D., Maniatis, T., and Harrison, S.C. (2007). An atomic model of the interferon-beta enhanceosome. *Cell* 129, 1111-1123.

Parker, S.C., Stitzel, M.L., Taylor, D.L., Orozco, J.M., Erdos, M.R., Akiyama, J.A., van Bueren, K.L., Chines, P.S., Narisu, N., Program, N.C.S., *et al.* (2013). Chromatin stretch enhancer states drive cell-specific gene regulation and harbor human disease risk variants. *Proceedings of the National Academy of Sciences of the United States of America* 110, 17921-17926.

Picaud, S., Fedorov, O., Thanasopoulou, A., Leonards, K., Jones, K., Meier, J., Olzscha, H., Monteiro, O., Martin, S., Philpott, M., *et al.* (2015). Generation of a Selective Small Molecule Inhibitor of the CBP/p300 Bromodomain for Leukemia Therapy. *Cancer Res* 75, 5106-5119.

Picaud, S., Wells, C., Felletar, I., Brotherton, D., Martin, S., Savitsky, P., Diez-Dacal, B., Philpott, M., Bountra, C., Lingard, H., *et al.* (2013). RVX-208, an inhibitor of BET transcriptional regulators with selectivity for the second bromodomain. *Proceedings of the National Academy of Sciences of the United States of America* 110, 19754-19759.

Ptashne, M. (2014). The chemistry of regulation of genes and other things. *J Biol Chem* 289, 5417-5435.

Pui, C.H., and Evans, W.E. (2006). Treatment of acute lymphoblastic leukemia. *N Engl J Med* 354, 166-178.

Raskatov, J.A., Meier, J.L., Puckett, J.W., Yang, F., Ramakrishnan, P., and Dervan, P.B. (2012). Modulation of NF-kappaB-dependent gene transcription using programmable DNA minor groove binders. *Proceedings of the National Academy of Sciences of the United States of America* 109, 1023-1028.

Rathert, P., Roth, M., Neumann, T., Muerdter, F., Roe, J.S., Muhar, M., Deswal, S., Cerny-Reiterer, S., Peter, B., Jude, J., *et al.* (2015). Transcriptional plasticity promotes primary and acquired resistance to BET inhibition. *Nature* 525, 543-547.

Rice, K.L., and de The, H. (2014). The acute promyelocytic leukaemia success story: curing leukaemia through targeted therapies. *J Intern Med* 276, 61-70.

Roderick, J.E., Tesell, J., Shultz, L.D., Brehm, M.A., Greiner, D.L., Harris, M.H., Silverman, L.B., Sallan, S.E., Gutierrez, A., Look, A.T., *et al.* (2014). c-Myc inhibition prevents leukemia initiation in mice and impairs the growth of relapsed and induction failure pediatric T-ALL cells. *Blood* 123, 1040-1050.

Roe, J.S., Mercan, F., Rivera, K., Pappin, D.J., and Vakoc, C.R. (2015). BET Bromodomain Inhibition Suppresses the Function of Hematopoietic Transcription Factors in Acute Myeloid Leukemia. *Molecular cell* 58, 1028-1039.

Roeder, R.G. (2005). Transcriptional regulation and the role of diverse coactivators in animal cells. *FEBS Lett* 579, 909-915.

Sainsbury, S., Bernecky, C., and Cramer, P. (2015). Structural basis of transcription initiation by RNA polymerase II. *Nat Rev Mol Cell Biol* 16, 129-143.

Sanda, T., Lawton, L.N., Barrasa, M.I., Fan, Z.P., Kohlhammer, H., Gutierrez, A., Ma, W., Tatarek, J., Ahn, Y., Kelliher, M.A., *et al.* (2012). Core transcriptional regulatory circuit controlled by the TAL1 complex in human T cell acute lymphoblastic leukemia. *Cancer cell* 22, 209-221.

Shi, J., and Vakoc, C.R. (2014). The mechanisms behind the therapeutic activity of BET bromodomain inhibition. *Molecular cell* 54, 728-736.

Shu, S., Lin, C.Y., He, H.H., Witwicki, R.M., Tabassum, D.P., Roberts, J.M., Janiszewska, M., Huh, S.J., Liang, Y., Ryan, J., *et al.* (2016). Response and resistance to BET bromodomain inhibitors in triple-negative breast cancer. *Nature* 529, 413-417.

Sikorski, T.W., and Buratowski, S. (2009). The basal initiation machinery: beyond the general transcription factors. *Curr Opin Cell Biol* 21, 344-351.

Spitz, F., and Furlong, E.E. (2012). Transcription factors: from enhancer binding to developmental control. *Nat Rev Genet* 13, 613-626.

Stellrecht, C.M., and Chen, L.S. (2011). Transcription inhibition as a therapeutic target for cancer. *Cancers (Basel)* 3, 4170-4190.

Sur, I.K., Hallikas, O., Vaharautio, A., Yan, J., Turunen, M., Enge, M., Taipale, M., Karhu, A., Aaltonen, L.A., and Taipale, J. (2012). Mice lacking a Myc enhancer that includes human SNP rs6983267 are resistant to intestinal tumors. *Science* 338, 1360-1363.

Taatjes, D.J. (2010). The human Mediator complex: a versatile, genome-wide regulator of transcription. *Trends Biochem Sci* 35, 315-322.

Thanos, D., and Maniatis, T. (1995). Virus induction of human IFN beta gene expression requires the assembly of an enhanceosome. *Cell* 83, 1091-1100.

Thurman, R.E., Rynes, E., Humbert, R., Vierstra, J., Maurano, M.T., Haugen, E., Sheffield, N.C., Stergachis, A.B., Wang, H., Vernot, B., *et al.* (2012). The accessible chromatin landscape of the human genome. *Nature* 489, 75-82.

Thurn, K.T., Thomas, S., Moore, A., and Munster, P.N. (2011). Rational therapeutic combinations with histone deacetylase inhibitors for the treatment of cancer. *Future Oncol* 7, 263-283.

Tuupanen, S., Turunen, M., Lehtonen, R., Hallikas, O., Vanharanta, S., Kivioja, T., Bjorklund, M., Wei, G., Yan, J., Niittymäki, I., *et al.* (2009). The common colorectal cancer predisposition SNP rs6983267 at chromosome 8q24 confers potential to enhanced Wnt signaling. *Nat Genet* 41, 885-890.

Van Vlierberghe, P., and Ferrando, A. (2012). The molecular basis of T cell acute lymphoblastic leukemia. *J Clin Invest* 122, 3398-3406.

Vaquerizas, J.M., Kummerfeld, S.K., Teichmann, S.A., and Luscombe, N.M. (2009). A census of human transcription factors: function, expression and evolution. *Nat Rev Genet* 10, 252-263.

Villicana, C., Cruz, G., and Zurita, M. (2014). The basal transcription machinery as a target for cancer therapy. *Cancer Cell Int* 14, 18.

Vogelstein, B., Papadopoulos, N., Velculescu, V.E., Zhou, S., Diaz, L.A., Jr., and Kinzler, K.W. (2013). Cancer genome landscapes. *Science* 339, 1546-1558.

Wang, Y., Zhang, T., Kwiatkowski, N., Abraham, B.J., Lee, T.I., Xie, S., Yuzugullu, H., Von, T., Li, H., Lin, Z., *et al.* (2015). CDK7-dependent transcriptional addiction in triple-negative breast cancer. *Cell* 163, 174-186.

Weng, A.P., Millholland, J.M., Yashiro-Ohtani, Y., Arcangeli, M.L., Lau, A., Wai, C., Del Bianco, C., Rodriguez, C.G., Sai, H., Tobias, J., *et al.* (2006). c-Myc is an important direct target of Notch1 in T-cell acute lymphoblastic leukemia/lymphoma. *Genes Dev* 20, 2096-2109.

Whyte, W.A., Orlando, D.A., Hnisz, D., Abraham, B.J., Lin, C.Y., Kagey, M.H., Rahl, P.B., Lee, T.I., and Young, R.A. (2013). Master transcription factors and mediator establish super-enhancers at key cell identity genes. *Cell* 153, 307-319.

Yan, C., and Higgins, P.J. (2013). Drugging the undruggable: transcription therapy for cancer. *Biochim Biophys Acta* 1835, 76-85.

Yang, Z., Yik, J.H., Chen, R., He, N., Jang, M.K., Ozato, K., and Zhou, Q. (2005). Recruitment of P-TEFb for stimulation of transcriptional elongation by the bromodomain protein Brd4. *Molecular cell* 19, 535-545.

Zuber, J., Shi, J., Wang, E., Rappaport, A.R., Herrmann, H., Sison, E.A., Magoon, D., Qi, J., Blatt, K., Wunderlich, M., *et al.* (2011). RNAi screen identifies Brd4 as a therapeutic target in acute myeloid leukaemia. *Nature* 478, 524-528.



## Chapter 2: Targeting transcription regulation in cancer with a covalent CDK7 inhibitor

---

Nicholas Kwiatkowski<sup>1,2,3\*</sup>, Tinghu Zhang<sup>1,2\*</sup>, Peter B Rahl<sup>3</sup>, Brian J Abraham<sup>3</sup>, Jessica Reddy<sup>3,4</sup>, Scott B Ficarro<sup>1,2,5</sup>, Anahita Dastur<sup>6</sup>, Arnaud Amzallag<sup>6,7</sup>, Sridhar Ramaswamy<sup>6,7</sup>, Bethany Tesar<sup>8,9</sup>, Christopher R Jenkins<sup>10</sup>, Nancy M Hannett<sup>3</sup>, Douglas McMillin<sup>8,9</sup>, Takaomi Sanda<sup>11,12</sup>, Taebo Sim<sup>13</sup>, Nam Doo Kim<sup>14</sup>, Thomas Look<sup>11,15</sup>, Constantine Mitsiades<sup>8,9</sup>, Andrew P Weng<sup>10</sup>, Jennifer R Brown<sup>8,9</sup>, Cyril H. Benes<sup>6</sup>, Jarrod A Marto<sup>1,2,5</sup>, Richard A Young<sup>3,4</sup>, Nathanael S. Gray<sup>1,2</sup>

<sup>1</sup>Department of Cancer Biology, Dana-Farber Cancer Institute, Boston, MA 02115, USA. <sup>2</sup>Department of Biological Chemistry and Molecular Pharmacology, Harvard Medical School, Boston, MA 02115, USA. <sup>3</sup>Whitehead Institute for Biomedical Research, 9 Cambridge Center, Cambridge, MA 02142, USA. <sup>4</sup>Department of Biology, Massachusetts Institute of Technology, Cambridge, MA 02139, USA. <sup>5</sup>Blais Proteomics Center, Dana-Farber Cancer Institute, Boston, MA 02115, USA. <sup>6</sup>Department of Medicine Massachusetts General Hospital Cancer Center and Harvard Medical School, Charlestown, MA 02129, USA. <sup>7</sup>Broad Institute of MIT and Harvard, 7 Cambridge Center, Cambridge, MA 02142, USA. <sup>8</sup>Department of Medical Oncology, Dana-Farber Cancer Institute, Harvard Medical School, Boston, MA 02115, USA. <sup>9</sup>Department of Medicine, Brigham and Women's Hospital, Harvard Medical School, Boston, MA 02115, USA. <sup>10</sup>Terry Fox Laboratory, British Columbia Cancer Agency, Vancouver, British Columbia, Canada. <sup>11</sup>Department of Pediatric Oncology, Dana-Farber Cancer Institute, Harvard Medical School, Boston, MA 02215, USA. <sup>12</sup>Cancer Science Institute of Singapore, National University of Singapore, Singapore 117599. <sup>13</sup>Chemical Kinomics Research Center, Korea Institute of Science and Technology, 39-1, Hawolgok-dong, Seongbuk-gu, Seoul, 136-791, Korea / KU-KIST Graduate School of Converging Science and Technology, 145, Anam-ro, Seoul, Korea. <sup>14</sup>Daegu-Gyeongbuk Medical Innovation Foundation, 2387 dalgubeol-daero, Suseong-gu, Daegu, 706-010, Korea. <sup>15</sup>Division of Hematology/Oncology, Children's Hospital, Boston, MA 02115 USA. \*These authors contributed equally to this work.

This chapter originally appeared in *Nature* 2014 vol. 511 (7511). pp 616-620. Corresponding Supplemental Material is appended. Supplemental tables and methods are available online at <http://dx.doi.org/10.1038/nature13393>.

### **Personal contribution to the Project**

This work was a collaborative effort from the laboratories of Prof. Nathanael S. Gray and Prof. Richard A. Young. Tinghu Zhang performed chemical synthesis and small molecule structure determination. Nicholas Kwiatkowski, Pete B. Rahl, and I performed experimental biological research. Specifically, I helped develop the experimental design and conduct genomics experiments depicted in Figure 4. Brian J. Abraham performed computational analyses.

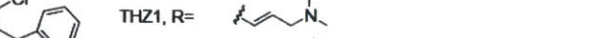
## Abstract

Tumor oncogenes include transcription factors that co-opt the general transcriptional machinery to sustain the oncogenic state, but direct pharmacological inhibition of transcription factors has thus far proven difficult. However, the transcriptional machinery contains various enzymatic co-factors that can be targeted for development of new therapeutic candidates, including cyclin-dependent kinases (CDKs). Here we present the discovery and characterization of the first covalent CDK7 inhibitor, THZ1, which has the unprecedented ability to target a remote cysteine residue located outside of the canonical kinase domain, providing an unanticipated means of achieving selectivity for CDK7. Cancer cell line profiling indicates that a subset of cancer cell lines, including T-ALL, exhibit exceptional sensitivity to THZ1. Genome-wide analysis in Jurkat T-ALL shows that THZ1 disproportionately affects transcription of *RUNX1* and suggests that sensitivity to THZ1 may be due to vulnerability conferred by the *RUNX1* super-enhancer and this transcription factor's key role in the core transcriptional regulatory circuitry of these tumor cells. Pharmacological modulation of CDK7 kinase activity may thus provide an approach to identify and treat tumor types exhibiting extreme dependencies on transcription for maintenance of the oncogenic state.

## Main text

In an effort to discover new inhibitors of kinases that regulate gene transcription, we performed cell-based screening and kinase selectivity profiling of a library of known and novel ATP-site directed kinase inhibitors (See Supplementary Table 1 for known CDK7 inhibitors). We identified THZ1 (Fig. 1a), a phenylaminopyrimidine bearing a potentially cysteine-reactive acrylamide moiety, as a low nanomolar inhibitor of cell proliferation and biochemical CDK7 activity (Fig. 1b, c). To investigate the functional relevance of the acrylamide moiety we prepared a non-cysteine reactive analog THZ1-R, which displayed diminished activity for CDK7 and reduced antiproliferative potency (Fig. 1b, c). KiNativ<sup>TM</sup> profiling (Patricelli et al., 2007), which measures the ability of a compound to block nucleotide-dependent enzymes from biotinylation with a reactive desthiobiotin-ATP probe, established CDK7 as the primary intracellular target of THZ1, but not of THZ1-R (Supplementary Table 2). Kinome-wide profiling identified additional kinase targets of THZ1; however, we confirmed CDK7 as the only target displaying time-dependent inhibition, which is suggestive of covalent binding (Supplementary Fig. 1a-c and Table 3).

As no covalent inhibitors of CDKs have been reported, we next focused our studies on the mechanism by which THZ1 could achieve covalent inhibition of CDK7. We first incubated recombinant CDK7/cyclin H/MAT1 trimeric complex with a biotinylated version of THZ1 (bio-THZ1, Fig. 1a) and demonstrated that it



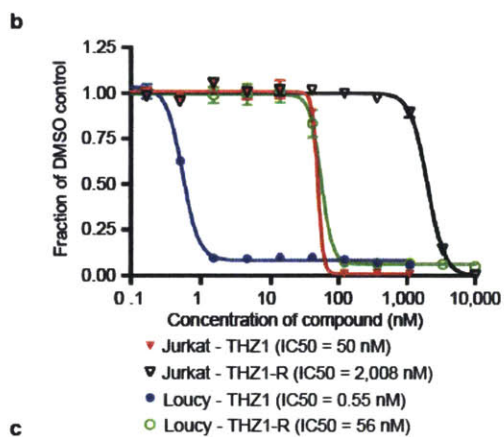


### Figure 1

**Figure 1 | Cell-based screening and kinome profiling identifies phenylamino-pyrimidines as a potential CDK7 scaffold.** **a**, Compound structures of THZ1, THZ1-R, and bio-THZ1. **b**, THZ1 potently inhibits proliferation of Jurkat and Loucy T-ALL cell lines. Cell lines were treated with THZ1 or THZ1-R for 72 hrs. Experiments were performed in biological triplicates and error bars are +/- SD. **c**, THZ1 and THZ1-R have different binding affinities for CDK7. LanthaScreen® Eu Kinase Binding assay was conducted at Life Technologies in a time-dependent manner. Here  $K_D$  values are shown following 180-minute incubation with compounds. Experiments were performed in biological triplicates and error bars are +/- SD.

indeed covalently modifies CDK7 (Fig. 2a; Supplementary Fig. 1d-g). Mass spectrometry identified the site of covalent modification as C312, a residue located outside the kinase domain (Supplementary Fig. 2a-d). Inspection of the crystal structure reveals that a C-terminal extension of CDK7 bearing C312 traverses the ATP cleft in the kinase domain and would be predicted to position Cys312 directly adjacent to the reactive acrylamide moiety of THZ1 (Fig. 2b). Mutation to serine (C312S), a less nucleophilic amino acid, prevented THZ1 from covalently binding to CDK7 and from inhibiting CDK7 activity in an irreversible fashion (Fig. 2c; Supplementary Fig. 2e). Sequence alignment of the 20-member CDK family suggests that Cys312 is unique to CDK7, however CDK12 and CDK13 also possess accessible cysteines within 4 amino acids of Cys312 (Supplementary Fig. 3a). Indeed, we found that THZ1 can inhibit CDK12 kinase activity at slightly higher concentrations (Supplementary Fig. 3b-f). THZ1 is the first inhibitor demonstrated to target a cysteine located outside of the kinase domain, which provides an unanticipated means of achieving covalent selectivity.

CDK7 kinase activity has been implicated in the regulation of both transcription, where it phosphorylates the C-terminal domain (CTD) of RNAP polymerase II (RNAPII) (Akhtar et al., 2009; Drapkin et al., 1996; Glover-Cutter et al., 2009) and CDK9 (Larochelle et al., 2012), and the cell cycle, where it functions as the CDK-activating kinase (CAK) for CDKs1/2/4/6 (Fisher and Morgan, 1994; Larochelle et al., 2007; Makela et al., 1994; Schachter et al., 2013; Solomon et al., 1992). THZ1, but not THZ1-R, completely inhibits the phosphorylation of the established intracellular CDK7 substrate RNAPII CTD at

Ser-5 and Ser-7 (Akhtar et al., 2009; Glover-Cutter et al., 2009), with concurrent loss of Ser-2 phosphorylation at 250 nM in Jurkat cells (Fig. 2d). Cellular washout experiments demonstrate that THZ1 indeed acts in an irreversible fashion (Fig. 2e, f; Supplementary Fig. 4a-e). We observed a loss of CAK activity, as evidenced by decreased phosphorylation of the activation loops of CDK1, 2 and 9, indicating disruption of both recognized CDK7 signaling pathways in Jurkat cells (Fig. 2d; Supplementary Fig. 4f, g) and Loucy cell lines (Supplementary Fig. 4). Ectopic expression of dox-inducible FLAG-CDK7 C312S, but not FLAG-CDK7 WT, in HeLa S3 cells restored RNAPII CTD p-Ser 5/7 to near WT levels at concentrations of THZ1 up to 2.5  $\mu$ M, establishing C312 as a critical determinant of the cellular pharmacology of the inhibitor (Supplementary Fig. 5a-b). Additionally, FLAG-CDK7 C312S expression restored CDK1/2 T-loop phosphorylation, reduced early induction of cleaved PARP and restored the expression of a subset of genes, including the highly – expressed transcription factors MYC, KLF4, ID1, and GATA2 (Supplementary Fig. 5c-e). The partial rescues of the hyperphosphorylated form of RNAPII (RNAPII0) and RNAPII p-Ser2 CTD phosphorylation combined with the incomplete restoration of gene expression may result, in part, from lower affinity cross-reactivity of THZ1 with CDK12/13, which are bona fide Ser2 kinases (Bartkowiak et al., 2010).

Our evidence that CDK7 inhibition leads to reduction in RNAPII CTD phosphorylation status appears in conflict with evidence that inhibition of CDK7



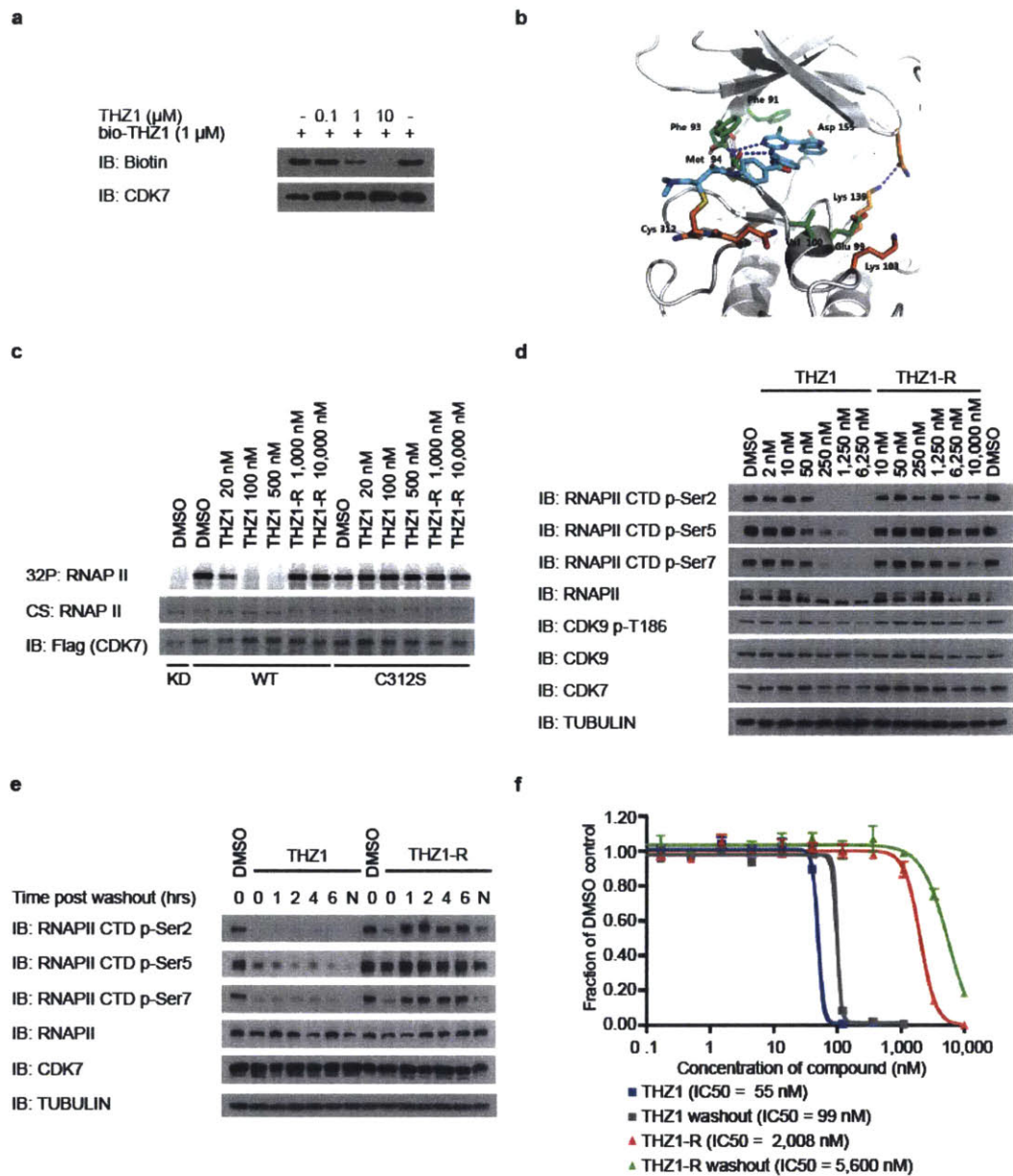


**Figure 2**

**Figure 2 | THZ1 irreversibly inhibits RNAPII CTD phosphorylation by covalently targeting a unique cysteine located outside the kinase domain of CDK7.** **a**, bio-THZ1 binds irreversibly to CDK7. Recombinant CAK complex was incubated with bio-THZ1 +/- THZ1 at 37°C for 4 hrs and biotinylated proteins were resolved by SDS-page. **b**, Docking model of THZ1 in the ATP-binding pocket of CDK7 (PDB code 1UA2). CDK7 depicted with grey ribbons and THZ1 in turquois. Key residues are indicated. C312 has been modeled into the crystal structure. **c**, Mutation of C312 to serine (C312S) rescues wild-type kinase activity in the presence of THZ1. HCT116 cells stably expressing FLAG-tagged CDK7 proteins were treated with THZ1 or THZ1-R for 4 hrs. Exogenous CDK7 proteins were immunoprecipitated with FLAG antibody and subjected to *in vitro* kinase assays. CS = coomassie stain. **d**, THZ1 inhibits RNAPII CTD phosphorylation. Jurkat cells were treated with THZ1 or THZ1-R for 4 hrs. and proteins of interest resolved by SDS page. **e**, THZ1, but not THZ1-R, shows irreversible inactivation of CDK7. Jurkat cells were treated with THZ1 or THZ1-R for 4 hrs followed by washout of inhibitor-containing medium. Cells were then allowed to grow in medium without inhibitor for 0 to 6 hrs. 'N' signifies cells where medium was never washed out (*ie* – 10 hr incubation with compounds). **f**, Antiproliferative effects of THZ1 are impervious to inhibitor washout. Jurkat cells were treated with THZ1 or THZ1-R in dose response format for 72 hrs. Experiments were performed in biological triplicates and error bars are +/- SD.

alone is insufficient to reduce RNAPII CTD phosphorylation in HCT116 cells (Larochelle et al., 2012). It is possible that covalent inhibition and reversible inhibition can engender different effects on kinase structure; we did not find evidence that THZ1 impacts TFIIH or CAK complex stability (Supplementary Fig. 4h). It is also possible that inhibition of CDK12/13 (or another undetected kinase) contributes to reduced RNAPII CTD phosphorylation, although our evidence that RNAPII CTD phosphorylation levels are restored following expression of CDK7 C312S suggests otherwise.

To better understand the breadth of antiproliferative activity of THZ1, we screened it against a diverse panel of over 1,000 cancer cell lines (Garnett et al., 2012). THZ1 displayed broad-based activity with  $IC_{50}$ s less than 200 nM against 53% of the cell lines tested (Fig. 3a; Supplementary Table 4). Elastic net regression analysis incorporating gene expression, copy number, and sequence variation genomics data (Garnett et al., 2012) across 527 of the cell lines tested were used to identify genomic features common to sensitive cell lines. Gene ontology (GO) term enrichment analysis (Huang et al., 2009) indicated a strong enrichment of (proto-)oncogenic transcription factors commonly overexpressed in cancer and factors involved in RNAPII -driven transcriptional regulation, suggesting the dominant activity of THZ1 was through modulation of transcription (Fig. 3b; Supplementary Table 5).

In agreement with the net elastic regression analysis, T-ALL cell lines that display characteristic misregulation of T-cell lineage-specific transcription factors,

were broadly sensitive to THZ1, but not THZ1-R (Fig. 3c; Supplementary Fig. 6a and Table 4). Treatment of T-ALL cell lines with THZ1 caused decreased cellular proliferation and an increase in apoptotic index with concomitant reduction in anti-apoptotic proteins, most notably MCL-1 and XIAP (Supplementary Fig. 6, 7). These strong antiproliferative responses induced at sub-effective doses of THZ1 suggest that these cells may be particularly sensitive to small perturbations in transcription and CDK7 kinase function. Indeed, THZ1 demonstrated efficacy against primary leukemia cells and in a bioluminescent xenografted model using the human T-ALL cell line, KOPTK1, when dosed twice daily (BID) at 10 mg/kg (Fig. 3d, e; Supplementary Fig. 8 and Table 6). Importantly, THZ1 was well tolerated at these doses with no observable body weight loss or behavioral changes (Supplementary Fig. 8f), suggesting no overt toxicity to the animals. These results were mirrored in cell culture with non-transformed BJ fibroblast and retinal pigment epithelial (RPE-1) cells responding to relatively high doses of THZ1 by undergoing cell cycle arrest rather than initiating apoptosis or cell death, further suggesting that normal cells might tolerate transcriptional disruption (Supplementary Fig. 9).

CDK7 is a component of the general transcription factor IIH (TFIIH) complex (Feaver et al., 1994; Serizawa et al., 1995; Shiekhataar et al., 1995), so we next investigated how THZ1 treatment affects genome-wide gene expression.

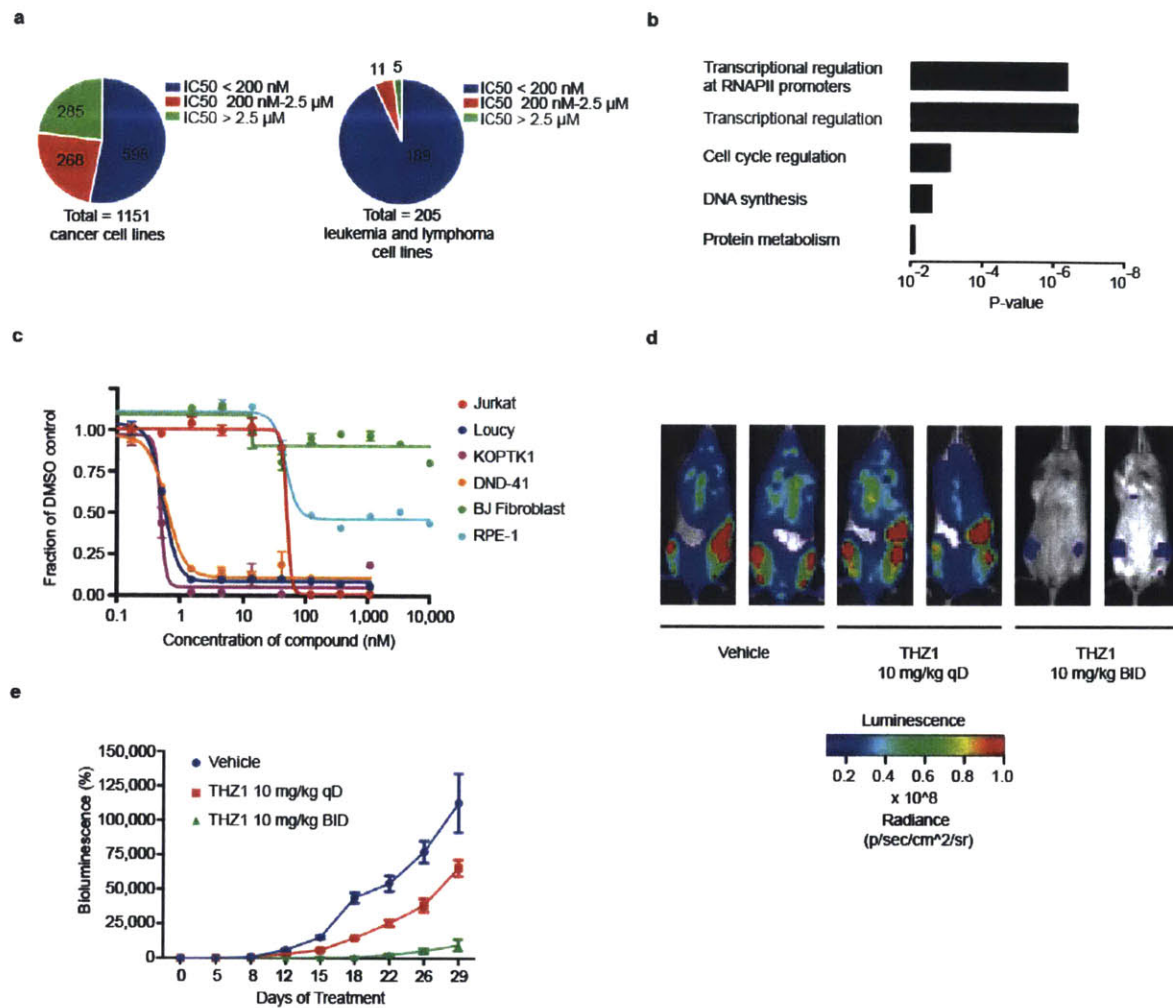


**Figure 3**

**Figure 3 | THZ1 strongly reduces the proliferation and cell viability of T-ALL cell lines.** **a**, THZ1 exhibits strong antiproliferative effect across a broad range of cancer cell lines from various cancer types. Cells were treated with THZ1 or DMSO vehicle for 72 hrs and assessed for antiproliferative effect using resazurin. **b**, Overexpression of transcriptional regulators, including (proto)oncogenic transcription factors, is a strong predictor of cell line sensitivity to THZ1. GO terms associated with overexpressed factors found in THZ1 –sensitive cell lines. **c**, THZ1 exhibits strong antiproliferative affect against T-ALL cell lines. BJ fibroblasts and RPE-1 cells are shown as normal cell lines. Cells were treated with THZ1 or DMSO vehicle for 72 hrs. Experiments were performed in biological triplicates and error bars are +/- SD. **d**, THZ1 reduces the proliferation of KOPTK1 T-ALL cells in a human xenograft mouse model. Bioluminescent images of two representative mice treated with either vehicle control, 10 mg/kg THZ1 qD (once daily), or 10 mg/kg/day THZ1 BID (twice daily) for 29 days. **e**, Relative bioluminescence (BLI) of mice treated with vehicle, 10 mg/kg THZ1 qD (once daily), or 10 mg/kg/day THZ1 BID (twice daily) during the 29 days of treatment. n=10 for all groups. Bioluminescence is shown relative to day 0 and is plotted as average  $\pm$  SEM. Analysis of the BLI data by repeated measures (RM) two-way ANOVA reveals the anti-proliferative effect of treatment with THZ1 BID is highly statistically significantly different ( $p < 0.0001$ ) as compared to the other treatments.

We chose Jurkat T-ALL for these studies because it is a well-studied T-ALL cell line model with a defined core transcriptional regulatory circuitry, consisting of key transcription factors, which is also found in human T-ALL primagrafts (Sanda et al., 2012). Treatment with 250 nM THZ1, but not THZ1-R, led to progressive reduction in global steady-state mRNA levels over time, with 75% and 96% of mRNAs showing greater than 2-fold reduction by 6 and 12 hrs, respectively (Fig. 4a, Supplementary Fig. 10a and Table 7). Consistent with global downregulation of mRNA transcripts, 250 nM THZ1 reduced RNAPII occupancy genome-wide at both promoters and gene bodies (Fig. 4b). By comparison, Flavopiridol reduced RNAPII density across only gene bodies (Fig. 4b). This is consistent with the model that CDK7 regulates RNAPII initiation and pausing while CDK9 regulates pause release leading to processive elongation (Feaver et al., 1994; Glover-Cutter et al., 2009; Larochelle et al., 2012; Rahl et al., 2010; Serizawa et al., 1995; Shiekhata et al., 1995; Watanabe et al., 2000; Yamada et al., 2006).

Although 250 nM THZ1 inhibits global transcription, we found that some cancer cell lines, particularly T-ALL, are sensitive to considerably lower concentrations of THZ1. We postulated that the expression of certain genes might be especially sensitive to low doses of THZ1 and therefore have a key role in driving the cellular response. Indeed, we found that transcripts for only a subset of genes were substantially affected by treatment with 50 nM THZ1, with that for RUNX1 among the most profoundly affected (Fig. 4c). There are at least two reasons that low dose THZ1 treatment might cause a preferential loss of RUNX1 expression. Tumor cell oncogenes can acquire super-enhancers,

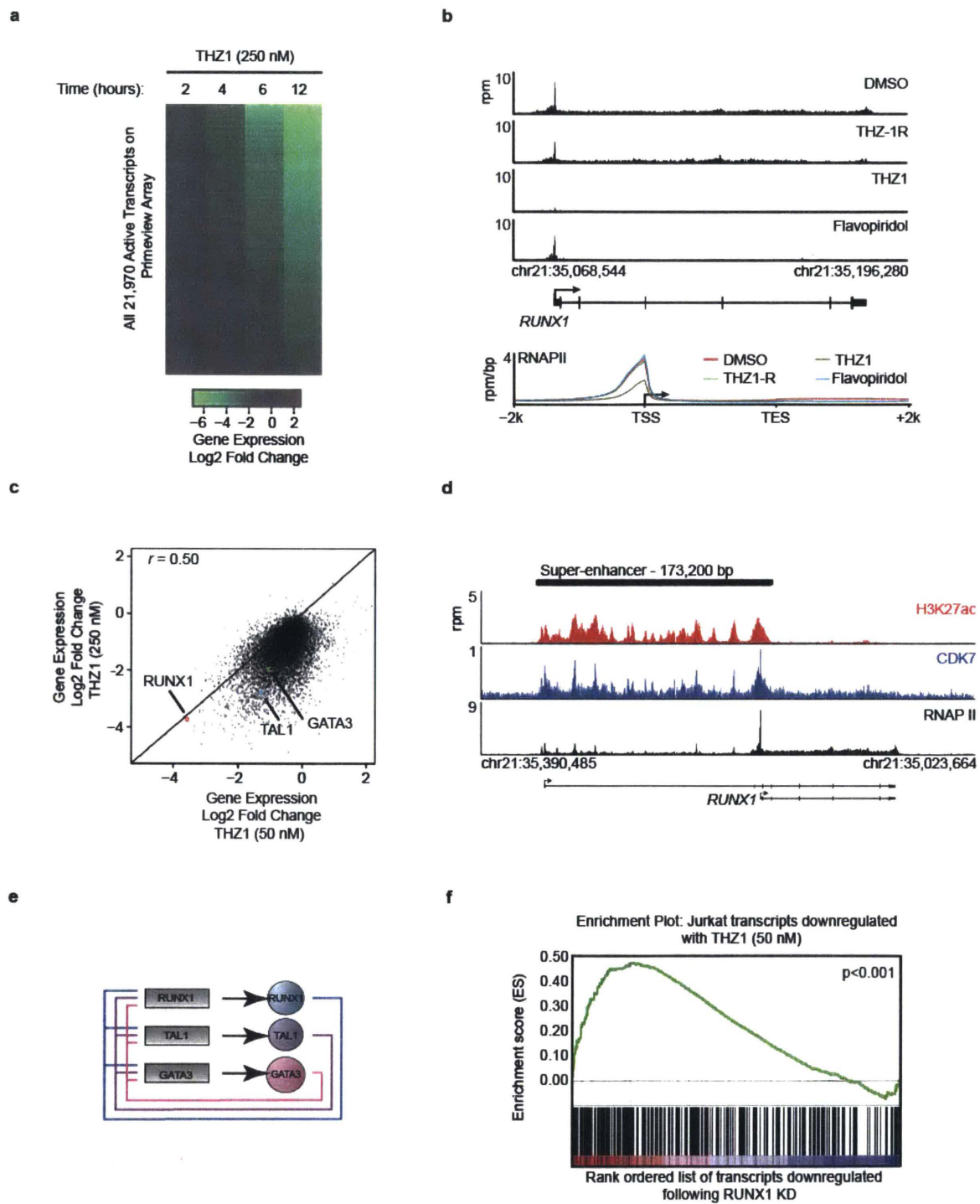


**Figure 4**



**Figure 4 | THZ1 preferentially downregulates Jurkat core transcriptional circuitry.** **a**, THZ1 treatment globally downregulates steady-state mRNA levels in a time-dependent manner. Jurkat cells were treated with THZ1 (250 nM) for the indicated amounts of time. Heatmaps display the Log2 fold change in gene expression vs. DMSO for the 21,970 transcripts expressed at 12h in DMSO. **b**, THZ1 reduces RNAPII occupancy across promoters and gene bodies. Metagene representation of global RNAPII occupancy at promoters and gene bodies (top). Average background subtracted ChIP-seq signal in 22,310 genes expressed in 6h DMSO conditions in units of rpm/bp. Gene tracks of RNAPII ChIP-seq occupancy at *RUNX1* following the indicated treatments (bottom). Signal of ChIP-seq occupancy is in units of reads per million (rpm). All treatments were 6 hrs with 250 nM of THZ1, THZ1-R, or Flavopiridol. **c**, THZ1 treatment delineates a subset of transcripts equally sensitive to low dose (50 nM) THZ1. Log2 fold change in gene expression for 50 nM (x axis) and 250 nM THZ1 (y axis) following a 4 hr treatment. Pearson coefficient  $r = 0.50$ . **d**, Gene tracks of H3K27Ac (top), CDK7 (middle), and RNAPII (bottom) ChIP-seq occupancy at the TSS, gene body, and a previously described enhancer region in the first intron of *RUNX1* (Nottingham et al., 2007). Total ChIP-seq signal is in units of rpm. **e**, Positive interconnected autoregulatory loop formed by RUNX1, TAL1, and GATA3. Genes are represented by rectangles, and proteins are represented by ovals (Sanda et al., 2012). **f**, Transcripts down-regulated by low dose THZ1 are enriched for transcripts downregulated following *RUNX1* knockdown. Gene set enrichment analysis of top 500 transcripts downregulated following a 4-hour

treatment with THZ1 (50 nM) in comparison to transcripts following a *RUNX1* knockdown (Sanda et al., 2012). GSEA-supplied p-value < 0.001.

which drive high-level expression yet can be especially sensitive to perturbation (Chapuy et al., 2013; Hnisz et al., 2013; Loven et al., 2013; Shi et al., 2013). Super-enhancer analysis in Jurkat cells revealed that *RUNX1* contains an exceptionally large super-enhancer domain containing a previously described hematopoietic cell –specific enhancer (Fig. 4d; Supplementary Fig. 10b-d and Table 8) (Nottingham et al., 2007). In addition, *RUNX1* forms a core regulatory circuitry with two additional transcription factors that play prominent roles in leukemia biology, *TAL1* and *GATA3* (Fig. 4e) (Sanda et al., 2012). These factors autoregulate their own gene expression while simultaneously regulating many other genes that comprise the active gene expression program of Jurkat cells. Treatment with 50 nM THZ1 led to significant reduction in both the transcript and protein levels of *RUNX1*, *TAL1*, and *GATA3* (Supplementary Fig. 10e and f). Loss of the *RUNX1* driven transcriptional program is likely key to the response to low dose THZ1 treatment, as gene set enrichment analysis revealed that the Jurkat transcripts downregulated by 50 nM THZ1 were enriched in transcripts similarly downregulated following *RUNX1* depletion using shRNA (Fig. 4f).

Here we have reported the discovery and characterization of the first covalent inhibitor of CDK7, THZ1. THZ1 employs a unique mechanism, combining ATP-site and allosteric covalent binding, as means of attaining potency and selectivity for CDK7. This mechanistic insight should be useful for designing next generation inhibitors of CDKs, where high sequence and shape homology in the ATP pocket has posed a formidable challenge to achieving selectivity with conventional ATP-competitive inhibitors. THZ1 displayed

exquisite antiproliferative activity for T-ALL cell lines and other blood cancers, where oncogenic transcription factors feature prominently in the disease state. In Jurkat cells, low dose THZ1 had a profound effect on a small subset of genes, including the key regulator *RUNX1*, thus contributing to subsequent loss of the greater gene expression program and cell death. Identification of additional cancer cell lines whose gene expression programs display vulnerability to THZ1 or other transcriptional inhibitors should delineate additional cancers that are exquisitely susceptible to perturbation of transcription.

## References

- Akhtar, M.S., Heidemann, M., Tietjen, J.R., Zhang, D.W., Chapman, R.D., Eick, D., and Ansari, A.Z. (2009). TFIIH kinase places bivalent marks on the carboxy-terminal domain of RNA polymerase II. *Molecular cell* 34, 387-393.
- Bartkowiak, B., Liu, P., Phatnani, H.P., Fuda, N.J., Cooper, J.J., Price, D.H., Adelman, K., Lis, J.T., and Greenleaf, A.L. (2010). CDK12 is a transcription elongation-associated CTD kinase, the metazoan ortholog of yeast Ctk1. *Genes & development* 24, 2303-2316.
- Chapuy, B., McKeown, M.R., Lin, C.Y., Monti, S., Roemer, M.G., Qi, J., Rahl, P.B., Sun, H.H., Yeda, K.T., Doench, J.G., *et al.* (2013). Discovery and characterization of super-enhancer-associated dependencies in diffuse large B cell lymphoma. *Cancer cell* 24, 777-790.
- Drapkin, R., Le Roy, G., Cho, H., Akoulitchiev, S., and Reinberg, D. (1996). Human cyclin-dependent kinase-activating kinase exists in three distinct complexes. *Proceedings of the National Academy of Sciences of the United States of America* 93, 6488-6493.
- Feaver, W.J., Svejstrup, J.Q., Henry, N.L., and Kornberg, R.D. (1994). Relationship of CDK-activating kinase and RNA polymerase II CTD kinase TFIIH/TFIIK. *Cell* 79, 1103-1109.
- Fisher, R.P., and Morgan, D.O. (1994). A novel cyclin associates with MO15/CDK7 to form the CDK-activating kinase. *Cell* 78, 713-724.
- Garnett, M.J., Edelman, E.J., Heidorn, S.J., Greenman, C.D., Dastur, A., Lau, K.W., Greninger, P., Thompson, I.R., Luo, X., Soares, J., *et al.* (2012). Systematic identification of genomic markers of drug sensitivity in cancer cells. *Nature* 483, 570-575.
- Glover-Cutter, K., Larochelle, S., Erickson, B., Zhang, C., Shokat, K., Fisher, R.P., and Bentley, D.L. (2009). TFIIH-associated Cdk7 kinase functions in phosphorylation of C-terminal domain Ser7 residues, promoter-proximal pausing, and termination by RNA polymerase II. *Mol Cell Biol* 29, 5455-5464.
- Hnisz, D., Abraham, B.J., Lee, T.I., Lau, A., Saint-Andre, V., Sigova, A.A., Hoke, H.A., and Young, R.A. (2013). Super-enhancers in the control of cell identity and disease. *Cell* 155, 934-947.
- Huang da, W., Sherman, B.T., and Lempicki, R.A. (2009). Bioinformatics enrichment tools: paths toward the comprehensive functional analysis of large gene lists. *Nucleic acids research* 37, 1-13.

Larochelle, S., Amat, R., Glover-Cutter, K., Sanso, M., Zhang, C., Allen, J.J., Shokat, K.M., Bentley, D.L., and Fisher, R.P. (2012). Cyclin-dependent kinase control of the initiation-to-elongation switch of RNA polymerase II. *Nature structural & molecular biology* 19, 1108-1115.

Larochelle, S., Merrick, K.A., Terret, M.E., Wohlbold, L., Barboza, N.M., Zhang, C., Shokat, K.M., Jallepalli, P.V., and Fisher, R.P. (2007). Requirements for Cdk7 in the assembly of Cdk1/cyclin B and activation of Cdk2 revealed by chemical genetics in human cells. *Molecular cell* 25, 839-850.

Loven, J., Hoke, H.A., Lin, C.Y., Lau, A., Orlando, D.A., Vakoc, C.R., Bradner, J.E., Lee, T.I., and Young, R.A. (2013). Selective inhibition of tumor oncogenes by disruption of super-enhancers. *Cell* 153, 320-334.

Loven, J., Orlando, D.A., Sigova, A.A., Lin, C.Y., Rahl, P.B., Burge, C.B., Levens, D.L., Lee, T.I., and Young, R.A. (2012). Revisiting global gene expression analysis. *Cell* 151, 476-482.

Makela, T.P., Tassan, J.P., Nigg, E.A., Frutiger, S., Hughes, G.J., and Weinberg, R.A. (1994). A cyclin associated with the CDK-activating kinase MO15. *Nature* 371, 254-257.

Nottingham, W.T., Jarratt, A., Burgess, M., Speck, C.L., Cheng, J.F., Prabhakar, S., Rubin, E.M., Li, P.S., Sloane-Stanley, J., Kong, A.S.J., *et al.* (2007). Runx1-mediated hematopoietic stem-cell emergence is controlled by a Gata/Ets/SCL-regulated enhancer. *Blood* 110, 4188-4197.

Patricelli, M.P., Szardenings, A.K., Liyanage, M., Nomanbhoy, T.K., Wu, M., Weissig, H., Aban, A., Chun, D., Tanner, S., and Kozarich, J.W. (2007). Functional interrogation of the kinome using nucleotide acyl phosphates. *Biochemistry* 46, 350-358.

Rahl, P.B., Lin, C.Y., Seila, A.C., Flynn, R.A., McCuine, S., Burge, C.B., Sharp, P.A., and Young, R.A. (2010). c-Myc regulates transcriptional pause release. *Cell* 141, 432-445.

Sanda, T., Lawton, L.N., Barrasa, M.I., Fan, Z.P., Kohlhammer, H., Gutierrez, A., Ma, W., Tatarek, J., Ahn, Y., Kelliher, M.A., *et al.* (2012). Core transcriptional regulatory circuit controlled by the TAL1 complex in human T cell acute lymphoblastic leukemia. *Cancer cell* 22, 209-221.

Schachter, M.M., Merrick, K.A., Larochelle, S., Hirschi, A., Zhang, C., Shokat, K.M., Rubin, S.M., and Fisher, R.P. (2013). A Cdk7-Cdk4 T-loop phosphorylation cascade promotes G1 progression. *Molecular cell* 50, 250-260.

Serizawa, H., Makela, T.P., Conaway, J.W., Conaway, R.C., Weinberg, R.A., and Young, R.A. (1995). Association of Cdk-activating kinase subunits with transcription factor TFIIH. *Nature* 374, 280-282.

Shi, J., Whyte, W.A., Zepeda-Mendoza, C.J., Milazzo, J.P., Shen, C., Roe, J.S., Minder, J.L., Mercan, F., Wang, E., Eckersley-Maslin, M.A., *et al.* (2013). Role of SWI/SNF in acute leukemia maintenance and enhancer-mediated Myc regulation. *Genes Dev* 27, 2648-2662.

Shiekhhattar, R., Mermelstein, F., Fisher, R.P., Drapkin, R., Dynlacht, B., Wessling, H.C., Morgan, D.O., and Reinberg, D. (1995). Cdk-activating kinase complex is a component of human transcription factor TFIIH. *Nature* 374, 283-287.

Solomon, M.J., Lee, T., and Kirschner, M.W. (1992). Role of phosphorylation in p34cdc2 activation: identification of an activating kinase. *Molecular biology of the cell* 3, 13-27.

Watanabe, Y., Fujimoto, H., Watanabe, T., Maekawa, T., Masutani, C., Hanaoka, F., and Ohkuma, Y. (2000). Modulation of TFIIH-associated kinase activity by complex formation and its relationship with CTD phosphorylation of RNA polymerase II. *Genes to cells : devoted to molecular & cellular mechanisms* 5, 407-423.

Yamada, T., Yamaguchi, Y., Inukai, N., Okamoto, S., Mura, T., and Handa, H. (2006). P-TEFb-mediated phosphorylation of hSpt5 C-terminal repeats is critical for processive transcription elongation. *Molecular cell* 21, 227-237.

## **Methods Summary**

**T-ALL culture conditions.** Jurkat, Loucy, KOPTK1, and DND-41 cell lines were grown in RPMI-1640 supplemented with 10% fetal bovine serum and 1% glutamine. All cell lines were cultured at 37°C in a humidified chamber in the presence of 5% CO<sub>2</sub>, unless otherwise noted.

**Inhibitor treatment experiments.** Time-course experiments such as those described in Supplementary Fig. 5a were conducted to determine the minimal time required for full inactivation of CDK7. Cells were treated with THZ1, THZ1-R, or DMSO for 0-6 hrs to assess the effect of time on the THZ1 –mediated inhibition of RNAPII CTD phosphorylation. For subsequent experiments cells were treated with compounds for 4 hrs as determined by time-course experiment described above, unless otherwise noted. For inhibitor washout experiments (Fig. 2e, f; Supplementary Fig. 5) cells were treated with THZ1, THZ1-R, or DMSO for 4 hrs. Medium containing inhibitors was subsequently removed to effectively ‘washout’ the compound and the cells were allowed to grow in the absence of inhibitor. For each experiment, lysates were probed for RNAPII CTD phosphorylation and other specified proteins.

**High-throughput cell line panel viability assay.** Cells were seeded in 384-well microplates at ~15% confluency in medium with 5% FBS and



penicillin/streptavidin. Cells were treated with THZ1 or DMSO for 72 hrs and cell viability was determined using resazurin.

**RNA Extraction and Synthetic RNA Spike-In.** Total RNA and sample preparation was performed as previously described(Loven et al., 2012). Briefly, following inhibitor treatment cell number was determined, total RNA was isolated, and ERCC RNA Spike-In Mix (Ambion, cat# 4456740) was added to total RNA relative to cell number.

### **Chapter 3: Small-molecule inhibition of functionally related transcriptional co-factors produces synergistic effects in T-cell acute lymphoblastic leukemia**

---

Jessica Reddy<sup>1,2</sup>, Brian J. Abraham<sup>1</sup>, Alla Sigova<sup>1</sup>, Richard Young<sup>1,2</sup>

<sup>1</sup>*Whitehead Institute for Biomedical Research, 9 Cambridge Center, Cambridge, MA 02142* <sup>2</sup>*Department of Biology, Massachusetts Institute of Technology, Cambridge, MA, 02139*

The results depicted in this chapter contribute to a manuscript currently in preparation entitled “Small-molecule inhibition of functionally related transcriptional co-factors produces synergistic effects in T-cell acute lymphoblastic leukemia”.

## **Personal contribution to the Project**

This research is an extension of the work contained in Chapter 2, and Prof. Young and I conceived the idea of combining BRD4 and CDK7 inhibition as a follow-up study. I led the project, designed and performed all experiments. Brian Abraham helped perform computational analyses. I wrote the chapter with assistance from Prof. Young and comments from all authors.

## Abstract

Inhibitors that target the general transcriptional cofactors CDK7 and BRD4 have been shown to each cause profound effects on tumor cell proliferation. These inhibitors affect two different but closely related steps in transcriptional control, but it is unknown if they produce additive, synergistic or antagonistic effects on tumor cells. Here, we show that concurrent inhibition of CDK7 and BRD4 in T-cell acute lymphoblastic leukemia cells with the tool compounds THZ1 and JQ1, respectively, produces synergistic effects on cell proliferation and apoptotic induction. Treatment of cells with each compound generally resulted in distinct effects on gene expression. Combination treatment affected expression of a larger set of genes than either inhibitor alone and, furthermore, had a more profound effect on expression of key oncogenes, such as the super-enhancer—driven *RUNX1* gene. These results reveal that simultaneous inhibition of transcriptional co-factors can produce synergistic effects on tumor cell growth phenotypes that are likely due to combinatorial effects on tumor cell gene expression.

## Introduction

Multiple studies have shown that inhibitors of the transcriptional cofactors CDK7 or BRD4 can have selective effects on expression of oncogenes in various cancer cells (Kwiatkowski et al., 2014; Chipumuro et al., 2014; Christensen et al., 2014; Wang et al., 2015; Loven et al., 2013; Chapuy et al., 2013; Shu et al., 2016). For examples, CDK7 inhibition by THZ1 leads to selective loss of expression of *RUNX1* in T-cell acute lymphoblastic leukemia (T-ALL) (Kwiatkowski et al., 2014), of *MYC* family proto-oncogenes and neuroendocrine lineage-specific factors in small cell lung cancer (SCLC) (Christensen et al., 2014), of *MYCN* expression in neuroblastoma (Chipumuro et al., 2014) and of an “Achilles cluster” of oncogenes in triple-negative breast cancer (TNBC) (Wang et al., 2015). BRD4 inhibition by JQ1 causes selective loss of expression of *MYC* in multiple myeloma (MM) (Loven et al., 2013; Delmore et al., 2011), of *POU2AF1* in diffuse large B cell lymphoma (DLBCL) (Chapuy et al., 2013) and of *MYC* and other oncogenes in TNBC (Shu et al., 2016). Although the effects of both inhibitors on gene expression have been studied individually, the effects of combined inhibition of CDK7 and BRD4 have yet to be investigated.

CDK7 and BRD4 contribute to two different but closely related steps in transcriptional control. As a component of TFIIF, CDK7 is thought to function in transcription initiation as well as elongation and does so, in part, by phosphorylating the C-terminal domain (CTD) of RNA polymerase II (Pol II) at serine 5 and 7 and CDK9 as part of the CAK complex (Akhtar et al., 2009; Larochelle et al., 2012). BRD4, however, occupies acetylated chromatin at active

regulatory elements and recruits CDK9, which functions as a transcriptional pause-release factor, permitting Pol II transcription elongation (Dey et al., 2003; Jang et al., 2005; Yang et al., 2005; Loven et al., 2013). Each factor contributes to several related but distinct steps of transcription that may be largely redundant or may suggest different results upon their perturbation.

Combination therapy can be clinically beneficial since it can help lower doses necessary for treatment, limit the emergence of resistant clones, and inhibit multiple oncogenic processes at once (Foucquier and Guedj, 2015). Due to the functional inter-connectedness of CDK7 and BRD4, combination treatments with inhibitors for the two proteins could result in additive, synergistic, or antagonistic effects. Synergistic or additive effects of the combination of inhibitors could inform future clinical investigation as well as lend insight into the functional inter-play between CDK7 and BRD4. Furthermore, understanding the effects of combined inhibition of multiple transcriptional steps with THZ1 and JQ1 could inform combinations with other inhibitors.

Here, we sought to understand the consequences of combining the two transcriptional inhibitors THZ1 and JQ1 on tumor cells. We discovered that the two inhibitors produce synergistic effects on T-ALL cell growth and survival. Consistent with their closely related roles in transcriptional regulation, CDK7 and BRD4 occupy similar transcriptional regulatory regions on the genome. However, the two inhibitors had vastly different effects on gene expression, suggesting that different genes may be especially dependent on CDK7 or BRD4 for their transcription. Simultaneous inhibition of CDK7 and BRD4 impacted more genes

than inhibition with either alone, and the effects on gene expression were overall greater when treating with the combination. These findings suggest that inhibiting two functionally related transcriptional co-factors produces enhanced cytotoxicity in T-ALL cells, likely due to combinatorial effects on tumor cell gene expression.

## Results

### *THZ1 and JQ1 have synergistic effects on T-ALL cell proliferation*

To confirm the separate effects of CDK7 and BRD4 inhibition on proliferation of a T-ALL cell line, we treated Jurkat cells with either THZ1, JQ1, or a combination of the two compounds. We first incubated the cells with varying doses of the individual inhibitors for 72 hours and measured the fraction of viable cells relative to cells treated with the vehicle control (Fig. 1A). Proliferation of the cells displayed a dose-dependent response, with an IC<sub>50</sub> of 38 nM and 490 nM for THZ1 (Fig. 1, left) and JQ1 (Fig. 1B, right), respectively. This is largely consistent with the range of IC<sub>50</sub> values reported for similar cells treated with these compounds (Kwiatkowski et al., 2014; Roderick et al., 2014).

To determine if combining THZ1 and JQ1 would result in additive, synergistic, or antagonistic effects on cell proliferation, Jurkat cells were treated with the two inhibitors over a range of doses and effects on proliferation were then measured (Fig. 1B). To obtain a reference point to which the data could be compared against, we used two separate models to predict an additive effect. Effects that were greater than additive were considered synergistic and lower

than additive were considered antagonistic. We first predicted the outcome of an additive relationship assuming Bliss independence (Fitzgerald et al., 2006) (Fig. 1B, left panel). The Bliss independence model treats drug effects as probabilistic processes (with values ranging from 0 to 1) and assumes that the drugs act independently of each other (Foucquier and Guedj, 2015). This additive prediction was then compared to the reduction in viability that we detected for each dose combination (Fig. 1B, middle panel). Changes in viability larger than those predicted through Bliss independence were tabulated (Fig. 1B, right panel; values  $> 0$  indicate synergism) and plotted (Fig. 1C). The two compounds reproducibly produced synergistic effects on cellular viability over a range of dose combinations, including those at or below the IC<sub>50</sub>s of the individual inhibitors (Fig. 1B, right panel, Fig. 1C). We used an additional method to model additivity, one that does not rely on the assumption that the drugs act independently. Based in Loewe additivity principles, the Chou-Talalay method predicts the concentration of a drug that could produce an effect that is equivalent to that resulting from a different drug (Chou, 2006). For a given effect, such as 50% inhibition of cell proliferation, an additive prediction across different dose combinations is represented by an “isobole” line with negative slope (Fig. 1D). Data-points from dose combinations below the isobole indicate that lower doses are necessary to produce a given effect when treated in combination and is thus considered synergistic (Fig. 1D; fractional inhibitory concentrations (FICs) of each drug  $< 1$ ).



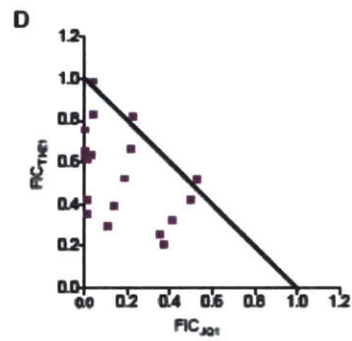
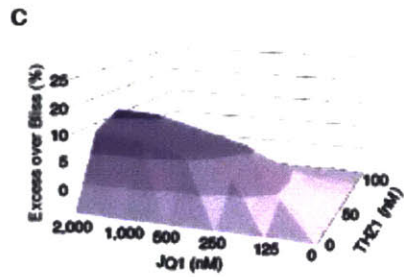
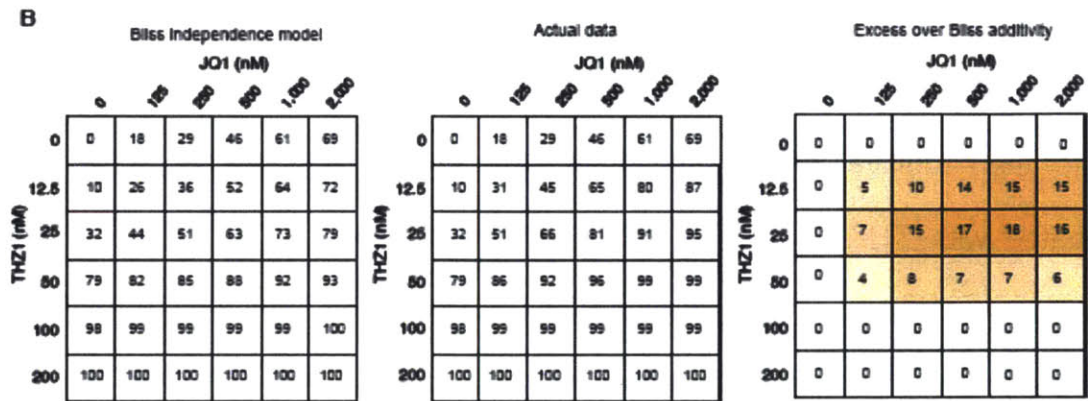
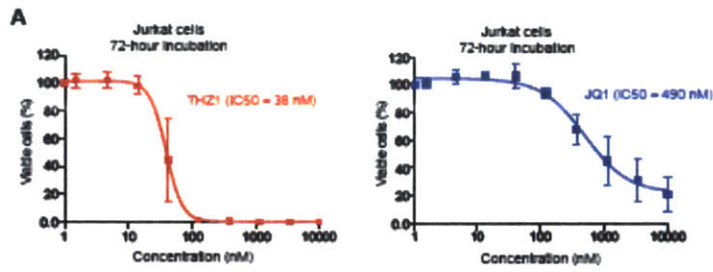


**Figure 1 | THZ1 and JQ1 have synergistic effects on T-ALL Jurkat cell proliferation.** **a.** THZ1 and JQ1 inhibit cell proliferation with differing IC50s. Jurkat cells were incubated with THZ1 or JQ1 over a range of doses (3, 10, 30, 100, 300, 1,000, 3,000, 10,000 nM) for 72 hours, and the fraction of proliferating cells were quantified relative to cells treated with vehicle. Error bars represent SD of 3 biological replicates. **b.** Combined treatment with THZ1 and JQ1 results in a greater-than-additive effect on Jurkat cell proliferation. Jurkat cells were incubated with THZ1 and JQ1 over a range of doses for 72 hours prior to measurement of the anti-proliferative effect of each dose combination relative to cells treated with vehicle. An additive relationship assuming Bliss independence (Fitzgerald et al., 2006) was calculated (left) and compared to the actual data (middle), and effects in excess of the predicted additive relationship were quantified (right). Numbers represent averages of 5 biological replicates. **c.** Excess over Bliss synergy plots for serial dilutions of JQ1 in combination with THZ1 in Jurkat cells. Excess over Bliss scores >0 indicate drug synergy, whereas negative scores indicate antagonism. **d.** Combined treatment with THZ1 and JQ1 results in synergistic effects on Jurkat cell proliferation. Chou-Talalay isobologram (Chou, 2006) of data presented in **c.** The numbers on the axes represent fractional inhibitory concentrations (FIC) for each inhibitor. The coordinates of the FIC scores are  $d_1/D_{x1}$  and  $d_2/D_{x2}$  where  $D_{x1}$  is the concentration of drug 1 that alone produces the effect  $x$ , and  $D_{x2}$  is the concentration of drug 2 that alone produces the effect  $x$ . Values below diagonal line indicate synergism.

Thus, the results of both the Bliss and Chou-Talalay analysis methods indicate that the two inhibitors have a synergistic effect on Jurkat cell proliferation.

To investigate whether the synergy observed with these inhibitors is specific to the Jurkat cell line, we carried out a similar study with another T-ALL cell line, KOPT-K1, which had comparable IC50 values for the separate inhibitors (Fig. 2A). A synergistic relationship was also observed with these (Fig. 2), demonstrating effects greater than those predicted through Bliss independence (Fig. 2B, C) and through isobologram analyses (Fig. 2D). These results indicate that the two inhibitors have a synergistic effect on proliferation of multiple T-ALL cell lines. We selected the Jurkat cell line for further analysis of synergy because our prior studies of these cells have explored their genetic alterations, super-enhancer driven oncogenes, and gene expression program (Sanda et al., 2013; Kwiatkowski et al., 2014; Mansour et al., 2014).

#### *Combined treatment with THZ1 and JQ1 results in synergistic apoptotic induction*

Decreases in cell proliferation can result from distinguishable cellular processes including apoptosis and/or cell cycle arrest, so we sought to distinguish between these possible phenotypes of treatment. To determine if treatment with THZ1 and JQ1 results in induction of apoptosis, we administered IC50 levels of THZ1, JQ1, or the combination of THZ1 and JQ1 to Jurkat cells and labeled them with Annexin V and propidium iodide for apoptotic/dead cell

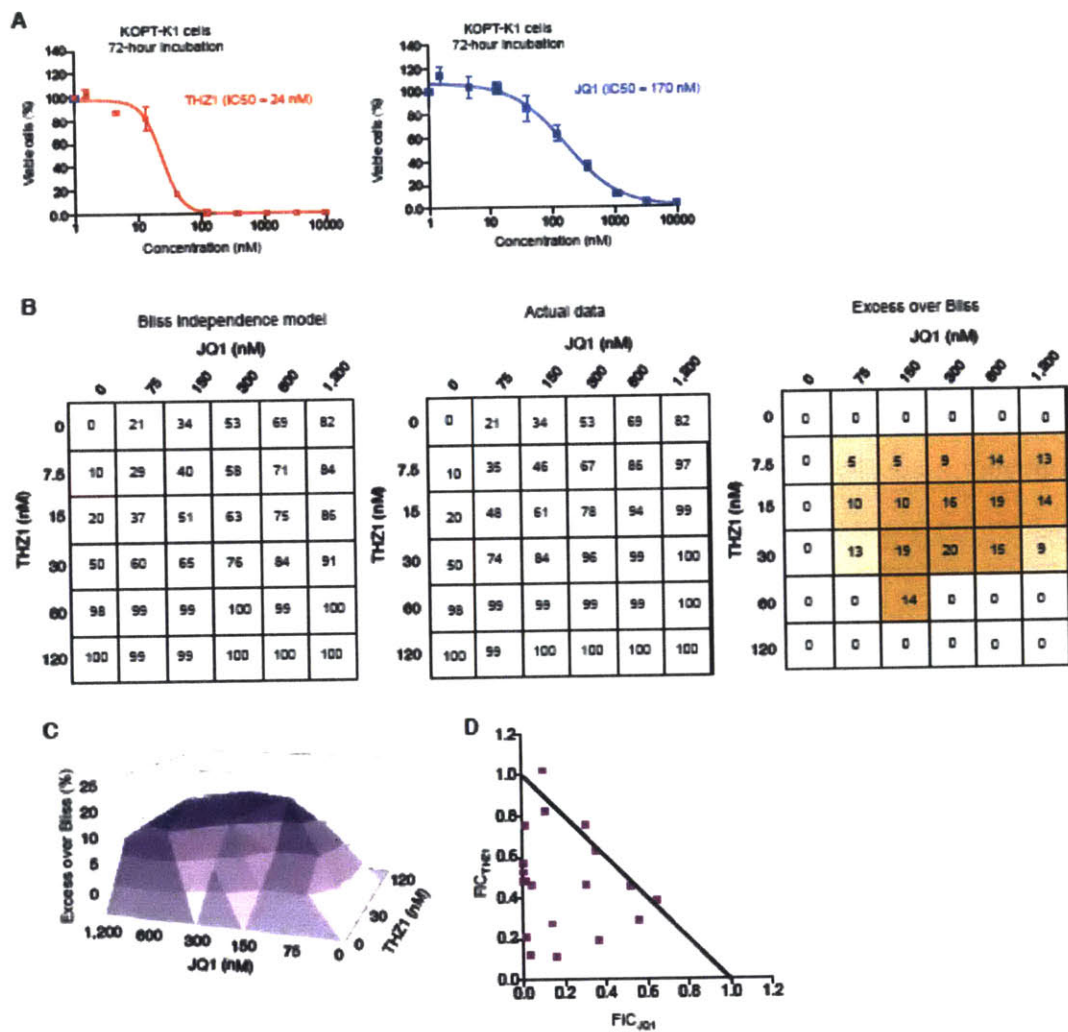


**Figure 2 | THZ1 and JQ1 have synergistic effects on T-ALL KOPTK-1 cell proliferation.** **a.** THZ1 and JQ1 inhibit cell proliferation with differing IC<sub>50</sub>s. KOPT-K1 cells were incubated with THZ1 or JQ1 over a range of doses (3, 10, 30, 100, 300, 1,000, 3,000, 10,000 nM) for 72 hours, and the fraction of proliferating cells were quantified relative to cells treated with vehicle. Error bars represent SD of 3 technical replicates. **b.** Combined treatment with THZ1 and JQ1 results in greater-than-additive effects on KOPT-K1 cell proliferation. KOPT-K1 cells were incubated with THZ1 or JQ1 over a range of doses for 72 hours prior to measurement of the anti-proliferative effect of each dose combination relative to cells treated with vehicle. An additive relationship assuming Bliss independence (Fitzgerald et al., 2006) was calculated (left) and compared to the actual data (middle), and the effects in excess of the predicted additive relationship were quantified (right). Numbers represent averages of 3 technical replicates. **c.** Excess over Bliss synergy plots for serial dilutions of JQ1 in combination with THZ1 in Jurkat cells. Excess over Bliss scores >0 indicate drug synergy, whereas negative scores indicate antagonism. **d.** Combined treatment with THZ1 and JQ1 results in synergistic effects on KOPT-K1 cell proliferation. Chou-Talalay isobolograms (Chou, 2006) of data presented in **c.** The numbers on the axes represent fractional inhibitory concentrations (FIC) for each inhibitor. The coordinates of the FIC scores are  $d_1/D_{x1}$  and  $d_2/D_{x2}$  where  $D_{x1}$  is the concentration of drug 1 that alone produces the effect  $x$ , and  $D_{x2}$  is the concentration of drug 2 that alone produces the effect  $x$ . Values below diagonal line indicate synergism.

detection (Fig. 3A). While treatment with THZ1 or JQ1 produced small numbers of Annexin V-positive cells, treatment with both inhibitors resulted in approximately 40% of cells staining positive for Annexin V (Fig. 3A-B), suggesting that treatment with the two inhibitors leads to synergistic induction of apoptosis.

Both CDK7 and BRD4 inhibition have been shown to separately cause cell cycle arrest (Kwiatkowski et al., 2014; Roderick et al., 2014), so we next examined the effects of the two inhibitors individually and in combination on cell cycle distribution. We treated the cells with THZ1, JQ1, or THZ1 and JQ1, ethanol-fixed and stained the cells with propidium iodide to measure DNA content per cell (Fig. 3C). Consistent with previous work, THZ1 or JQ1 alone resulted in small but measurable cell cycle changes, but the combination treatment substantially increased the fraction of cells with <2N DNA staining, an indication of inviable cells (Fig. 3C-D). These findings indicate that cell fitness is markedly decreased upon combination treatment with THZ1 and JQ1, as cell cycle defects likely contribute to the observed increases in apoptosis and cell death.

#### *Protein targets of THZ1 and JQ1 co-occupy transcriptional regulatory elements*

To gain insights into the molecular basis of the synergistic relationship of THZ1 and JQ1, we first investigated the genomic occupancy of their targets, CDK7 and BRD4, in Jurkat cells. CDK7 and BRD4 are thought to function in the context of an active transcription apparatus at transcriptionally active enhancers

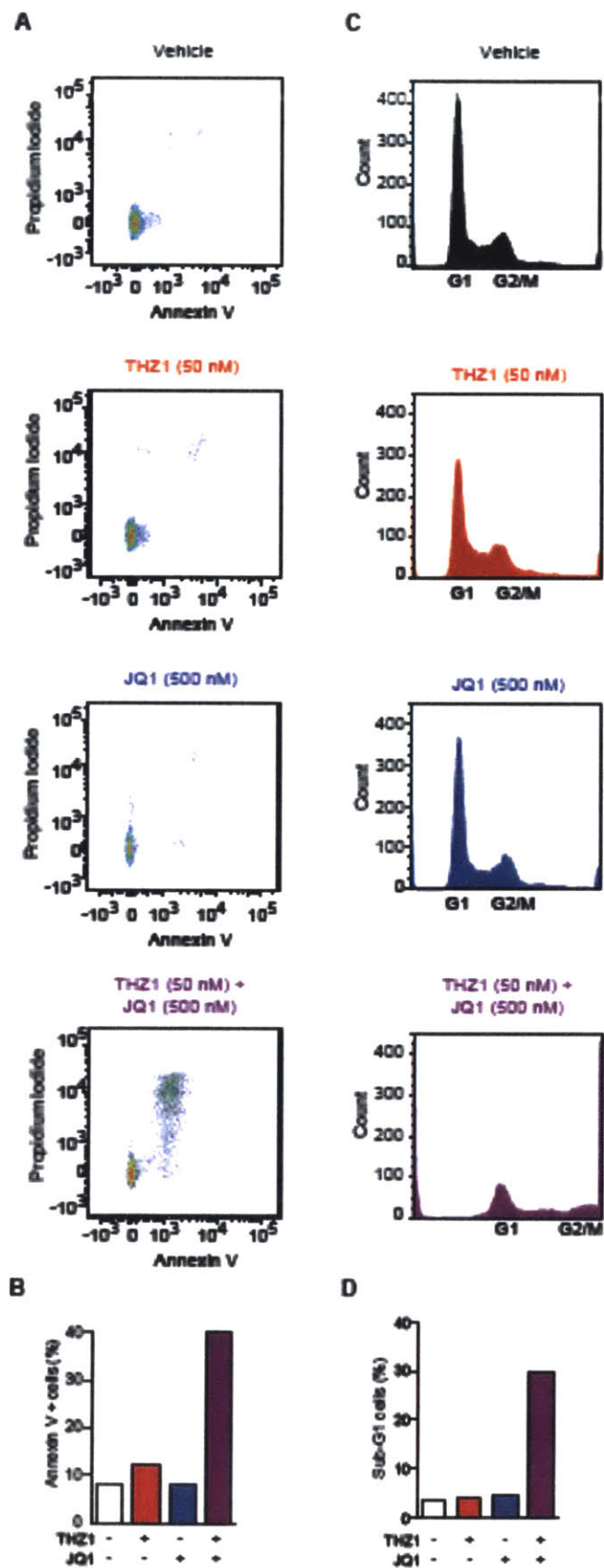


**Figure 3 | Treatment with THZ1 and JQ1 has synergistic effects on apoptosis**

**a.** Combined treatment with THZ1 and JQ1 results in a greater level of apoptosis and cell death than either inhibitor alone. Jurkat cells were treated with THZ1 (50 nM), JQ1 (500 nM), THZ1 (50 nM) and JQ1 (500 nM) for 72 hours and stained with Annexin V and propidium iodide for detection of apoptotic and dead cells. **b.** Quantification of Annexin V+ cells. **c.** Combined treatment with THZ1 and JQ1 results in a greater level of sub-G1 cells than either inhibitor alone. Jurkat cells were treated with THZ1 (50 nM), JQ1 (500 nM), THZ1 (50 nM) and JQ1 (500 nM) for 72 hours, fixed, and stained with propidium iodide for cell cycle analysis. **d.** Quantification of sub-G1 cells.

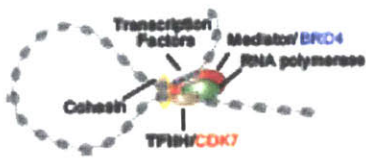


and promoters (Fig. 4A), but the two regulatory proteins may preferentially occupy one type of element. We performed chromatin immunoprecipitation-sequencing (ChIP-seq) using antibodies against CDK7 and BRD4, which confirmed that CDK7 and BRD4 co-occupy active promoters, enhancers, and constituents of super-enhancers (Fig. 4B-E). However, CDK7 signal was also found across the body of many highly transcribed genes with RNA polymerase II (Pol II); this was not typically observed with BRD4 (Fig. 4B). This is consistent with the view that CDK7 may be bound to actively transcribing Pol II at some genes (Glover-Cutter et al., 2009). Relative to CDK7, BRD4 was found to preferentially occupy super-enhancers (Fig. 4D). These results indicate that CDK7 and BRD4 can both occupy active enhancers and promoters across the genome, but also indicates that the two proteins can have somewhat different distributions at super-enhancers and gene bodies.

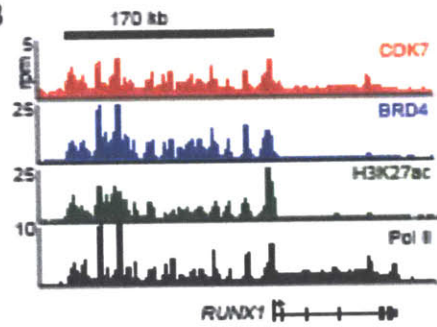
#### *Effects of THZ1 and JQ1 on global gene expression*

Previous studies have noted that treatment of tumor cells with THZ1 or JQ1 can produce striking gene-selective effects (Kwiatkowski et al., 2014; Chipumuro et al., 2014; Christensen et al., 2014; Wang et al., 2015; Loven et al., 2013; Chapuy et al., 2013; Shu et al., 2016), but it is not known whether the same set of genes is especially sensitive to the two inhibitors because a side-by-side comparison has yet to be examined in a tumor cell line. We performed side-by-side treatments with THZ1 and JQ1 to compare the effects of the two inhibitors on global gene expression. To assess the immediate and thus most likely direct

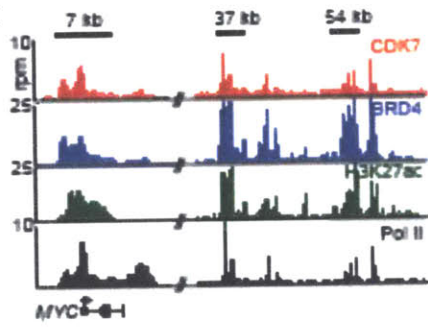
A



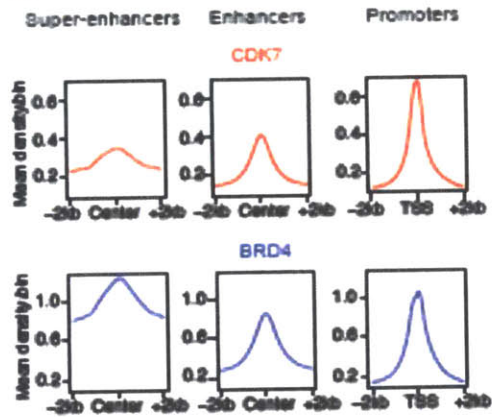
B



C



D



E

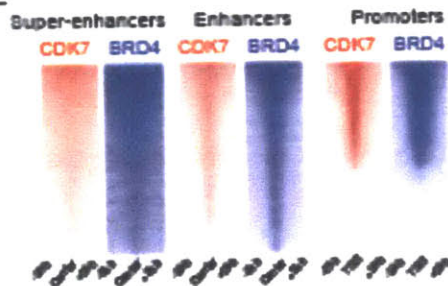


**Figure 4 | CDK7 and BRD4 co-occupy regulatory regions in T-ALL Jurkat cells.**

**a.** Cartoon depicting roles for CDK7 and BRD4 in transcriptional regulation

**b.** Gene tracks of CDK7, BRD4, H3K27ac and RNA Pol II ChIP-seq occupancy at the *RUNX1* locus, with the upstream super-enhancer indicated with a black box. The x axis shows genomic position and the y axis shows signal of ChIP-seq occupancy in units of reads per million.

**c.** Gene tracks of CDK7, BRD4, H3K27ac and RNA Pol II ChIP-seq occupancy at the *MYC* locus, with upstream and downstream super-enhancers indicated with black boxes. The x axis shows genomic position and the y axis shows signal of ChIP-seq occupancy in units of reads per million.

**d.** Meta-gene representation of average CDK7 (top, red line) and BRD4 (bottom, blue line) occupancy at super-enhancer constituents, all enhancers, and promoters. The x axis shows regions +/- 2kb around enhancer constituents (left and middle displays) or transcription start sites (right). The y axis shows signal in rpm/bp.

**e.** Heat-map representation of CDK7 (red) and BRD4 (blue) occupancy at individual super-enhancer constituents (left), all enhancers (middle), and promoters (right). Each row represents the +/- 2kb centered on the middle of each super-enhancer, enhancer, or TSS. Color scaled intensities are in units of rpm/bp.

transcriptional effects, Jurkat cells were incubated for a short time (4 hours) with THZ1 (50 nM) or JQ1 (500 nM), or a combination of these inhibitors, and the effects on gene expression were monitored with microarrays (Fig. 5). Doses similar to proliferation IC50 values were chosen as, at least for THZ1, similar IC50 values were derived from changes in RNA Polymerase II phosphorylation states (Kwiatkowski et al., 2014). Treatment with THZ1 alone led to reduced levels (> 1.5-fold loss) of 264 gene transcripts, whereas treatment with JQ1 alone led to reduced levels (> 1.5-fold loss) of 1,356 gene transcripts (Figure 5A, B). Approximately 40% of transcripts sensitive to THZ1 were also sensitive to JQ1, and 8% of transcripts sensitive to JQ1 were also sensitive to THZ1 (Figure 5B). These results demonstrate that THZ1 and JQ1 treatments both result in gene-selective effects, but groups of genes are differentially sensitive to the two inhibitors, suggesting that certain genes may possess unique dependencies on CDK7 and BRD4 for full expression.

Treatment of Jurkat cells with both inhibitors had substantial effects on a larger number of genes than treatment with either inhibitor alone (2,249 with combination vs. 264 and 1,356 with THZ1 and JQ1)(Fig. 5A-B). As expected, most genes affected by either inhibitor were also sensitive to the combined treatment (Fig. 5B). For the set of genes sensitive to THZ1 and JQ1, the combined treatment typically caused a more substantial decrease in expression than treatment with the individual inhibitors (Fig. 5C; p-values < 2.2e-16 for comparisons to either THZ1 or JQ1 with Student's two-tailed t-test). Furthermore, the sum of the gene expression responses to individual treatments were largely

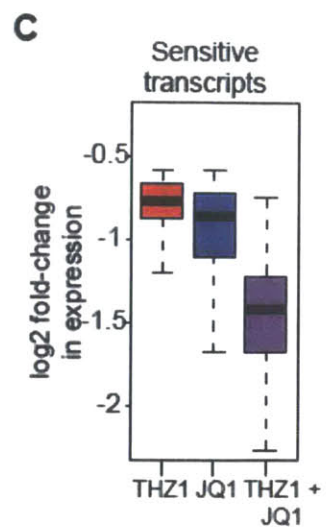
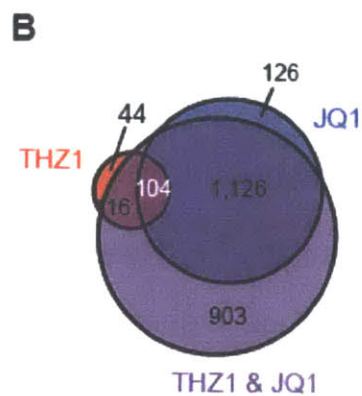
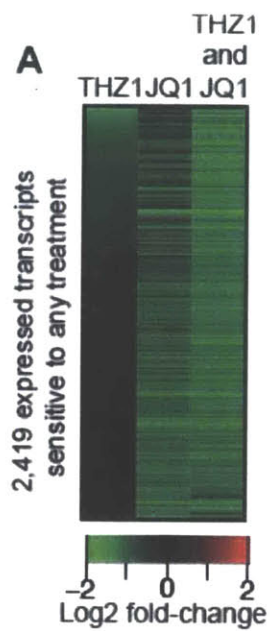


**Figure 5 | Combined treatment of THZ1 and JQ1 results in greater effects on global gene expression than either inhibitor alone**

**a.** Combined treatment with THZ1 and JQ1 affects the expression of a greater number of transcripts than either inhibitor alone. Jurkat cells were treated with THZ1 (50 nM), JQ1 (500 nM), or THZ1 (50 nM) and JQ1 (500 nM) for 4 hours followed by isolation of RNA, addition of synthetic RNA spike-in, and hybridization on expression microarrays. Heatmap displays the log<sub>2</sub> fold change in gene expression versus vehicle for the 2,419 expressed transcripts that are downregulated at least 1.5-fold with any of the three treatments.

**b.** A greater number of transcripts are sensitive to combined THZ1 and JQ1 treatment than with the individual inhibitors. Venn diagram over-lap of sensitive (>1.5-fold loss in expression) transcripts from treatments with THZ1, JQ1, and the two inhibitors together. 903 transcripts were sensitive to the combined treatment but unaffected by THZ1 and JQ1 when treated alone.

**c.** Combining THZ1 and JQ1 results in greater changes in gene expression than either inhibitor alone. Expression changes were quantified for each condition of the 160 transcripts that were sensitive (>1.5-fold reduction in expression) to all three treatments.

predictive of their response to the combined treatment (data not shown), consistent with an additive effect on gene expression. These results suggest that the combination of THZ1 and JQ1 impacts a larger number of genes, and has a more substantial effect on transcript levels for these genes, than does treatment with either inhibitor alone.

## **Discussion**

Despite growing evidence of THZ1 and JQ1 as effective anti-tumor agents, the effects of treating the two inhibitors together have not been investigated. Combination therapy has the potential to enhance therapeutic effects while allowing for dose and toxicity reduction (Lehar et al., 2009; Fitzgerald et al., 2006; Chou, 2010). Drug synergism decreases the likelihood of resistance (Lowe et al., 2014), and, given recent studies describing resistance to JQ1 in tumor cells (Rathert et al. 2015, Fong et al. 2015), combined treatment with another inhibitor could hypothetically limit these effects. Indeed, the combination of THZ1 and JQ1 had enhanced effects on T-ALL cell proliferation and apoptosis, and experiments with various levels of the two drugs (Figs. 1, 2) suggests that lower doses of the combination of inhibitors may be more effective than either inhibitor alone.

Both THZ1 and JQ1 have been shown to produce anti-tumor effects in a variety of cancer models by selectively affecting the expression of key genes on which tumor cells depend for survival (Kwiatkowski et al., 2014; Chipumuro et al., 2014; Christensen et al., 2014; Wang et al., 2015; Loven et al., 2013; Chapuy et

al., 2013; Shu et al., 2016). We previously found that THZ1 treatment selectively reduced the expression of *RUNX1* while causing dramatic levels of apoptosis in T-ALL cells (Kwiatkowski et al. 2014), consistent with previous work showing that high levels of *RUNX1* are required for survival (Sanda et al., 2012). Likewise, in T-ALL cells JQ1 treatment has been shown reduce the levels of *MYC* and cause anti-proliferative effects (Roderick et al., 2014; Knoechel, et al., 2014). Our results confirm these findings. However, the question remains whether targeting two regulatable steps of transcription has additional effects on gene expression beyond targeting each one individually.

Treatment with both inhibitors affected more genes than treatment with the inhibitors individually and increased the magnitude of expression changes for several genes, which was particularly evident for *RUNX1*. This suggests that inhibiting multiple steps of transcription may cause effects on tumor gene expression programs that lead to a synergistic cellular response. We found that both BRD4 and CDK7 proteins co-occupy enhancers and super-enhancers (Fig. 3B-E), but the genes sensitive to inhibition of either protein were largely different (Fig. 4A-B), suggesting unique dependencies on the two proteins for gene expression. More broadly, our results suggest that inhibiting two steps within the transcriptional cascade can have increased effects on cell death, likely due to the increased number and magnitude of gene expression responses.

Synergy between THZ1 and JQ1 suggests that combining different transcriptional inhibitors may be therapeutically beneficial. It remains to be tested if this relationship also exists in animal models of T-ALL. Our results



suggest that genes depend on specific general transcriptional regulators in a combinatorial manner, and, as a result, these inhibitors may cause unanticipated and desirable effects on tumor cells. Thus, different nodes in transcriptional control may be effectively targeted together in cancer therapy, and the relationships between inhibitors of the pharmacologically tractable nodes should be further explored.

## References

- Akhtar, M.S., Heidemann, M., Tietjen, J.R., Zhang, D.W., Chapman, R.D., Eick, D., and Ansari, A.Z. (2009). TFIIH kinase places bivalent marks on the carboxy-terminal domain of RNA polymerase II. *Molecular cell* 34, 387-393.
- Cai, S.F., Chen, C.W., and Armstrong, S.A. (2015). Drugging Chromatin in Cancer: Recent Advances and Novel Approaches. *Molecular cell* 60, 561-570.
- Chapuy, B., McKeown, M.R., Lin, C.Y., Monti, S., Roemer, M.G., Qi, J., Rahl, P.B., Sun, H.H., Yeda, K.T., Doench, J.G., *et al.* (2013). Discovery and characterization of super-enhancer-associated dependencies in diffuse large B cell lymphoma. *Cancer cell* 24, 777-790.
- Chipumuro, E., Marco, E., Christensen, C.L., Kwiatkowski, N., Zhang, T., Hatheway, C.M., Abraham, B.J., Sharma, B., Yeung, C., Altabef, A., *et al.* (2014). CDK7 inhibition suppresses super-enhancer-linked oncogenic transcription in MYCN-driven cancer. *Cell* 159, 1126-1139.
- Chou, T.C. (2006). Theoretical basis, experimental design, and computerized simulation of synergism and antagonism in drug combination studies. *Pharmacol Rev* 58, 621-681.
- Chou, T.C. (2010). Drug combination studies and their synergy quantification using the Chou-Talalay method. *Cancer Res* 70, 440-446.
- Chou, T.C., and Talalay, P. (1984). Quantitative analysis of dose-effect relationships: the combined effects of multiple drugs or enzyme inhibitors. *Adv Enzyme Regul* 22, 27-55.
- Christensen, C.L., Kwiatkowski, N., Abraham, B.J., Carretero, J., Al-Shahrour, F., Zhang, T., Chipumuro, E., Herter-Sprie, G.S., Akbay, E.A., Altabef, A., *et al.* (2014). Targeting transcriptional addictions in small cell lung cancer with a covalent CDK7 inhibitor. *Cancer cell* 26, 909-922.
- Dawson, M.A., Prinjha, R.K., Dittmann, A., Giotopoulos, G., Bantscheff, M., Chan, W.I., Robson, S.C., Chung, C.W., Hopf, C., Savitski, M.M., *et al.* (2011). Inhibition of BET recruitment to chromatin as an effective treatment for MLL-fusion leukaemia. *Nature* 478, 529-533.
- Delmore, J.E., Issa, G.C., Lemieux, M.E., Rahl, P.B., Shi, J., Jacobs, H.M., Kastiris, E., Gilpatrick, T., Paranal, R.M., Qi, J., *et al.* (2011). BET bromodomain inhibition as a therapeutic strategy to target c-Myc. *Cell* 146, 904-917.
- Dey, A., Chitsaz, F., Abbasi, A., Misteli, T., and Ozato, K. (2003). The double bromodomain protein Brd4 binds to acetylated chromatin during interphase and

mitosis. *Proceedings of the National Academy of Sciences of the United States of America* 100, 8758-8763.

Feaver, W.J., Svejstrup, J.Q., Henry, N.L., and Kornberg, R.D. (1994). Relationship of CDK-activating kinase and RNA polymerase II CTD kinase TFIIH/TFIIK. *Cell* 79, 1103-1109.

Ferri, E., Petosa, C., and McKenna, C.E. (2016). Bromodomains: Structure, function and pharmacology of inhibition. *Biochem Pharmacol* 106, 1-18.

Fesquet, D., Labbe, J.C., Derancourt, J., Capony, J.P., Galas, S., Girard, F., Lorca, T., Shuttleworth, J., Doree, M., and Cavadore, J.C. (1993). The MO15 gene encodes the catalytic subunit of a protein kinase that activates cdc2 and other cyclin-dependent kinases (CDKs) through phosphorylation of Thr161 and its homologues. *The EMBO journal* 12, 3111-3121.

Fisher, R.P., and Morgan, D.O. (1994). A novel cyclin associates with MO15/CDK7 to form the CDK-activating kinase. *Cell* 78, 713-724.

Fitzgerald, J.B., Schoeberl, B., Nielsen, U.B., and Sorger, P.K. (2006). Systems biology and combination therapy in the quest for clinical efficacy. *Nat Chem Biol* 2, 458-466.

Fong, C.Y., Gilan, O., Lam, E.Y., Rubin, A.F., Ftouni, S., Tyler, D., Stanley, K., Sinha, D., Yeh, P., Morison, J., *et al.* (2015). BET inhibitor resistance emerges from leukaemia stem cells. *Nature* 525, 538-542.

Foucquier, J., and Guedj, M. (2015). Analysis of drug combinations: current methodological landscape. *Pharmacol Res Perspect* 3, e00149.

Ganuza, M., Saiz-Ladera, C., Canamero, M., Gomez, G., Schneider, R., Blasco, M.A., Pisano, D., Paramio, J.M., Santamaria, D., and Barbacid, M. (2012). Genetic inactivation of Cdk7 leads to cell cycle arrest and induces premature aging due to adult stem cell exhaustion. *The EMBO journal* 31, 2498-2510.

Garraway, L.A., and Sellers, W.R. (2006). Lineage dependency and lineage-survival oncogenes in human cancer. *Nature reviews Cancer* 6, 593-602.

Greco, W.R., Faessel, H., and Levasseur, L. (1996). The search for cytotoxic synergy between anticancer agents: a case of Dorothy and the ruby slippers? *J Natl Cancer Inst* 88, 699-700.

Herranz, D., Ambesi-Impiombato, A., Palomero, T., Schnell, S.A., Belver, L., Wendorff, A.A., Xu, L., Castillo-Martin, M., Llobet-Navas, D., Cordon-Cardo, C., *et al.* (2014). A NOTCH1-driven MYC enhancer promotes T cell development,

transformation and acute lymphoblastic leukemia. *Nature medicine* 20, 1130-1137.

Hnisz, D., Abraham, B.J., Lee, T.I., Lau, A., Saint-Andre, V., Sigova, A.A., Hoke, H.A., and Young, R.A. (2013). Super-enhancers in the control of cell identity and disease. *Cell* 155, 934-947.

Hnisz, D., Schuijers, J., Lin, C.Y., Weintraub, A.S., Abraham, B.J., Lee, T.I., Bradner, J.E., and Young, R.A. (2015). Convergence of developmental and oncogenic signaling pathways at transcriptional super-enhancers. *Molecular cell* 58, 362-370.

Jain, M., Arvanitis, C., Chu, K., Dewey, W., Leonhardt, E., Trinh, M., Sundberg, C.D., Bishop, J.M., and Felsher, D.W. (2002). Sustained loss of a neoplastic phenotype by brief inactivation of MYC. *Science* 297, 102-104.

Jang, M.K., Mochizuki, K., Zhou, M., Jeong, H.S., Brady, J.N., and Ozato, K. (2005). The bromodomain protein Brd4 is a positive regulatory component of P-TEFb and stimulates RNA polymerase II-dependent transcription. *Molecular cell* 19, 523-534.

Johnson-Farley, N., Veliz, J., Bhagavathi, S., and Bertino, J.R. (2015). ABT-199, a BH3 mimetic that specifically targets Bcl-2, enhances the antitumor activity of chemotherapy, bortezomib and JQ1 in "double hit" lymphoma cells. *Leuk Lymphoma* 56, 2146-2152.

King, B., Trimarchi, T., Reavie, L., Xu, L., Mullenders, J., Ntziachristos, P., Aranda-Orgilles, B., Perez-Garcia, A., Shi, J., Vakoc, C., *et al.* (2013). The ubiquitin ligase FBXW7 modulates leukemia-initiating cell activity by regulating MYC stability. *Cell* 153, 1552-1566.

Knoechel, B., Roderick, J.E., Williamson, K.E., Zhu, J., Lohr, J.G., Cotton, M.J., Gillespie, S.M., Fernandez, D., Ku, M., Wang, H., *et al.* (2014). An epigenetic mechanism of resistance to targeted therapy in T cell acute lymphoblastic leukemia. *Nat Genet* 46, 364-370.

Kwiatkowski, N., Zhang, T., Rahl, P.B., Abraham, B.J., Reddy, J., Ficarro, S.B., Dastur, A., Amzallag, A., Ramaswamy, S., Tesar, B., *et al.* (2014). Targeting transcription regulation in cancer with a covalent CDK7 inhibitor. *Nature* 511, 616-620.

Langmead, B., Trapnell, C., Pop, M., and Salzberg, S.L. (2009). Ultrafast and memory-efficient alignment of short DNA sequences to the human genome. *Genome Biol* 10, R25.

Larochelle, S., Amat, R., Glover-Cutter, K., Sanso, M., Zhang, C., Allen, J.J., Shokat, K.M., Bentley, D.L., and Fisher, R.P. (2012). Cyclin-dependent kinase control of the initiation-to-elongation switch of RNA polymerase II. *Nat Struct Mol Biol* 19, 1108-1115.

Larochelle, S., Merrick, K.A., Terret, M.E., Wohlbald, L., Barboza, N.M., Zhang, C., Shokat, K.M., Jallepalli, P.V., and Fisher, R.P. (2007). Requirements for Cdk7 in the assembly of Cdk1/cyclin B and activation of Cdk2 revealed by chemical genetics in human cells. *Molecular cell* 25, 839-850.

Lee, T.I., and Young, R.A. (2013). Transcriptional regulation and its misregulation in disease. *Cell* 152, 1237-1251.

Lehar, J., Krueger, A.S., Avery, W., Heilbut, A.M., Johansen, L.M., Price, E.R., Rickles, R.J., Short, G.F., 3rd, Staunton, J.E., Jin, X., *et al.* (2009). Synergistic drug combinations tend to improve therapeutically relevant selectivity. *Nat Biotechnol* 27, 659-666.

Li, H., Handsaker, B., Wysoker, A., Fennell, T., Ruan, J., Homer, N., Marth, G., Abecasis, G., Durbin, R., and Genome Project Data Processing, S. (2009). The Sequence Alignment/Map format and SAMtools. *Bioinformatics* 25, 2078-2079.

Loven, J., Hoke, H.A., Lin, C.Y., Lau, A., Orlando, D.A., Vakoc, C.R., Bradner, J.E., Lee, T.I., and Young, R.A. (2013). Selective inhibition of tumor oncogenes by disruption of super-enhancers. *Cell* 153, 320-334.

Makela, T.P., Tassan, J.P., Nigg, E.A., Frutiger, S., Hughes, G.J., and Weinberg, R.A. (1994). A cyclin associated with the CDK-activating kinase MO15. *Nature* 371, 254-257.

Mansour, M.R., Abraham, B.J., Anders, L., Berezovskaya, A., Gutierrez, A., Durbin, A.D., Etchin, J., Lawton, L., Sallan, S.E., Silverman, L.B., *et al.* (2014). Oncogene regulation. An oncogenic super-enhancer formed through somatic mutation of a noncoding intergenic element. *Science* 346, 1373-1377.

Mazur, P.K., Herner, A., Mello, S.S., Wirth, M., Hausmann, S., Sanchez-Rivera, F.J., Lofgren, S.M., Kuschma, T., Hahn, S.A., Vangala, D., *et al.* (2015). Combined inhibition of BET family proteins and histone deacetylases as a potential epigenetics-based therapy for pancreatic ductal adenocarcinoma. *Nature medicine* 21, 1163-1171.

Northcott, P.A., Lee, C., Zichner, T., Stutz, A.M., Erkek, S., Kawauchi, D., Shih, D.J., Hovestadt, V., Zapatka, M., Sturm, D., *et al.* (2014). Enhancer hijacking activates GFI1 family oncogenes in medulloblastoma. *Nature* 511, 428-434.

Poon, R.Y., Yamashita, K., Adamczewski, J.P., Hunt, T., and Shuttleworth, J. (1993). The cdc2-related protein p40MO15 is the catalytic subunit of a protein kinase that can activate p33cdk2 and p34cdc2. *The EMBO journal* 12, 3123-3132.

Rathert, P., Roth, M., Neumann, T., Muerdter, F., Roe, J.S., Muhar, M., Deswal, S., Cerny-Reiterer, S., Peter, B., Jude, J., *et al.* (2015). Transcriptional plasticity promotes primary and acquired resistance to BET inhibition. *Nature* 525, 543-547.

Roderick, J.E., Tesell, J., Shultz, L.D., Brehm, M.A., Greiner, D.L., Harris, M.H., Silverman, L.B., Sallan, S.E., Gutierrez, A., Look, A.T., *et al.* (2014). c-Myc inhibition prevents leukemia initiation in mice and impairs the growth of relapsed and induction failure pediatric T-ALL cells. *Blood* 123, 1040-1050.

Roy, R., Adamczewski, J.P., Seroz, T., Vermeulen, W., Tassan, J.P., Schaeffer, L., Nigg, E.A., Hoeijmakers, J.H., and Egly, J.M. (1994). The MO15 cell cycle kinase is associated with the TFIIH transcription-DNA repair factor. *Cell* 79, 1093-1101.

Sanda, T., Lawton, L.N., Barrasa, M.I., Fan, Z.P., Kohlhammer, H., Gutierrez, A., Ma, W., Tatarek, J., Ahn, Y., Kelliher, M.A., *et al.* (2012). Core transcriptional regulatory circuit controlled by the TAL1 complex in human T cell acute lymphoblastic leukemia. *Cancer cell* 22, 209-221.

Schachter, M.M., Merrick, K.A., Larochelle, S., Hirschi, A., Zhang, C., Shokat, K.M., Rubin, S.M., and Fisher, R.P. (2013). A Cdk7-Cdk4 T-loop phosphorylation cascade promotes G1 progression. *Molecular cell* 50, 250-260.

Serizawa, H., Makela, T.P., Conaway, J.W., Conaway, R.C., Weinberg, R.A., and Young, R.A. (1995). Association of Cdk-activating kinase subunits with transcription factor TFIIH. *Nature* 374, 280-282.

Shaffer, A.L., Emre, N.C., Lamy, L., Ngo, V.N., Wright, G., Xiao, W., Powell, J., Dave, S., Yu, X., Zhao, H., *et al.* (2008). IRF4 addiction in multiple myeloma. *Nature* 454, 226-231.

Sharma, S.V., and Settleman, J. (2007). Oncogene addiction: setting the stage for molecularly targeted cancer therapy. *Genes Dev* 21, 3214-3231.

Shiekhata, R., Mermelstein, F., Fisher, R.P., Drapkin, R., Dynlacht, B., Wessling, H.C., Morgan, D.O., and Reinberg, D. (1995). Cdk-activating kinase complex is a component of human transcription factor TFIIH. *Nature* 374, 283-287.

Shu, S., Lin, C.Y., He, H.H., Witwicki, R.M., Tabassum, D.P., Roberts, J.M., Janiszewska, M., Huh, S.J., Liang, Y., Ryan, J., *et al.* (2016). Response and resistance to BET bromodomain inhibitors in triple-negative breast cancer. *Nature* 529, 413-417.

Solomon, M.J., Harper, J.W., and Shuttleworth, J. (1993). CAK, the p34cdc2 activating kinase, contains a protein identical or closely related to p40MO15. *The EMBO journal* 12, 3133-3142.

Soucek, L., Whitfield, J., Martins, C.P., Finch, A.J., Murphy, D.J., Sodir, N.M., Karnezis, A.N., Swigart, L.B., Nasi, S., and Evan, G.I. (2008). Modelling Myc inhibition as a cancer therapy. *Nature* 455, 679-683.

Wang, Y., Zhang, T., Kwiatkowski, N., Abraham, B.J., Lee, T.I., Xie, S., Yuzugullu, H., Von, T., Li, H., Lin, Z., *et al.* (2015). CDK7-dependent transcriptional addiction in triple-negative breast cancer. *Cell* 163, 174-186.

Weinstein, I.B. (2002). Cancer. Addiction to oncogenes--the Achilles heel of cancer. *Science* 297, 63-64.

Weng, A.P., Millholland, J.M., Yashiro-Ohtani, Y., Arcangeli, M.L., Lau, A., Wai, C., Del Bianco, C., Rodriguez, C.G., Sai, H., Tobias, J., *et al.* (2006). c-Myc is an important direct target of Notch1 in T-cell acute lymphoblastic leukemia/lymphoma. *Genes Dev* 20, 2096-2109.

Yang, Z., Yik, J.H., Chen, R., He, N., Jang, M.K., Ozato, K., and Zhou, Q. (2005). Recruitment of P-TEFb for stimulation of transcriptional elongation by the bromodomain protein Brd4. *Molecular cell* 19, 535-545.

Zhang, Y., Liu, T., Meyer, C.A., Eeckhoute, J., Johnson, D.S., Bernstein, B.E., Nusbaum, C., Myers, R.M., Brown, M., Li, W., *et al.* (2008). Model-based analysis of ChIP-Seq (MACS). *Genome Biol* 9, R137.

Zuber, J., Shi, J., Wang, E., Rappaport, A.R., Herrmann, H., Sison, E.A., Magoon, D., Qi, J., Blatt, K., Wunderlich, M., *et al.* (2011). RNAi screen identifies Brd4 as a therapeutic target in acute myeloid leukaemia. *Nature* 478, 524-528.

## Methods

### *Cell culture*

Jurkat and KOPTK1 T-ALL cells were cultured in RPMI GlutaMAX (Invitrogen, 61870-127), supplemented with 10% fetal bovine serum, 100 U/ml penicillin and 100 µg/ml streptomycin (Invitrogen, 15140-122). Cell lines were cultured at 37C in a humidified chamber in the presence of 5% CO<sub>2</sub>.

### *Proliferation Assays*

Proliferation assays were conducted using Cell Titer Glo assay kit (Promega cat# G7571). T-ALL cells grown in suspension were resuspended in fresh media containing THZ1, JQ1, THZ1 and JQ1, or DMSO at the indicated concentrations and then plated in 96-well plates at 10,000 cells/ well in a volume of 100 µL. Anti-proliferative effects of compounds were assessed following 72 hr incubations. Anti-proliferative effects were then determined using Cell Titer Glo as described in product manual by luminescence measurements on a Tecan Safire plate reader. IC<sub>50</sub>s were determined using GraphPad Prism 6 non-linear regression curve fit.

### *Apoptosis Assays*

Cells were treated with THZ1 (50 nM), JQ1 (500 nM), or THZ1 (50 nM) and JQ1 (500 nM) or with DMSO for 72 hours, collected by centrifugation and then washed once in PBS, and processed with the Dead Cell Apoptosis kit



according to manufacturers protocol (Invitrogen cat# V13242). Samples were analyzed on a BD LSR (BD Biosciences) instrument and processed on FlowJo (Treestar).

#### *Cell cycle analyses*

Cells were treated with THZ1 (50 nM), JQ1 (500 nM), or THZ1 (50 nM) and JQ1 (500 nM) or with DMSO for 72 hours, collected by centrifugation and then washed once in ice-cold phosphate-buffered saline (PBS), and fixed overnight at -20C with 80% ethanol in PBS. Cells were then washed 3x, pelleted, and resuspended in FxCycle PI/RNase staining solution (Life Technologies, F10797) prior to FACS analysis. Samples were analyzed on a BD LSR (BD Biosciences) instrument and processed on FlowJo (Treestar).

#### *RNA extraction and Synthetic RNA Spike-In Addition*

Total RNA and sample preparation was performed as previously described (Loven). Briefly, Jurkat cells were incubated in media containing THZ1 (50 nM), JQ1 (500 nM), or THZ1 (50 nM) and JQ1 (500 nM) or with DMSO for four hours. Cell numbers were determined with a Z Series Coulter Counter (Beckman Coulter) prior to lysis and RNA extraction. Biological duplicates (equivalent to 10 million cells per replicate) were collected, and RNA was isolated using the RNeasy Plus kit (Qiagen, 74136) following the manufacturer's instructions. ERCC RNA Spike-In Mix (Ambion, 4456740) was added to total RNA relative to cell number, RNA was analyzed on Agilent 2100 Bioanalyzer for

integrity. RNA with the RNA Integrity Number (RIN) above 9.8 was hybridized to GeneChip PrimeView Human Gene Expression Arrays (Affymetrix).

#### *Microarray Sample Preparation and Analysis*

For microarray analysis, 100 ng of total RNA containing ERCC RNA Spike-In Mix was used to prepare biotinylated aRNA (cRNA) according to the manufacturer's protocol (30 IVT Express Kit, Affymetrix 901228). Briefly, total RNA undergoes T7 oligo(dT)-primed reverse transcription to synthesize first-strand cDNA containing a T7 promoter sequence. This cDNA is then converted into a double-stranded DNA template for transcription using DNA Polymerase and RNase H to simultaneously degrade the RNA and synthesize second strand cDNA. In vitro transcription synthesizes aRNA and incorporates a biotin-conjugated nucleotide. The aRNA is then purified to remove unincorporated NTPs, salts, enzymes, and inorganic phosphate. Fragmentation of the biotin-labeled aRNA prepares the sample for hybridization onto GeneChip 3' expression arrays. Samples were prepared for hybridization using 10 µg of biotinylated aRNA in a 1X hybridization cocktail according the Affymetrix hybridization manual. Additional hybridization cocktail components were provided in the Affymetrix GeneChip Hybridization, Wash and Stain Kit. GeneChip arrays (Human PrimeView, Affymetrix 901837) were hybridized in a GeneChip Hybridization OvRPM. Washing was done using a GeneChip Fluidics Station 450 according to the manufacturer's instructions, using the buffers provided in the Affymetrix GeneChip Hybridization, Wash and Stain Kit. Images were extracted

with Affymetrix GeneChip Command Console (AGCC), and analyzed using GeneChip Expression Console. A Primeview CDF that included probe information for the ERCC controls (GPL16043), provided by Affymetrix, was used to generate .CEL files. We processed the CEL files using standard tools available within the affy package in R. The CEL files were processed with the `expresso` command to convert the raw probe intensities to probeset expression values. The parameters of the `expresso` command were set to generate Affymetrix MAS5-normalized probeset values. We used a *loess* regression to re-normalize these MAS5 normalized probeset values, using only the spike-in probesets to fit the *loess*. The `affy` package provides a function, `loess normalize`, which will perform *loess* regression on a matrix of values (defined using the parameter `mat`) and allows for the user to specify which subset of data to use when fitting the *loess* (defined using the parameter `subset`, see the `affy` package documentation for further details). For this application the parameters `mat` and `subset` were set as the MAS5-normalized values and the row-indices of the ERCC control probesets, respectively. The default settings for all other parameters were used. The result of this was a matrix of expression values normalized to the control ERCC probes. Probe set-level expression was collapsed to log2 RefSeq transcript-level transcription by taking the probe-set with the maximum average signal across all experiments. Log2 values of biological replicates were averaged. Fold-changes were taken by subtracting average log2 DMSO signal from average log2 treatment signal. Expressed genes

were those with  $\log_2(\text{expression}) > \log_2(100)$  in the corresponding DMSO sample. Expression heatmaps in Figure 5A were made using heatmap.2.

### *Chromatin Immunoprecipitation and Sequencing*

Cells were crosslinked for 20 min at room temperature by the addition of one-tenth of the volume of 11% formaldehyde solution (11% formaldehyde, 50mM HEPES pH 7.3, 100mM NaCl, 1mM EDTA pH 8.0, 0.5mM EGTA pH 8.0) to the growth media followed by 5 min quenching with 100 mM glycine. Cells were washed twice with PBS, then the supernatant was aspirated and the cell pellet was flash frozen in liquid nitrogen. Frozen crosslinked cells were stored at -80°C. 50  $\mu$ L of Dynal magnetic beads (Sigma) were blocked with 0.5% BSA (w/v) in PBS. Magnetic beads were bound with 5  $\mu$ g of the indicated antibody. For CDK7 occupied genomic regions, we performed ChIP-Seq experiments using a Bethyl Laboratories (A300-405A-1) antibody. The affinity-purified antibody was raised in rabbit against an epitope corresponding to amino acids 300-346 of human CDK7. For H3K27Ac occupied genomic regions, we performed ChIP-Seq experiments using an Abcam (AB4729A) antibody. The affinity-purified antibody was raised in rabbit against an epitope corresponding to amino acids 1-100 of human Histone H3 that is acetylated at K27. For RNA polymerase II occupied genomic regions, we performed ChIP-Seq experiments using a SantaCruz Biotechnology (sc-899) antibody. The affinity purified antibody was raised in rabbit against an epitope mapping to the N-terminus of murine RBP1, the largest subunit of RNA Pol II. For BRD4 occupied genomic regions,

we performed ChIP-Seq experiments using a Bethyl Laboratories (A301-985A) antibody. The affinity purified antibody was raised in rabbit against an epitope corresponding to amino acids 1312-1362 of human BRD4. Crosslinked cells were lysed with lysis buffer 1 (50mM HEPES pH 7.5, 140mM NaCl, 1mM EDTA, 10% glycerol, 0.5% NP-40, and 0.25% Triton X-100), pelleted and resuspended in lysis buffer 2 (10 mM TrisHCl pH 8.0, 200 mM NaCl, 1 mM EDTA, 0.5 mM EGTA). The subsequent pellet was resuspended in and sonicated in sonication buffer (50 mM HEPES pH 7.5, 140 mM NaCl, 1 mM EDTA pH 8.0, 1 mM EGTA, 0.1% Na-deoxycholate, 0.1% SDS, and 1% Triton X-100). Cells were sonicated for 10 cycles at 30 s each on ice (21-24 W) with 60 s on ice between cycles. Sonicated lysates were cleared and incubated overnight at 4C with magnetic beads bound with antibody to enrich for DNA fragments bound by the indicated factor. Beads were washed two times with sonication buffer, one time with sonication buffer with 500 mM NaCl, one time with LiCl wash buffer (10 mM TrisHCl pH 8.0, 1 mM EDTA, 250 mM LiCl, 0.5% NP-40, 0.5% Na-deoxycholate) and one time with TE. DNA was eluted in elution buffer (50 mM TrisHCl pH 8.0, 10 mM EDTA, 1% SDS). Cross-links were reversed overnight. RNA and protein were digested using RNase A and Proteinase K, respectively and DNA was purified with phenol chloroform extraction and ethanol precipitation.

### *ChIP-Seq analysis*

Raw ChIP-Seq reads were mapped to the hg19 revision of the human reference genome using bowtie (Langmead, Genome Biology, 2009) with parameters `-k 2 -m 2 -sam -best` and `-l` set to the read length. Wiggle files for

displaying read counts in bins relative to genomic regions (Figure 4B, C) were created using MACS (Zhang, Genome Biology, 2008) with parameters `–space=50 –nomodel –shiftsize=200` and were subsequently normalized to the millions of mapped reads (RPM).

Enhancers and super-enhancers (Figure 4B, C, D, E) were identified by their enrichment in H3K27ac ChIP-Seq signal and were identified as in Mansour et al, 2014. Briefly, enhancer peaks of H3K27ac ChIP-Seq signal were identified with MACS with input control and parameters `–keep-dup=auto –p 1e-9`. For super-enhancers, two sets of MACS peaks identified with `–keep-dup=auto –p 1e-9` or `–keep-dup=all –p 1e-9` were collapsed and used as input for ROSE ([https://bitbucket.org/young\\_computation/rose/](https://bitbucket.org/young_computation/rose/)) with parameters `–s 12500 –t 2000 –g hg19` and input control. Constituent enhancers of super-enhancers were identified as those H3K27ac peaks (`--keep-dup=auto –p 1e-9`) that contacted super-enhancers.

Metagenes and heatmaps are both produced from a matrix of adjusted read counts in bins across a set of genomic loci created using bamToGFF (<https://github.com/BradnerLab/pipeline>). Presumed PCR duplicate reads were removed using samtools rmdup (Li, Bioinformatics, 2009). Promoters were defined as regions  $\pm 2000$  bp from the transcription start sites of RefSeq transcripts. Enhancer and super-enhancer constituents were created by taking  $\pm 2000$  bp from the center of peaks as defined above. Metagenes and heatmaps (Figure 4D, E) were created at promoters, enhancers, and super-

enhancer constituents using bamToGFF with parameters `-m 200 -r -d` to get the RPM-normalized density of reads in these 200 equally-sized bins. Metagenes were produced from the mean of each bin across all genomic regions. Heatmaps were created using the values of each bin in each region and are sorted by the means of CDK7 density across all bins in that region.

## Chapter 4: Conclusions and future directions

---

### Conclusions

Transcription factors are attractive targets in cancer therapy, but developing potent inhibitors against them has proven difficult. General transcriptional regulator proteins are more chemically tractable as they can contain substrate-binding or catalytic domains, but targeting them might result in substantial off-target toxicities, given their supposed general functions in transcription. Recent work, however, has demonstrated that inhibitors against GTRs can result in gene-selective effects on tumor cell oncogenes. Tumor cells appear to be especially vulnerable to GTR inhibitors because of their dependency on high-level expression of these oncogenes. The cells in turn possess dependencies, or “addictions” on the GTRs that regulate oncogene expression.

Several GTRs contain substrate-binding or catalytic domains, and, in my thesis I examined the cellular and molecular effects of inhibiting one such GTR, CDK7, with the novel small-molecule inhibitor THZ1. In addition, I determined whether combining THZ1 and BRD4 inhibitor JQ1 could result in synergy in cancer cells. Furthermore, we are currently testing potential synergy in a xenograft mouse model of human T-ALL in collaboration with Kwok-Kin Wong’s laboratory at the Dana-Farber Cancer Institute. In Chapter 2, I described results demonstrating exquisite sensitivity of T-ALL cells to THZ1, suggesting that these



cells may be “transcriptionally addicted” to CDK7, which was likely due at least in part to selective down-regulation of the oncogenic TF *RUNX1*. In Chapter 3, I showed that THZ1 and JQ1 treatment results in synergistic effects on T-ALL cell survival. The two inhibitors cause vastly different effects on gene expression, suggesting that different genes may be especially dependent on CDK7 and BRD4. Furthermore, combining the two inhibitors increases the number of sensitive genes and severity of effect on gene expression. These results suggest that critical oncogenes may be differentially dependent on CDK7 and BRD4, and the sum of these transcriptional changes may have caused the synergistic cellular response.

## **Future directions**

Overall, my results provide evidence for CDK7 as a transcriptional dependency in tumor cells, synergism between CDK7 and BRD4 inhibition, and differential dependency on the two GTRs for oncogene expression. My work inspires three main avenues for future research, of which I discuss next: 1) further study into the molecular basis underlying synergism between THZ1 and JQ1, 2) investigation of the mechanisms contributing to THZ1 and JQ1 resistance, and 3) the discovery of other transcriptional addictions in cancer cells.

## **Investigation into the molecular basis underlying THZ1 and JQ1 synergism**

### *Molecular basis of differential dependencies on GTRs*

Studies with JQ1 and THZ1 have demonstrated gene-selective effects in response to BRD4 or CDK7 inhibition in cancer cells (Loven et al., 2010; Chapuy et al., 2013; Kwiatkowski et al., 2014; Christensen et al., 2014; Chipumuro et al., 2014; Wang et al., 2015). My results indicate that these gene-selective effects are largely dissimilar, suggesting that different genes may be especially dependent on the two GTRs for expression. This unique reliance on certain GTRs could result from the absence of functionally redundant pathways. For example, other kinases have been shown to phosphorylate Serine 5 on the Pol II CTD, including CDK8 (Ramanathan et al., 2001), CDK9 (Czudnochowski et al., 2012), and the MAP kinase ERK2 (Tee et al., 2014). Likewise, other pause release factors, such as MYC, likely contribute to P-TEFb recruitment in addition to BRD4 (Rahl et al., 2010; Lin et al., 2012). Genes that appear uniquely dependent on BRD4 may lack alternative mechanisms for P-TEFb recruitment.

Because CDK7 and BRD4 have differing mechanistic functions, genes that are uniquely dependent on either inhibitor are expected to have different transcriptional defects. Transcription initiation is expected to change with CDK7 loss, in contrast to BRD4 inhibition, which predominantly affects elongation. Therefore, THZ1 treatment likely causes transcription initiation defects at CDK7-dependent genes, and these changes are not expected for BRD4-dependent genes. To investigate this possibility, changes in transcription initiation and elongation can be assessed by examining the distribution of Pol II molecules in its various phosphorylated states on the bodies of genes uniquely sensitive to each inhibitor. For example, genes uniquely sensitive to THZ1 may have reduced

levels of phosphorylated Serine 5 of Pol II CTD at regions proximal to promoters as compared to genes insensitive to the inhibitor. Likewise, reduced levels of phosphorylated Serine 2 of Pol II CTD are expected in response to JQ1 treatment for genes sensitive to the inhibitor. These experiments could provide a molecular explanation for why certain genes may be sensitive to one GTR inhibitor but not the other, and vice versa.

Genetic heterogeneity among different cells within a tumor cell population influences the oncogenic addictions that drive individual cells. Since different oncogenes appear to be especially dependent on different GTRs, cell-to-cell heterogeneity in drug sensitivity likely exists within tumor populations. This is exemplified by the portion of cells corresponding to leukemic stem cells in AML and T-ALL that are tolerant to JQ1 (Rathert et al., 2015; Fong et al., 2015) and NOTCH inhibition (Knoechel et al., 2014). Single cell methodologies, such as single molecule RNA fluorescence in situ hybridization (RNA-FISH), can be used to detect cell-to-cell variability in oncogene sensitivity to GTR inhibitors. Furthermore, single-cell quantification of nascent and steady-state transcript levels following combined treatment could reveal heterogeneous responses to the inhibitors within the cell population.

#### *Functional interdependence of CDK7 and BRD4*

Approximately 100 transcripts were sensitive to treatment with either THZ1 or JQ1, suggesting that activities of each target are required for full expression of these genes. Furthermore, combined treatment of the drugs

affected expression to a greater extent than single-drug treatments, further supporting the idea that CDK7 and BRD4 both contribute to expression of these genes. The combined treatment resulted in gene expression changes corresponding in magnitude to the sum of changes with single-drug treatments, suggesting a functionally non-redundant role for CDK7 and BRD4 at these genes. If functional redundancy existed between CDK7 and BRD4, combined inhibitor treatment would be expected to “unmask” any compensatory action of the two proteins. However, the question still remains of how functionally inter-connected are CDK7 and BRD4 at these genes.

CDK7 and BRD4 are generally thought to function in a sequential order through their regulation of Pol II and P-TEFb, respectively. An additional layer of regulation might also implicate functional convergence of the two proteins. CDK7 has been shown to phosphorylate CDK9 through its CAK activity, which contributes to full activation of P-TEFb (Larochelle et al., 2012). Furthermore, studies have shown that CDK7, CDK9, and BRD4 can regulate the activities of each other through CDK-mediated phosphorylation and atypical BRD4 kinase activity (Devaiah et al., 2012; Devaiah and Singer, 2012). These collective functional links may therefore contribute to defects in transcription elongation that are enhanced with the combined treatment. These upstream transcriptional defects may play roles in driving synergistic cellular responses in response to the two inhibitors. If CDK7 and BRD4 have inter-connected roles in regulating their activities and that of Pol II, investigating the reciprocal effects of inhibiting each protein on a genome-wide level would reveal these functional differences. For

example, phosphorylated substrates of CDK7 could be affected by BRD4 inhibition, and likewise, THZ1 treatment may affect the genomic occupancy of BRD4.

### **Investigate mechanisms of resistance to THZ1 and JQ1**

#### *Compare transcriptional states of drug-resistant and drug-sensitive cells*

Cancer cells can acquire resistance to transcriptional inhibitors through activation of alternative enhancers to maintain expression of critical oncogenes. This has been shown in AML cells in response to prolonged sub-lethal treatment with JQ1 (Rathert et al., 2015). A unique enhancer was found in MLL-AF9-driven AML cells that had become resistant to JQ1, but not in JQ1-sensitive cells, which drove high-level expression of *MYC*. This enhancer did not rely on BRD4 activity, but instead was bound by Wnt pathway effector TFs. Furthermore, JQ1-resistant cells were more sensitive to treatment with a Wnt inhibitor than JQ1-sensitive cells. T-ALL cells that acquired resistance to NOTCH1 inactivation with gamma secretase inhibitors (GSIs) were found to be more sensitive to JQ1 than GSI-sensitive cells (Knoechel et al., 2014). A new enhancer proximal to *MYC* was found in the GSI-resistant cells and was heavily occupied by BRD4. These studies exemplify the plasticity of enhancer activation in the development of resistance to transcriptional inhibitors.

Monitoring transcriptional changes following prolonged treatment with the inhibitors would lend insight into mechanisms that confer resistance. ChIP-seq

experiments with H3K27ac antibodies after prolonged inhibitor treatment would capture these changes and allow for the identification of new enhancers that drive oncogene expression in resistant cells. Monitoring genome-wide H3K27ac occupancy over time would reveal the dynamics of these enhancers: the rate at which they are formed or whether or not they are maintained after the drug is withdrawn. Examining transcription factor binding motifs within these acquired enhancers would help generate hypotheses of new transcriptional drivers in resistant cells. The role of these candidate drivers in maintaining resistant cell states could be determined through loss-of-function experiments with small-molecule inhibitors, if available, or through CRISPR/Cas9-mediated editing or silencing methods. Furthermore, examining genome-wide occupancy of other drug targets in resistant cells could indicate if cancer cells shift dependencies on one GTR to another during the acquisition of resistance to transcriptional inhibitors.

*Determine if THZ1-resistant cells display increased sensitivity to JQ1 (and vice versa)*

Cells that acquire resistance to one inhibitor could have increased sensitivity to another, as evidenced by JQ1-resistant AML cells with enhanced sensitivity to Wnt inhibition. Increased sensitivity to other inhibitors in drug-resistant cells could demonstrate the possible utility of these drugs as second-line therapeutics. Furthermore, cancer cell line profiling of the anti-proliferative effects of THZ1 and JQ1 have revealed cell lines relatively insensitive to the two drugs. The K562 chronic myelogenous leukemia cells are insensitive to JQ1

(IC<sub>50</sub> > 5  $\mu$ M), likely due to activation of new enhancers driving *MYC* expression immediately following treatment with JQ1 (Rathert et al., 2015). Short, 2-hour treatments with JQ1 led to the reduction in *MYC* expression levels in K562 cells, but these levels rebounded after two days, along with concomitant activation of a new 3' enhancer proximal to the *MYC* gene. Additionally, combination treatment with both JQ1 and another transcriptional inhibitor, such as THZ1, could negate this compensatory activity and render these cells sensitive to treatment. Cancer cell lines resistant to THZ1 have been identified (for example, D1.1, P31/FUJ, and L-428 hematopoietic cancer lines), and these cells may likewise be more sensitive to JQ1 on its own or when treated in combination.

### **Side-by-side comparisons with other transcriptional inhibitors**

Understanding the functional relationships between GTRs will inform rational design of drug combinations. Combining certain inhibitors targeting transcriptional regulators may result in unfavorable or antagonistic effects (Prebet et al., 2014; Isaa et al., 20015). These results necessitates studying the functional interdependence between GTRs and developing models describing synergistic, additive, or antagonist relationships between inhibitors that target them. DOT1L and BET inhibitors – two classes of inhibitors that are currently being evaluated separately in clinical trials—were recently shown to be synergistic, likely through an unanticipated functional relationship involving CBP/P300-induced acetylation bridging the activities of the two proteins (Gilan et al., 2016). This study could potentially inform rational combinations involving

BET inhibition, perhaps with members of the super elongation complex that have been shown to interact with DOT1L (Wong et al., 2015). Lastly, GTR inhibitors that affect different oncogenes will potentially provide novel strategies to target previously-undruggable oncogenic transcription factors whilst increasing our understanding of oncogene-specific dependencies.

There are several GTRs with catalytic or substrate-binding domains that serve as potential targets. Kinase activities include CDK8, CDK12, CDK13, CDK19, and TFIIF subunit RAP74. CDK8 is a known oncogene in colorectal cancer, and tool compounds have been recently developed that target it (Dale et al., 2015; Koehler et al., 2016; Schiemann et al., 2016; Bergeron et al., 2016). Studies have demonstrated gene-selective functions of CDK8 in regulating genes involved in Wnt/B-catenin, interferon beta, HIF1 alpha, response to serum starvation pathways (Firestein et al., 2008; Bancerek et al., 2013; Galbraith et al., 2013; Donner et al., 2010). Furthermore, CDK8 has been shown to phosphorylate Smad proteins, which are effectors of TGF- $\beta$  and BMP receptor signaling (Kato et al., 2002; Alarcon et al., 2009). Consistent with other Mediator subunits, CDK8 is bound to enhancers and promoters of actively transcribed genes and at greater levels to super-enhancers (Kagey et al., 2010). Examining the functional relationships of CDK8 and other SE-bound factors could therefore lend insight into the outcomes of inhibiting them together. Lastly, CDK12 and CDK13 are kinases thought to function in transcription elongation through phosphorylation of Pol II CTD Serine 2. CDK19 is paralogous to CDK8 and is another Mediator kinase, and RAP74 has been shown capable of auto-



phosphorylation (Rossignol et al., 1999).

In addition to CBP/p300, the TFIID subunit TAFII250 has been shown to have HAT activity (Lee and Young, 2000). If TAFII250 share substrates and is functionally redundant with CBP/p300, inhibitors targeting these proteins could affect similar genes and combined treatment could exacerbate the expression of this set. Alternatively, it is possible that the two HAT complexes acetylate vastly different substrates, or that different genes are especially dependent on either one. In this case, combined inhibition would affect a larger set of genes. In addition, combination with JQ1 and TAFII250 inhibitors could be synergistic as was shown with CBP/p300 bromodomain inhibitor (Picaud et al., 2015).

Cohesin, which is a ring-like complex involved in chromosomal organization, contains two subunits with ATPase activity, SMC1 and SMC3, that serve as potential targets, as cohesin is critical for enhancer-promoter interactions and has been shown to preferentially occupy super-enhancers. Importantly, recent data demonstrates the critical contribution of inappropriate chromosomal interactions in driving tumorigenesis (Hnisz et al., 2016), necessitating a means to target these aberrant structural processes. Furthermore, the SMC1B cohesin subunit was among the group of transcripts sensitive to both THZ1 and JQ1, and its loss in expression was accentuated with the combined treatment. If SMC1B is required for proper complex formation, these changes might affect enhancer-promoter interactions, as well as higher order structures facilitated by cohesin, that ultimately influence cellular responses to the drugs. Analyzing how chromatin interactions are affected in response to

the inhibitors, through technologies such as chromatin interaction analysis by paired-end tag sequencing (ChIA-PET), could reveal effects on chromosome structure of GTR inhibitors. Cohesin mediates chromosomal loops that help insulate groups of genes from surrounding transcriptional activity, facilitating the formation of insulated neighborhoods. GTR inhibitors could coordinately affect the expression of genes that exist within the same insulated neighborhood, and this aspect may also influence sensitivity to inhibitors.

Lastly, drugs initially developed to target processes other than transcription could directly influence it. For example, chromatin immunoprecipitation experiments recently demonstrated binding of the cell cycle kinase CDK6 to the *P16* promoter (Kollmann et al., 2013), suggesting that it may also function in transcriptional control. CDK6 inhibitors, such as abemaciclib, are currently in clinical trials. In addition, the heat shock factor HSP90 has been shown to be involved in transcriptional pause release (Sawarkar et al., 2012), and the ERK2 kinase has recently been implicated in transcription initiation through its ability to phosphorylate the CTD of Pol II at Serine 5 (Tee et al., 2014). These non-canonical transcriptional functions highlight that drugs in development for different molecular processes may have mechanisms of action that are unexpectedly similar to those of transcriptional inhibitors.

## **Conclusions**

My studies with THZ1, as monotherapy and in combination with JQ1,

demonstrate how gene-selective effects could result in tumor cell sensitivity. Transcription of certain oncogenes appears to be especially dependent on particular GTRs, suggesting that different oncogenes may respond to different inhibitors of GTRs. Inhibition of multiple GTRs can result in synergistic effects, and combining multiple GTR inhibitors may negate the emergence of resistant clones caused by transcriptional re-wiring. GTR inhibitors may also be suitable adjuvants in therapies involving other targeted inhibitors and chemotherapeutics that are currently in practice.

## References

- Alarcon, C., Zaromytidou, A.I., Xi, Q., Gao, S., Yu, J., Fujisawa, S., Barlas, A., Miller, A.N., Manova-Todorova, K., Macias, M.J., *et al.* (2009). Nuclear CDKs drive Smad transcriptional activation and turnover in BMP and TGF-beta pathways. *Cell* 139, 757-769.
- Bancerek, J., Poss, Z.C., Steinparzer, I., Sedlyarov, V., Pfaffenwimmer, T., Mikulic, I., Dolken, L., Strobl, B., Muller, M., Taatjes, D.J., *et al.* (2013). CDK8 kinase phosphorylates transcription factor STAT1 to selectively regulate the interferon response. *Immunity* 38, 250-262.
- Bergeron, P., Koehler, M.F., Blackwood, E.M., Bowman, K., Clark, K., Firestein, R., Kiefer, J.R., Maskos, K., McClelland, M.L., Orren, L., *et al.* (2016). Design and Development of a Series of Potent and Selective Type II Inhibitors of CDK8. *ACS Med Chem Lett* 7, 595-600.
- Chapuy, B., McKeown, M.R., Lin, C.Y., Monti, S., Roemer, M.G., Qi, J., Rahl, P.B., Sun, H.H., Yeda, K.T., Doench, J.G., *et al.* (2013). Discovery and characterization of super-enhancer-associated dependencies in diffuse large B cell lymphoma. *Cancer cell* 24, 777-790.
- Chipumuro, E., Marco, E., Christensen, C.L., Kwiatkowski, N., Zhang, T., Hatheway, C.M., Abraham, B.J., Sharma, B., Yeung, C., Altabef, A., *et al.* (2014). CDK7 inhibition suppresses super-enhancer-linked oncogenic transcription in MYCN-driven cancer. *Cell* 159, 1126-1139.
- Christensen, C.L., Kwiatkowski, N., Abraham, B.J., Carretero, J., Al-Shahrour, F., Zhang, T., Chipumuro, E., Herter-Sprie, G.S., Akbay, E.A., Altabef, A., *et al.* (2014). Targeting transcriptional addictions in small cell lung cancer with a covalent CDK7 inhibitor. *Cancer cell* 26, 909-922.
- Czudnochowski, N., Bosken, C.A., and Geyer, M. (2012). Serine-7 but not serine-5 phosphorylation primes RNA polymerase II CTD for P-TEFb recognition. *Nat Commun* 3, 842.
- Dale, T., Clarke, P.A., Esdar, C., Waalboer, D., Adeniji-Popoola, O., Ortiz-Ruiz, M.J., Mallinger, A., Samant, R.S., Czodrowski, P., Musil, D., *et al.* (2015). A selective chemical probe for exploring the role of CDK8 and CDK19 in human disease. *Nat Chem Biol* 11, 973-980.
- Devaiah, B.N., Lewis, B.A., Cherman, N., Hewitt, M.C., Albrecht, B.K., Robey, P.G., Ozato, K., Sims, R.J., 3rd, and Singer, D.S. (2012). BRD4 is an atypical kinase that phosphorylates serine2 of the RNA polymerase II carboxy-terminal domain. *Proceedings of the National Academy of Sciences of the United States of America* 109, 6927-6932.

Devaiah, B.N., and Singer, D.S. (2012). Cross-talk among RNA polymerase II kinases modulates C-terminal domain phosphorylation. *J Biol Chem* 287, 38755-38766.

Donner, A.J., Ebmeier, C.C., Taatjes, D.J., and Espinosa, J.M. (2010). CDK8 is a positive regulator of transcriptional elongation within the serum response network. *Nat Struct Mol Biol* 17, 194-201.

Firestein, R., Bass, A.J., Kim, S.Y., Dunn, I.F., Silver, S.J., Guney, I., Freed, E., Ligon, A.H., Vena, N., Ogino, S., *et al.* (2008). CDK8 is a colorectal cancer oncogene that regulates beta-catenin activity. *Nature* 455, 547-551.

Fong, C.Y., Gilan, O., Lam, E.Y., Rubin, A.F., Ftouni, S., Tyler, D., Stanley, K., Sinha, D., Yeh, P., Morison, J., *et al.* (2015). BET inhibitor resistance emerges from leukaemia stem cells. *Nature* 525, 538-542.

Galbraith, M.D., Allen, M.A., Bensard, C.L., Wang, X., Schwinn, M.K., Qin, B., Long, H.W., Daniels, D.L., Hahn, W.C., Dowell, R.D., *et al.* (2013). HIF1A employs CDK8-mediator to stimulate RNAPII elongation in response to hypoxia. *Cell* 153, 1327-1339.

Gilan, O., Lam, E.Y., Becher, I., Lugo, D., Cannizzaro, E., Joberty, G., Ward, A., Wiese, M., Fong, C.Y., Ftouni, S., *et al.* (2016). Functional interdependence of BRD4 and DOT1L in MLL leukemia. *Nat Struct Mol Biol* 23, 673-681.

Hnisz, D., Weintraub, A.S., Day, D.S., Valton, A.L., Bak, R.O., Li, C.H., Goldmann, J., Lajoie, B.R., Fan, Z.P., Sigova, A.A., *et al.* (2016). Activation of proto-oncogenes by disruption of chromosome neighborhoods. *Science* 351, 1454-1458.

Issa, J.P., Garcia-Manero, G., Huang, X., Cortes, J., Ravandi, F., Jabbour, E., Borthakur, G., Brandt, M., Pierce, S., and Kantarjian, H.M. (2015). Results of phase 2 randomized study of low-dose decitabine with or without valproic acid in patients with myelodysplastic syndrome and acute myelogenous leukemia. *Cancer* 121, 556-561.

Kato, Y., Habas, R., Katsuyama, Y., Naar, A.M., and He, X. (2002). A component of the ARC/Mediator complex required for TGF beta/Nodal signalling. *Nature* 418, 641-646.

Knoechel, B., Roderick, J.E., Williamson, K.E., Zhu, J., Lohr, J.G., Cotton, M.J., Gillespie, S.M., Fernandez, D., Ku, M., Wang, H., *et al.* (2014). An epigenetic mechanism of resistance to targeted therapy in T cell acute lymphoblastic leukemia. *Nat Genet* 46, 364-370.

Koehler, M.F., Bergeron, P., Blackwood, E.M., Bowman, K., Clark, K.R., Firestein, R., Kiefer, J.R., Maskos, K., McClelland, M.L., Orren, L., *et al.* (2016). Development of a Potent, Specific CDK8 Kinase Inhibitor Which Phenocopies CDK8/19 Knockout Cells. *ACS Med Chem Lett* 7, 223-228.

Kollmann, K., Heller, G., Schneckenleithner, C., Warsch, W., Scheicher, R., Ott, R.G., Schafer, M., Fajmann, S., Schlederer, M., Schiefer, A.I., *et al.* (2013). A kinase-independent function of CDK6 links the cell cycle to tumor angiogenesis. *Cancer cell* 24, 167-181.

Kwiatkowski, N., Zhang, T., Rahl, P.B., Abraham, B.J., Reddy, J., Ficarro, S.B., Dastur, A., Amzallag, A., Ramaswamy, S., Tesar, B., *et al.* (2014). Targeting transcription regulation in cancer with a covalent CDK7 inhibitor. *Nature* 511, 616-620.

Larochelle, S., Amat, R., Glover-Cutter, K., Sanso, M., Zhang, C., Allen, J.J., Shokat, K.M., Bentley, D.L., and Fisher, R.P. (2012). Cyclin-dependent kinase control of the initiation-to-elongation switch of RNA polymerase II. *Nat Struct Mol Biol* 19, 1108-1115.

Lee, T.I., and Young, R.A. (2000). Transcription of eukaryotic protein-coding genes. *Annu Rev Genet* 34, 77-137.

Lin, C.Y., Loven, J., Rahl, P.B., Paranal, R.M., Burge, C.B., Bradner, J.E., Lee, T.I., and Young, R.A. (2012). Transcriptional amplification in tumor cells with elevated c-Myc. *Cell* 151, 56-67.

Loven, J., Hoke, H.A., Lin, C.Y., Lau, A., Orlando, D.A., Vakoc, C.R., Bradner, J.E., Lee, T.I., and Young, R.A. (2013). Selective inhibition of tumor oncogenes by disruption of super-enhancers. *Cell* 153, 320-334.

Picaud, S., Fedorov, O., Thanasopoulou, A., Leonards, K., Jones, K., Meier, J., Olzscha, H., Monteiro, O., Martin, S., Philpott, M., *et al.* (2015). Generation of a Selective Small Molecule Inhibitor of the CBP/p300 Bromodomain for Leukemia Therapy. *Cancer Res* 75, 5106-5119.

Prebet, T., Sun, Z., Figueroa, M.E., Ketterling, R., Melnick, A., Greenberg, P.L., Herman, J., Juckett, M., Smith, M.R., Malick, L., *et al.* (2014). Prolonged administration of azacitidine with or without entinostat for myelodysplastic syndrome and acute myeloid leukemia with myelodysplasia-related changes: results of the US Leukemia Intergroup trial E1905. *J Clin Oncol* 32, 1242-1248.

Rahl, P.B., Lin, C.Y., Seila, A.C., Flynn, R.A., McCuine, S., Burge, C.B., Sharp, P.A., and Young, R.A. (2010). c-Myc regulates transcriptional pause release. *Cell* 141, 432-445.

Ramanathan, Y., Rajpara, S.M., Reza, S.M., Lees, E., Shuman, S., Mathews, M.B., and Pe'ery, T. (2001). Three RNA polymerase II carboxyl-terminal domain kinases display distinct substrate preferences. *J Biol Chem* 276, 10913-10920.

Rathert, P., Roth, M., Neumann, T., Muerdter, F., Roe, J.S., Muhar, M., Deswal, S., Cerny-Reiterer, S., Peter, B., Jude, J., *et al.* (2015). Transcriptional plasticity promotes primary and acquired resistance to BET inhibition. *Nature* 525, 543-547.

Rossignol, M., Keriél, A., Staub, A., and Egly, J.M. (1999). Kinase activity and phosphorylation of the largest subunit of TFIIF transcription factor. *J Biol Chem* 274, 22387-22392.

Sawarkar, R., Sievers, C., and Paro, R. (2012). Hsp90 globally targets paused RNA polymerase to regulate gene expression in response to environmental stimuli. *Cell* 149, 807-818.

Schiemann, K., Mallinger, A., Wienke, D., Esdar, C., Poeschke, O., Busch, M., Rohdich, F., Eccles, S.A., Schneider, R., Raynaud, F.I., *et al.* (2016). Discovery of potent and selective CDK8 inhibitors from an HSP90 pharmacophore. *Bioorg Med Chem Lett* 26, 1443-1451.

Tee, W.W., Shen, S.S., Oksuz, O., Narendra, V., and Reinberg, D. (2014). Erk1/2 activity promotes chromatin features and RNAPII phosphorylation at developmental promoters in mouse ESCs. *Cell* 156, 678-690.

Wang, Y., Zhang, T., Kwiatkowski, N., Abraham, B.J., Lee, T.I., Xie, S., Yuzugullu, H., Von, T., Li, H., Lin, Z., *et al.* (2015). CDK7-dependent transcriptional addiction in triple-negative breast cancer. *Cell* 163, 174-186.

Wong, M., Polly, P., and Liu, T. (2015). The histone methyltransferase DOT1L: regulatory functions and a cancer therapy target. *Am J Cancer Res* 5, 2823-2837.

## **Appendix: Supplemental information for Chapter 2**

---



### **Supplementary Table 1 | Literature compounds that inhibit CDK7**

Compounds (with references) that have demonstrated activity against CDK7 and other CDKs.

### **Supplementary Table 2 | KiNativ™ kinome profiling identifies CDK7 as a target of phenylamino-pyrimidine-based compounds.**

Loucy cells were treated with DMSO, THZ1 (1  $\mu$ M), or THZ1-R (1  $\mu$ M) for 4 hrs. PBS-washed cell pellets were flash frozen and subjected to KiNativ™ kinome profiling at ActivX Biosciences, Inc. according to their specifications using their desthiobiotin-ATP probe. Peptide sequences shown above belong to the indicated kinase(s) and were detected by mass spectrometry (MS) under DMSO control conditions following enrichment for biotinylated proteins by streptavidin pulldown and subsequent proteolysis. Kinases labeled by the reactive desthiobiotin-ATP probe indicate that the kinase was accessible to desthiobiotin-ATP probe binding. Results shown are normalized to these paired DMSO controls and numbers represent the percentage (compared to DMSO control) of MS signal lost for sequences of an indicated kinase, eg – numbers approaching 100% indicate that test compound effectively out-competed the desthiobiotin ATP probe for binding to the kinase, resulting in decreased labeling and enrichment for peptides representing this kinase.

### **Supplementary Table 3 | THZ1 displays time-dependent inactivation of recombinant CDK7.**

CDK7 is inhibited in a time-dependent manner.  $K_D$  values

were determined at three different time points (20, 60, and 180 minutes) for THZ1 and THZ1-R using the LanthaScreen® Eu Kinase Binding Assay for each individual kinase according to the manufacturer's specifications. The ratio of the  $K_D$  values generated at 20 and 180 minutes was used to assess whether kinases displayed time-dependent inactivation.

**Supplementary Table 4 | THZ1 displays broad-based antiproliferative activity against cancer cell lines.** THZ1 exhibits strong antiproliferative effects across a broad range of cancer cell lines from various cancer types including blood cancers. Cancer cells were treated with THZ1 or DMSO vehicle for 72 hrs and assessed for antiproliferative effect using resazurin.

**Supplementary Table 5 | Genomic features identified as predictors of response to CDK-7-IN-1 by elastic net regression.** IC50 data was used to identify genomic features across 527 number of cell lines with available genomic data (mRNA, copy number variations and mutational data). For each gene association the frequency and the magnitude of the effect of the interaction are presented. Negative effects correspond to sensitivity features (for gene expression, high expression in sensitive cell lines for mutation presence of the mutation in sensitive cell lines). Functional enrichment analysis of the genomic features identified by elastic net regression. The functional enrichment tool (DAVID) from the National Institute of Allergy and Infectious Diseases was used to identify functional classes of genes enriched in the elastic net output.

**Supplementary Table 6 | Pharmacokinetics properties of THZ1 in KOPTK1 T-ALL xenograft mouse model.** Blood plasma and liver harvested from THZ1 – treated mice were analyzed for the presence of THZ1. Concentration is given in ng/ mL and micromolar ( $\mu$ M).

**Supplementary Table 7 | Gene expression tables.** Spike-in normalized mean Log2 treatment microarray expression grouped with corresponding DMSO or untreated controls and corresponding treatment-vs.-DMSO fold-changes.

**Supplementary Table 8 | Super-enhancer identification and gene assignment.** Total H3K27Ac ChIP-seq signal (length \* density) and Input DNA control signal in all stitched enhancers in Jurkat. Enhancers are ranked by increasing Input-subtracted H3K27Ac ChIP-seq signal. Super-enhancers were assigned to the RefSeq transcript whose TSS falls nearest to the center of the super-enhancer.

**Extended Data Figure 1 | THZ1 demonstrates time-dependent inhibition of CDK7 *in vitro* and covalent binding of intracellular CDK7.** **a**, THZ1 but not THZ1-R shows time-dependent inhibition. LanthaScreen® Eu Kinase Binding assay was conducted at Life Technologies in a time-dependent manner (20, 60, and 180 min.) showing that THZ1 but not THZ1-R shows time-dependent inhibition of CDK7. **b and c**, Pre-incubation of THZ1 increases CDK7 inhibitory

activity *in vitro*. Recombinant CAK complex was incubated with THZ1 (**b**) or THZ1-R (**c**) in dose response format with or without pre-incubation prior to ATP (25  $\mu$ M) addition. Kinase reaction was then allowed to proceed for 45 minutes at 30°C. **d**, Workflow of bio-THZ1 pull down competition experiment. **e**, bio-THZ1 pulls down CDK7 from cellular lysates. Loucy cellular lysates were incubated with bio-THZ1 (1  $\mu$ M) with or without THZ1 (10  $\mu$ M) and streptavidin-precipitated proteins were probed for CDK7. IB = immunoblot. **f**, Free intracellular THZ1 competes in a dose-dependent manner for bio-THZ1 binding to CDK7. Loucy cells were treated with increasing concentrations of THZ1 or with 10  $\mu$ M THZ1-R for 4 hrs. Cellular lysates were incubated with bio-THZ1 and processed as indicated in **a**. **g**, bio-THZ1 labels CDK7 in lysates. Loucy cellular lysates were incubated with bio-THZ1 at 4°C for 12 hrs followed by immunoprecipitation of CDK7 at 4°C for 3 hrs. Precipitated proteins were washed and probed with streptavidin-HRP.

### **Extended Data Figure 2 | THZ1 covalently binds CDK7 C312**

**a** and **b**, Total ion chromatograms (TIC) and extracted ion chromatograms (XIC) for CDK7 peptides recorded during analysis of CAK complexes treated with DMSO (**a**) or THZ1 (**b**). **c**, Efficiency of labeling was estimated to be approximately 85% gauged by the reduction in signal of triply and quadruply charged YFSNRPGPTPGCQLPRPNCPVETLK ions (residues 294-318). The peptides VPFLPGDSDLQLTR (residues 180-194) and LDFLGEGQFATVYK (residues 15-28) were used for normalization. **d**, Orbitrap HCD MS/MS spectrum

of a quadruply charged CDK7 derived peptide (residues 294-318) labeled by THZ1 at C312. Fragment ions containing the peptide C-terminus (y-type) or N-terminus (b-type), along with the associated mass errors are shown in red and blue, respectively. Fragment ions marked by (\*) contain the inhibitor and have the expected heavy isotope contribution from chlorine. The site of labeling was determined to be C312 (as opposed to C305) based on fragment ions observed in additional MS/MS spectra (for example  $y11^{3+}$  observed with  $< 3$  ppm mass error by fragmentation of the +6 charged precursor; see inset mass spectrum). **e**, C312S mutation eliminates THZ1 covalent binding. Cellular lysates from HCT116 cells expressing either FLAG-CDK7 WT or C312S were incubated with bio-THZ1 for 12 hrs at 4°C and then room temperature for 3 hrs to facilitate covalent binding. Precipitated proteins were then probed for the presence of FLAG-tagged CDK7.

**Extended Data Figure 3 | THZ1 inhibits CDK12 but at higher concentrations compared to CDK7.** **a**, Protein sequence alignment of the C-terminal regions of all human (hs) CDKs and mouse (m) CDK7 using Uniprot default settings. Note that the canonical cell cycle CDKs 1,2,4 as well as 5 do not have C-terminal domains that extent to the equivalent position of CDK7 C312 and therefore do not display aligned sequence in this region. **b**, bio-THZ1 covalently pulls down CDK7 from cellular lysates. Jurkat cellular lysates were incubated with bio-THZ1 (1  $\mu$ M) at 4°C for 12 hrs and 2 hrs at room temperature. Precipitated proteins were washed with or without urea (4M), here used as a denaturing agent, and

probed for the indicated CDKs. **c**, bio-THZ1 pulls down FLAG-CDK12 from lysates. Lysates from 293A cells stably expressing FLAG-tagged WT CDK12 were incubated with bio-THZ1 (1  $\mu$ M) at 4°C for 12 hrs and 2 hrs at rt. Immunoprecipitated proteins were probed with FLAG antibody to recognize CDK12 or with CDK7 antibody. **d**, bio-THZ1 pulls down cyclin K from cellular lysates. Jurkat cellular lysates were incubated with bio-THZ1 (1  $\mu$ M) at 4°C for 12 hrs and 2 hrs at rt. Precipitated proteins were probed for the indicated proteins. **e**, THZ1 inhibits CDK12 in an *in vitro* kinase assay. 293A cells stably expressing FLAG-tagged WT CDK12 were treated with THZ1 or THZ1-R for 4 hrs. Exogenous CDK12 was immunoprecipitated from cellular lysates using FLAG antibody. Precipitated proteins were washed and subjected to *in vitro* kinase assays at 30°C for 30 minutes using the large subunit of RNAPII (RPB1) as substrate and 25  $\mu$ M ATP. CS = coomassie stain. **f**, Quantitation of *in vitro* kinase assay conducted in (d).

**Extended Data Figure 4 | THZ1 irreversibly inhibits RNAPII CTD and CAK phosphorylation.** **a**, THZ1 exhibits time-dependent inactivation of intracellular CDK7. Loucy cells were treated with THZ1 or THZ1-R for 0 to 4 hrs. At each time point cells were harvested, lysed, and the cellular lysates were probed with antibodies against the specified proteins. **b**, THZ1 inhibits RNAPII CTD phosphorylation. Loucy cells were treated with THZ1 or THZ1-R for 4 hrs. Cellular lysates were then probed with antibodies recognizing the Ser-2, Ser-5, and Ser-7 CTD RNAPII phosphoepitopes. **c**, Loucy cells were treated with THZ1

or THZ1-R for 4 hrs followed by washout of inhibitor-containing medium. Cells were allowed to grow in medium without inhibitor for 0 to 6 hrs. At each time point cells were lysed and the cellular lysates were probed with antibodies against the specified proteins. 'N' signifies cells where medium was never washed out. **d**, Apoptotic signaling is maintained despite washout of THZ1. Loucy cells were treated with THZ1 or THZ1-R for 4 hrs followed by washout of inhibitor-containing medium, at which point cells were allowed to grow in medium with or without inhibitor for 0 to 48 hrs. At each time point cells were lysed and the cellular lysates were probed with antibodies against the specified proteins. **e**, Antiproliferative effects of THZ1 are impervious to inhibitor washout. Loucy cells were treated with THZ1 or THZ1-R in dose response format for 72 hrs. Antiproliferative effects were determined using cell titer glo analysis. **f**, THZ1 reduces the T-loop phosphorylation status of CDK1 and CDK2 in Jurkat cells over a 3 hour exposure. Asynchronous cells were treated with increasing concentrations of THZ1 or THZ1-R for 3 hrs. Cellular lysates were then probed with antibodies against the indicated proteins or phosphoproteins. **g**, THZ1, but not THZ1-R, completely inhibits T-loop phosphorylation of CDK1 and CDK2 following treatment over one cell cycle. Loucy cells were treated with THZ1, THZ1-R, Flavopiridol, or DMSO vehicle at the indicated concentrations for 24 and 14 hrs, respectively (roughly one cell cycle). Cell lysates were harvested and probed with antibodies against the specified proteins or phosphoproteins. **h**, Hela S3 cells stably expressing FLAG-WT CDK7 were treated with THZ1 (1  $\mu$ M) or DMSO vehicle for 5 hrs with and without the presence of doxycycline.

Proteins were immunoprecipitated using FLAG antibody. Precipitated proteins were probed using the indicated antibodies. \* indicates heavy-chain from IgG antibody.

**Extended Data Figure 5 | Mutation of CDK7 Cys-312 to serine rescues Ser-5/7 and partially Ser2 RNAPII CTD phosphorylation.** **a**, Expression of C312S rescues Ser-5/7 and partially rescues Ser-2 RNAPII CTD phosphorylation. HeLa S3 cells stably carrying a doxycycline-inducible FLAG-C312S CDK7 construct were treated with THZ1 or DMSO for 5 hrs with and without the presence of doxycycline. Cellular lysates were then probed for the indicated proteins. **b**, Phenotypic rescue is specific to C312S mutation as rescue is not achieved with overexpression of FLAG-WT CDK7. HeLa S3 cells stably carrying doxycycline-inducible FLAG-WT and C312S CDK7 constructs (or empty vector) were treated with THZ1 or DMSO for 5 hrs in the presence of doxycycline. **c**, Expression of C312S largely restores CDK1/2 T-loop phosphorylation. HeLa S3 cells stably carrying a doxycycline-inducible FLAG-C312S CDK7 construct were treated with THZ1 or DMSO for 5 hrs with and without the presence of doxycycline. Cellular lysates were then probed for the indicated proteins or phosphoproteins. **d**, Overexpression of FLAG-CDK7 C312 rescues the expression of a subset of transcripts in HeLa S3 cells. Log2 fold change in gene expression in HeLa S3 cells expressing FLAG-CDK7 WT (x axis) and FLAG-CDK7 C312S (y axis) following a 4 hr treatment with 500 nM THZ1. **e**, Gene ontology molecular function analysis of transcripts increased by 1 log2 order or more following



expression of FLAG-CDK7 C312S compared to FLAG-CDK7 WT in the presence of 500 nM THZ1.

**Extended Data Figure 6 | THZ1 potently disrupts T-ALL proliferation.**

**a**, THZ1, but not THZ1-R, exhibits strong antiproliferative effect against T-ALL cell lines. Cells were treated with THZ1, THZ1-R, or DMSO vehicle for 72 hrs and assessed for antiproliferative effect by Cell Titer Glo analysis. Error bars are +/- SD. **b**, THZ1 causes cell cycle arrest. Jurkat (top) and Loucy (bottom) T-ALL cells were treated with THZ1 for the indicated time periods. Cell cycle progression was assessed using FACS cell cycle analysis. 2N = G1, 4N = G2. **c**, Treatment with THZ1 decreases CDK1/2 T-loop phosphorylation. Jurkat cells were incubated with THZ1 for the indicated duration of time and lysates were probed for the specified proteins.

**Extended Data Figure 7 | Treatment with THZ1 induces apoptosis in T-ALL cells.**

**a**, Representative Annexin V and propidium iodide stainings for Jurkat cells incubated with THZ1 for the indicated amount of time and harvested to determine the percentage of apoptotic and/ or dead cells by Annexin V and propidium iodide staining, respectively. The percentage of cells in each cell population is shown in the four quadrants. **b**, Treatment with THZ1 induces apoptosis. Quantitation of Annexin V and propidium iodide staining data from **a**. Experiments were performed in biological triplicates and error bars are +/- SD.

c, Representative Annexin V and propidium iodide stainings for Loucy cells incubated with THZ1 for the indicated amount of time and harvested to determine the percentage of apoptotic and/ or dead cells by Annexin V and propidium iodide staining, respectively. The percentage of cells in each cell population is shown in the four quadrants. d, Treatment with THZ1 induces apoptosis. Quantitation of Annexin V and propidium iodide staining data from c. Experiments were performed in biological triplicates and error bars are +/- SD. e and f, Sustained treatment with THZ1 induces apoptosis coincident with loss of RNAPII CTD phosphorylation and reduction in anti-apoptotic proteins. Jurkat (e) and Loucy (f) cells were incubated with THZ1 for the indicated duration of time and lysates were probed for the specified proteins. Apoptosis was monitored by PARP cleavage.

**Extended Data Figure 8 | THZ1 demonstrates potent killing of primary chronic lymphocytic leukemia (CLL) cells and anti-proliferative activity against primary T-ALL cells and *in vivo* against a human T-ALL xenograft.**

a, CLL cells were cultured *in vitro* for 24 hrs in the presence of multiple doses of the specified compound. Results shown are mean normalized % death based on Annexin V / PI single and double positive cells (+/- SD) normalized to baseline death in the DMSO control wells. 10 patient samples were exposed to THZ1, THZ1-R and Flavopiridol (THZ1 vs. THZ1-R  $p = 1.5E-38$ ; THZ1 vs. Flavopiridol  $p = 0.05$ ). P-values were generated using an analysis of variance model. b, Patient-derived xenografts (patient ID# 3255-1, M18-1-5, D135-1-5;  $n=3$ ) were

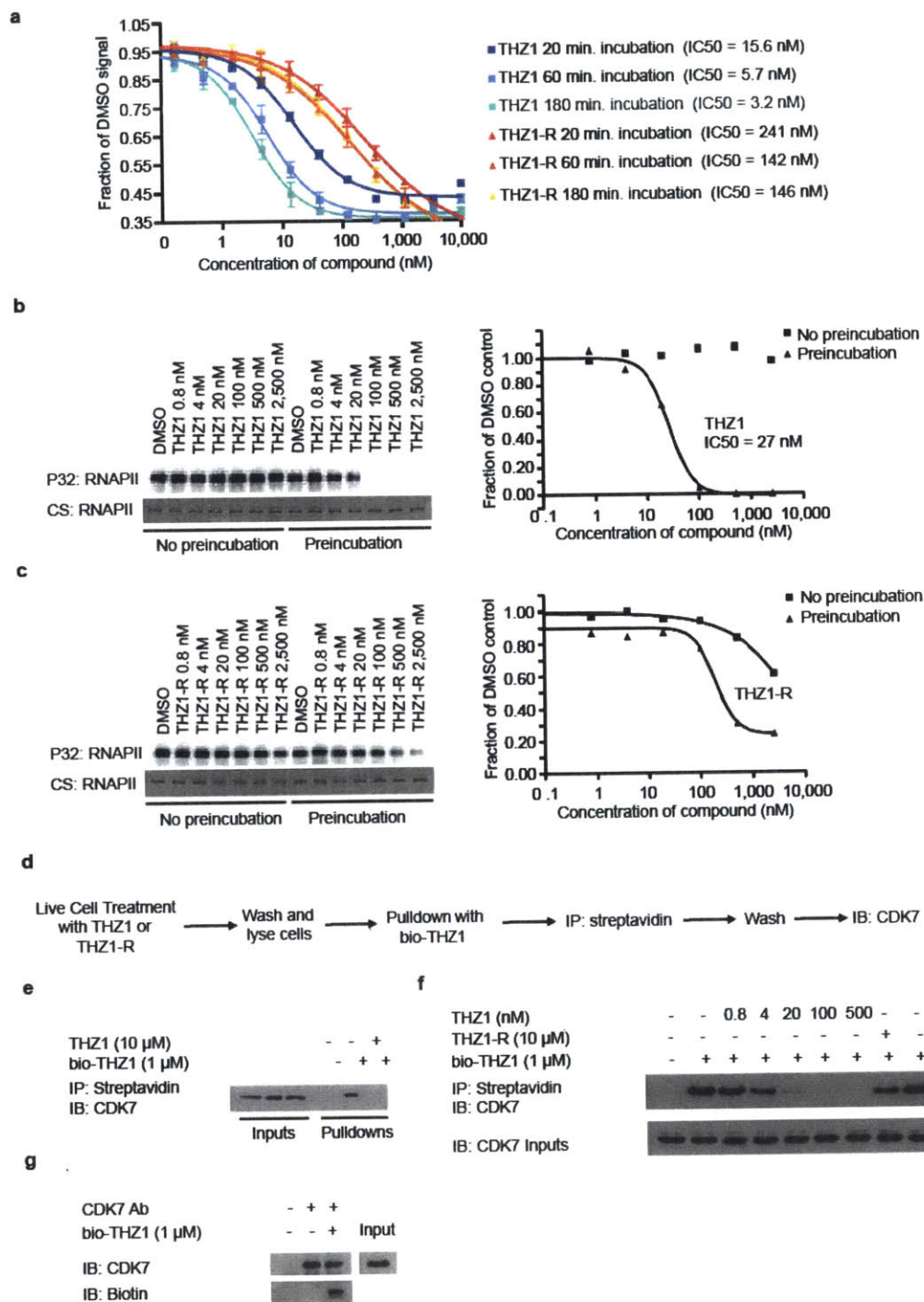
treated with THZ1 for 3 hrs followed by compound washout. An aliquot of input cells was then counted by flow cytometry using a known quantity of flow cytometry calibration beads (data not shown; Molecular Probes). The remaining cells were plated onto MS5-DL1 feeder cells in the presence of serum-free media (supplemented with 0.75 $\mu$ M SR1, 10ng/ml IL7, 10ng/ml IL2). 72 hrs later, cultures were harvested by vigorous pipetting with Trypsin, filtered through nylon mesh to deplete feeders, and counted by flow cytometry using a known quantity of flow cytometry calibration beads and with gating to discriminate between T-ALL cells and carryover feeders. The final cell number was normalized to the input cell number to calculate fold expansion. This experiment was performed once per patient-derived sample. **c**, Bioluminescent images of two representative mice treated with either vehicle control, 10 mg/kg THZ1 qD (once daily), or 10 mg/kg/day THZ1 BID (twice daily) for indicated number of days. **d**, Spleen tissue from mice treated with THZ1 show decreased RNAPII CTD phosphorylation. Mice were treated with THZ1 10 mg/kg qD or BID or vehicle control. The animals were sacrificed and spleen tissues were isolated. Lysates prepared from homogenized spleen tissue were probed for RNAPII CTD phosphoepitopes. **e**, THZ1 binds directly to CDK7 in mouse tissues. Mice were treated with THZ1 10 mg/kg qD or BID or vehicle control. The animals were sacrificed and spleen tissues were isolated. Lysates prepared from homogenized spleen tissue were incubated with bio-THZ1 for 12 hrs at 4 °C and 2 hrs at rt to induce covalent bond formation. Proteins pulled down were then probed for the presence of CDK7. **f**, Body weights of mice treated with either

vehicle control, 10 mg/kg THZ1 qD (once daily), or 10 mg/kg/day THZ1 BID (twice daily) over the duration of the drug treatment.

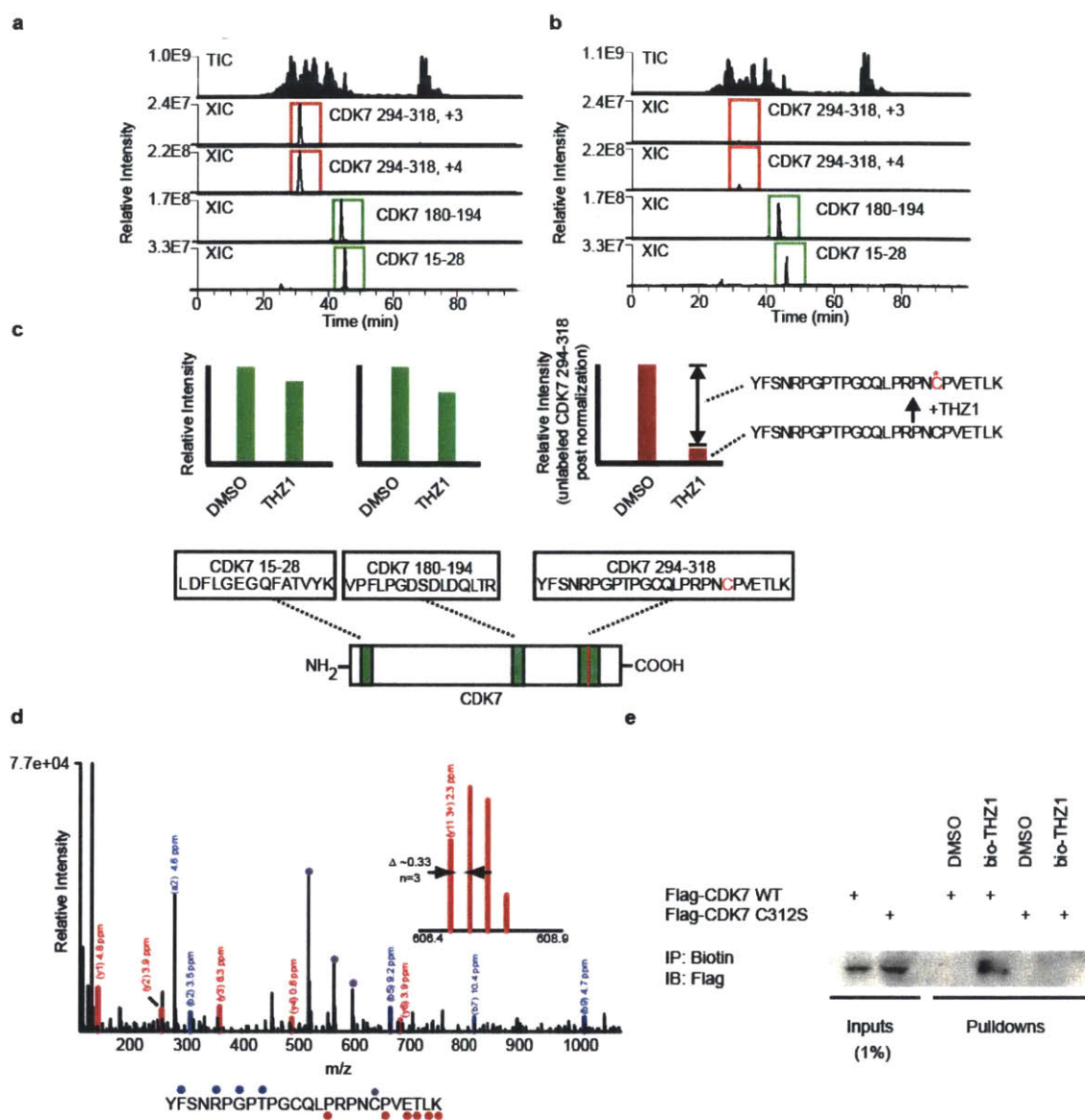
**Extended Data Figure 9 | THZ1 inhibits RNAPII CTD phosphorylation and causes cell cycle arrest in non-transformed cell lines.** **a** and **b**, THZ1 inhibits RNAPII CTD phosphorylation. RPE-1 (**a**), and BJ fibroblasts (**b**) were treated with THZ1 or THZ1-R for 4 hrs. Cellular lysates were then probed with antibodies against the indicated proteins. **c** and **d**, THZ1 causes cell cycle arrest in non-transformed cells. RPE-1 (**c**) and BJ fibroblasts (**d**) cells were treated with THZ1, Flavopiridol, Staurosporine, or DMSO vehicle for the indicated time periods. Cell cycle progression was analyzed following permeabilization and staining with propidium iodide. **e** and **f**, THZ1 inhibits proliferation of non-transformed cell lines. RPE-1 (**e**) and BJ fibroblasts (**f**) cells were treated with THZ1, THZ1-R, Flavopiridol, or Staurosporine for 72 hrs and antiproliferative effect was determined by Cell Titer Glo. Error bars are +/- SD.

**Extended Data Figure 10 | High dose THZ1 reduces global steady-state mRNA levels, but low dose THZ1 preferentially downregulates components of the TAL1/RUNX1/GATA3 transcriptional circuit.** **a**, THZ1, but not THZ1-R, causes global downregulation of steady-state mRNA levels. Jurkat cells were treated with THZ1 (250 nM) or THZ1-R (250 nM) for 4 hrs. Total RNA was isolated and ERCC spike-in controls were added relative to cell number and analyzed using Affymetrix Primeview microarrays. Heatmaps displaying the

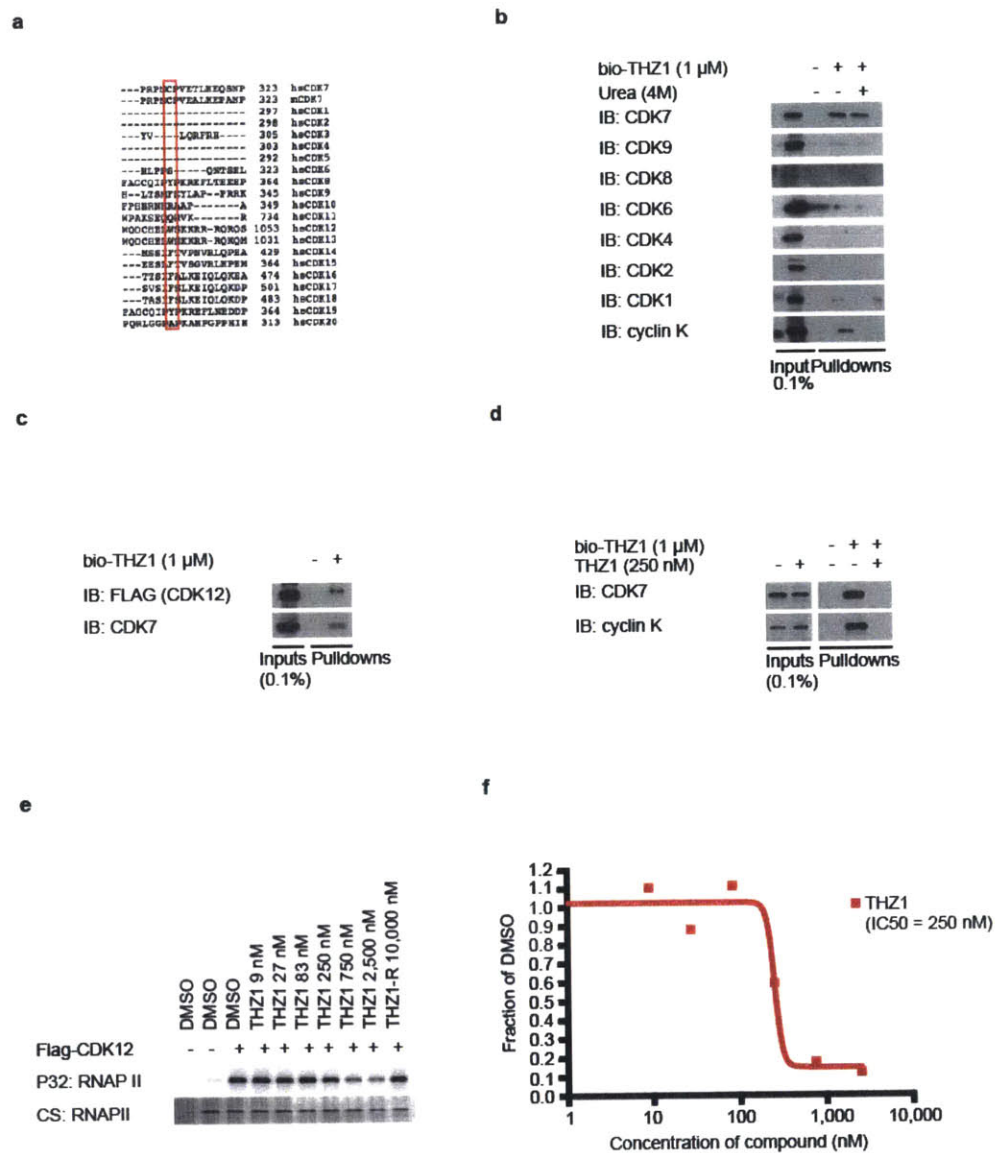
Log2 fold change in gene expression vs. DMSO for 22,310 genes expressed in DMSO conditions at 6h in THZ1 or THZ1-R. **b**, Total H3K27Ac ChIP-seq signal (length \* density) in enhancer regions for all stitched enhancers in Jurkat. Enhancers are ranked by increasing H3K27Ac ChIP-seq signal. **c** and **d**, Gene tracks of H3K27Ac (top), CDK7 (middle), and RNAPII (bottom) ChIP-seq occupancy at the TSS, gene body, and enhancer regions of *TAL1* (**c**) and *MYB* (**d**). **e**, THZ1 downregulates mRNA transcripts of the TAL1/RUNX1/GATA3 transcriptional circuitry. RT-qPCR expression analysis in Jurkat cells of transcripts identified as downregulated following THZ1 treatment relative to DMSO. All experiments shown were performed in biological triplicate. Each individual biological sample was qPCR-amplified in technical triplicate. Error bars are +/- SD. Taqman universal expression probes and normalized to ACTB. **f**, THZ1 treatment reduces the protein levels of TAL1/RUNX1/GATA3 transcriptional circuitry. Jurkat cells treated with THZ1 for the indicated time points were probed for the specified proteins.



Extended Data Figure 1



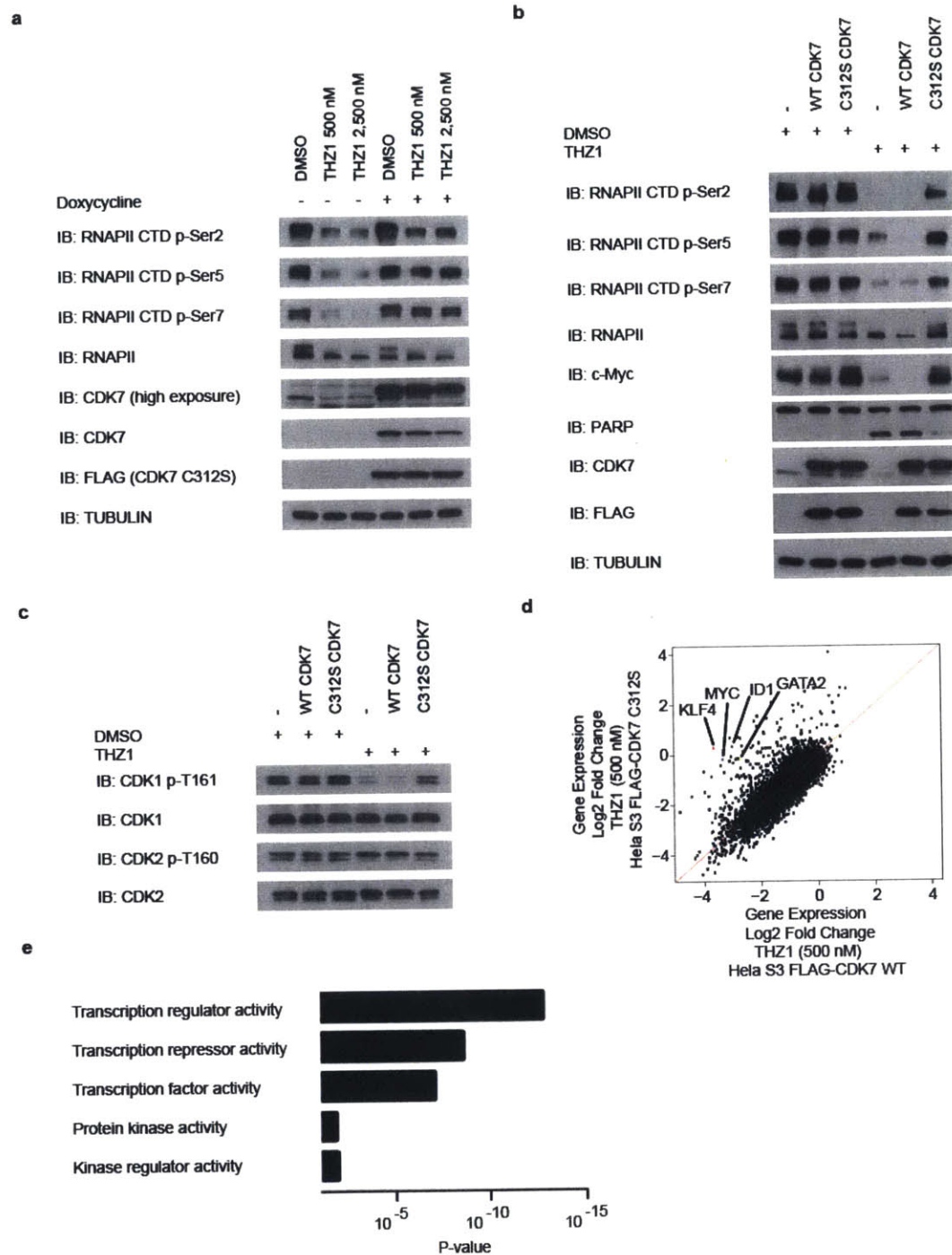
Extended Data Figure 2



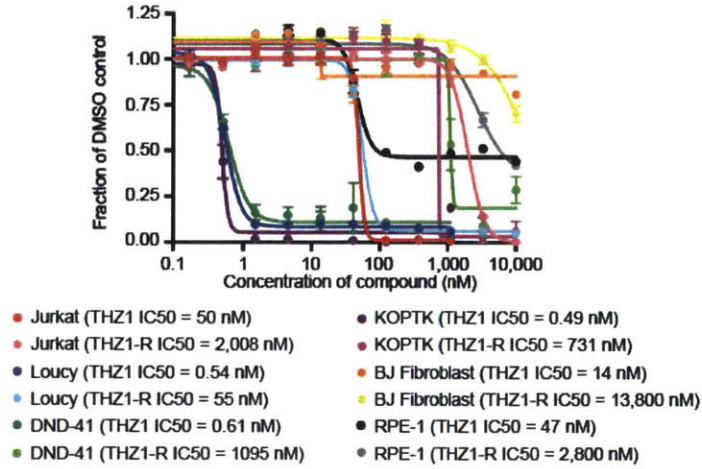
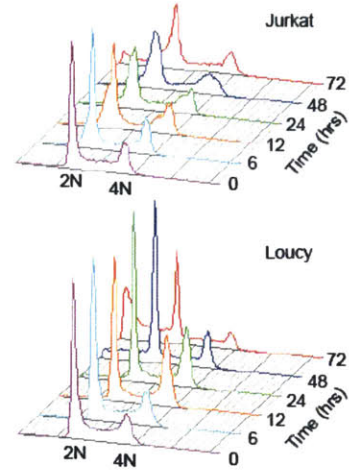
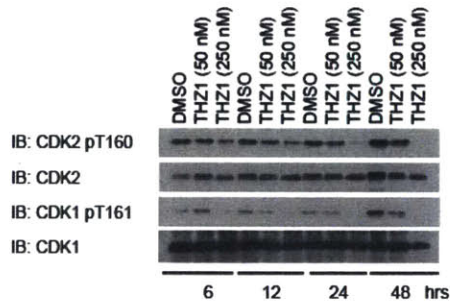
Extended Data Figure 3

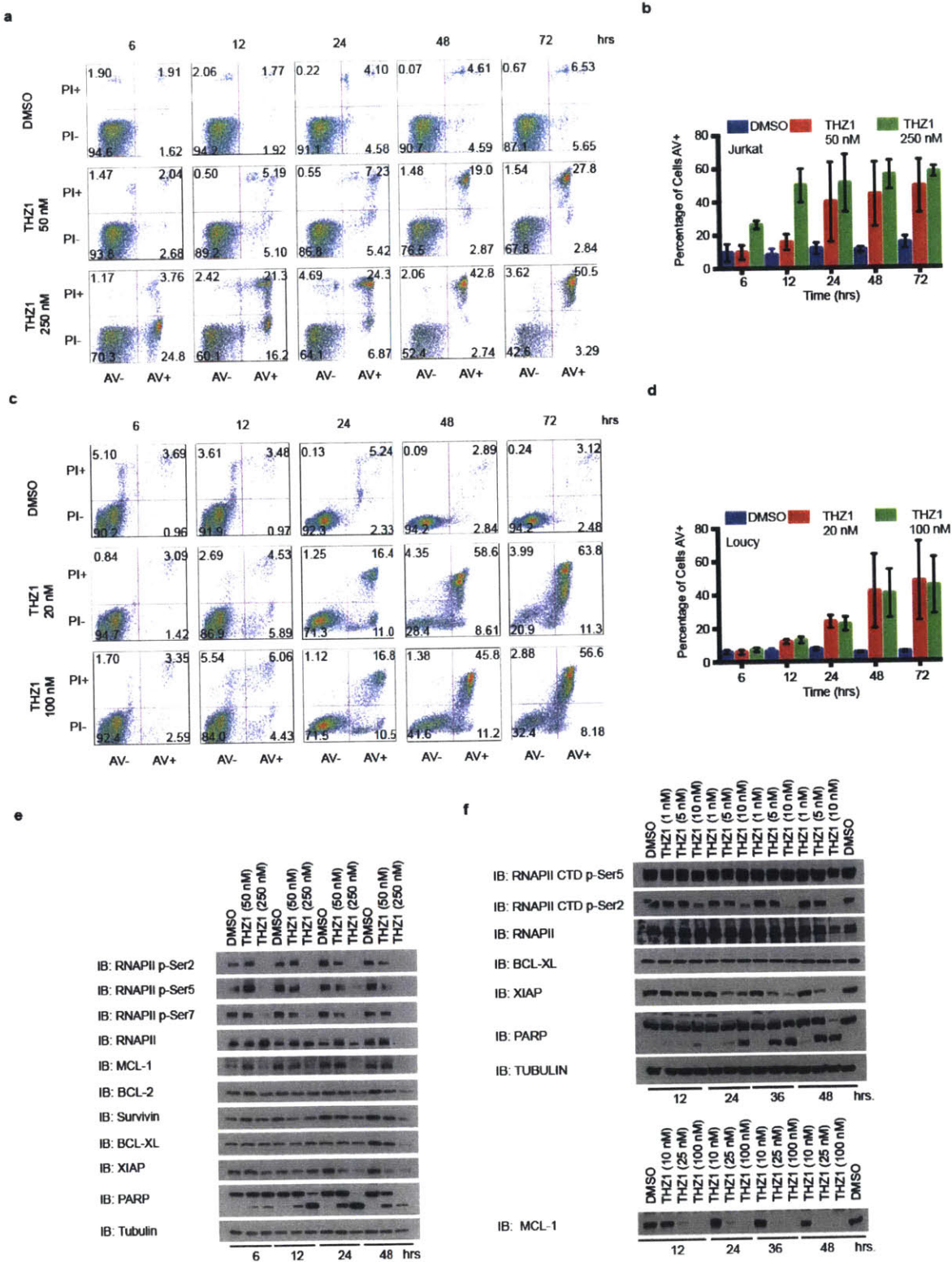






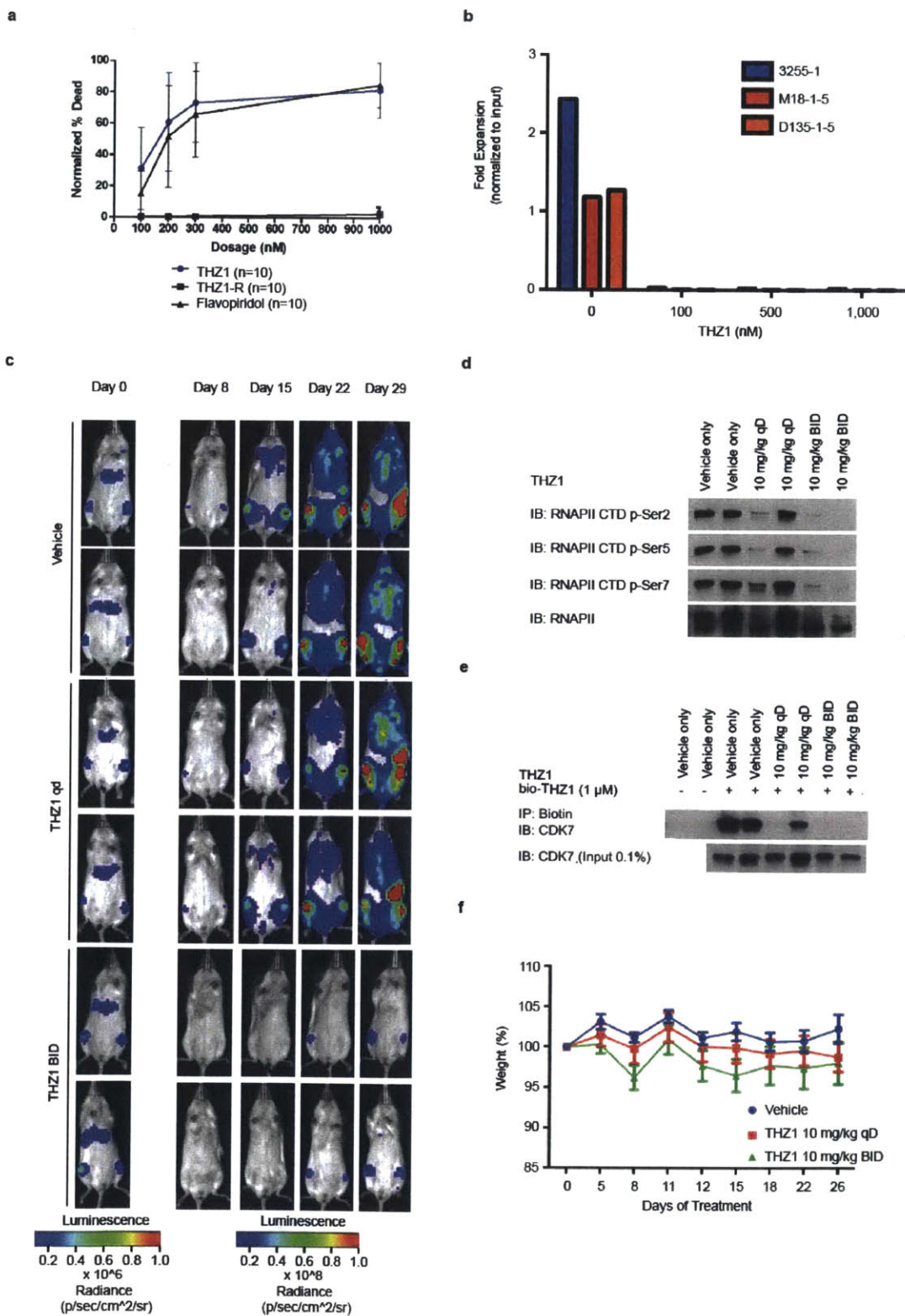
Extended Data Figure 5

**a****b****c****Extended Data Figure 6**

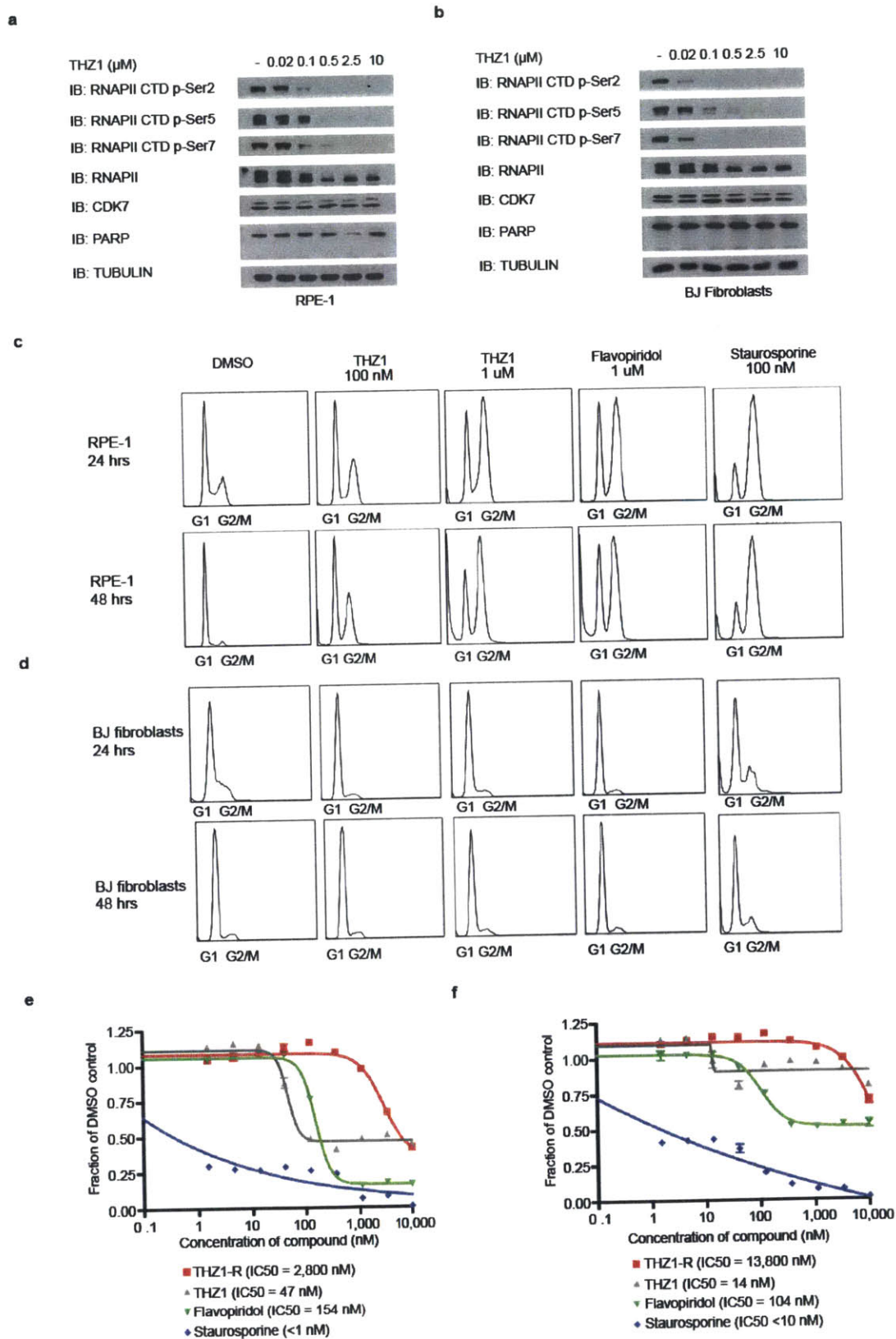


Extended Data Figure 7

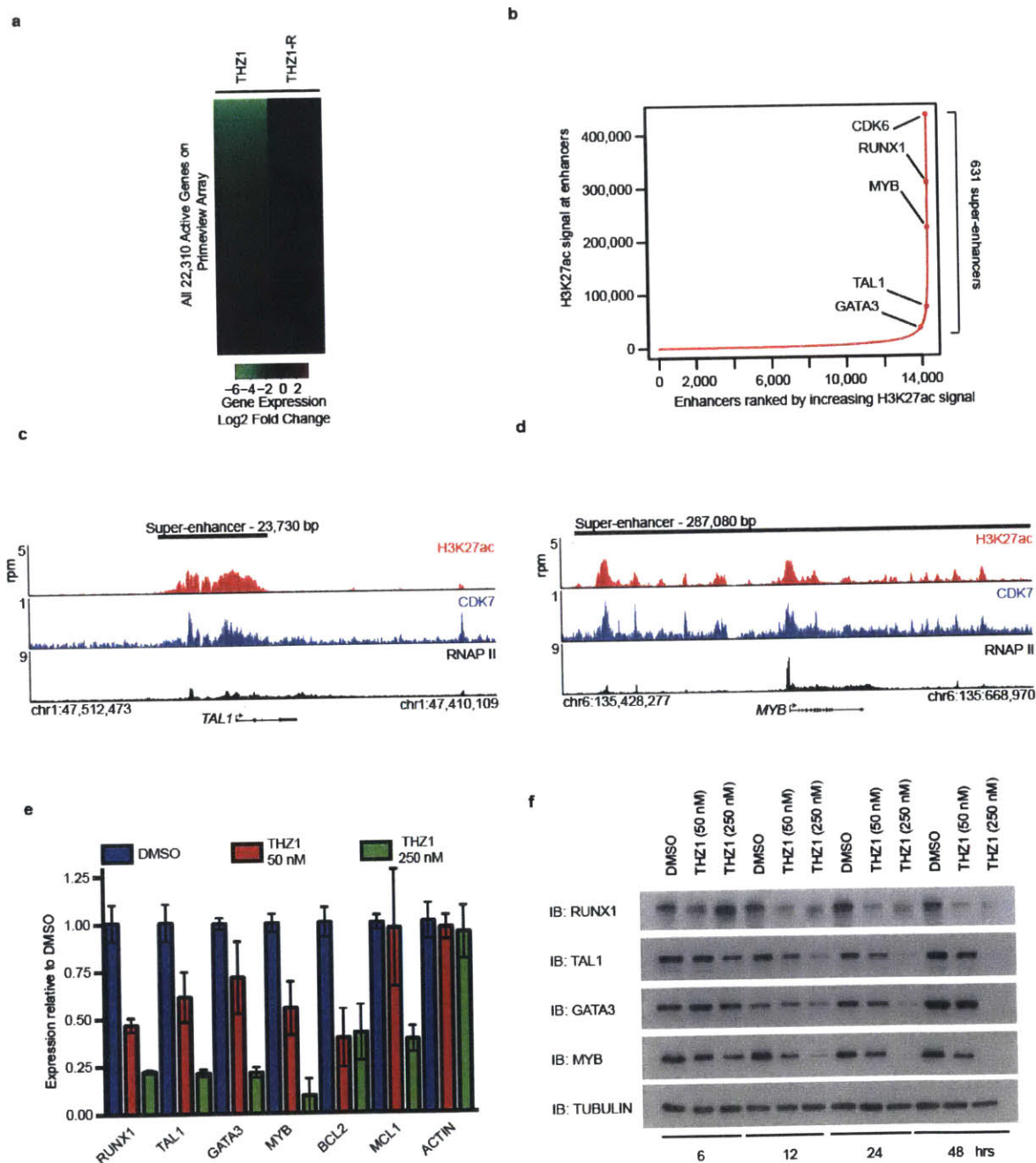




Extended Data Figure 8



Extended Data Figure 9



Extended Data Figure 10